A MODERN DEPOSITIONAL MODEL OF THE GREAT SALT PLAINS AND ITS POTENTIAL AS A CLIMATE ARCHIVE

By

KATHRYN GAIL JACKSON

Bachelor of Science in Geology

Texas Tech University

Lubbock, Texas

2008

Submitted to the Faculty of the
Graduate College of the
Oklahoma State University
in partial fulfillment of
the requirements for
the Degree of
MASTER OF SCIENCE
December, 2011

A MODERN DEPOSITIONAL MODEL OF THE GREAT SALT PLAINS AND ITS POTENTIAL AS A CLIMATE ARCHIVE

Thesis Approved:

Dr. Todd Halihan

Thesis Adviser

Dr. Alexander R. Simms

Dr. Anna M. Cruse

Sheryl A. Tucker

Dean of the Graduate College

TABLE OF CONTENTS

LIST OF TABLES

Table Page

LIST OF FIGURES

Figure Page

CHAPTER I

INTRODUCTION

Climate records for the south central High Plains of North America are sparse. The two commonly cited archives for climate reconstructions from the south central High Plains include the pollen record from Cheyenne bottoms, Kansas and the eolian deposits of the Nebraska sand hills. The Cheyenne bottoms pollen record contains two litho and bio-stratigraphic units have been identified. Radiocarbon ages from these units suggest that two periods of eolian activity occurred from 30,000 yr BP – 24,000 yr BP and from 11,000 yr BP – present day (Fredlund 1994). In Nebraska, Quaternary loess, such as the Peoria and Bignell Loess are deposited intermittently throughout the Holocene and are chronologically constrained via radiocarbon & optically stimulated luminescence (OSL) (Miao, et al., 2006; Muhs 2008). Loess has proven to be an important archive of Quaternary climate change and provides one of the most complete terrestrial records of interglacial cycles (Porter 2001; Muhs 2003). Miao et al. (2006) obtained OSL ages of the Bignell loess ranging from 10,250±610 years BP within the lowermost deposits to 100±10 years BP within the uppermost deposits. Both of these records provide excellent archives for paleoclimate interpretations. However, the record between 24,000 yr BP and 11,000 yr BP is absent from Cheyenne bottoms and the loess of the Nebraska sand hills was only deposited intermittently. A continuous record of late Quaternary deposition is needed. One potential source of a continuous late Pleistocene/Holocene record is the Great Salt Plains (GSP)

of NW Oklahoma. However, no detailed studies of its sedimentology and potential to contain a climate archive have been conducted.

The GSP is a continental sabkha with very little relief. The low-relief surface of the GSP is in a deflation-depositional equilibrium dictated by the local level of the groundwater table (Kinsman 1969; Gunatilaka 1987; Amiel 1971; Handford 1982). A well developed splay has been created by The Salt Fork of the Arkansas on the north side of the GSP. The Salt Fork of the Arkansas is the largest stream feeding water and sediment to the flats, but other minor creeks flow across the GSP as well (Figure 1). Some of the depositional environments were created by the dam completed in 1941; however, the vast majority of the flats not submerged by the reservoir are natural.

A continental sabkha is a dry land deposit associated with arid to dry environments. The fact that the GSP resides in a sub-humid environment creates a contrasting situation of an isolated dry land area within a sub-humid environment that is undocumented elsewhere. In general, examples of Holocene continental evaporites are largely lacking, so further study of the GSP will contribute more insight into the processes operating in the continental sabkhas in sub-humid settings (Handford 1982). The purpose of the project is to evaluate the potential of the GSP as a climate archive by documenting the sedimentary processes and facies of the GSP and gain a better understanding of the processes and deposits of continental sabkhas. In addition to its potential as a climate archive, mapping the GSP and its depositional environments will provide a modern analogue for analogous subsurface petroleum systems (Fisher 2008). Subsurface systems analogous to terminal splays, such as those found on the GSP, rely on few modern analogues, which has led to a tremendous amount of unsupported speculation regarding the processes and deposits of terminal splays (Fisher 2008; North et al., 2007). Continental sabkha systems also are a host for valuable ecological sites.

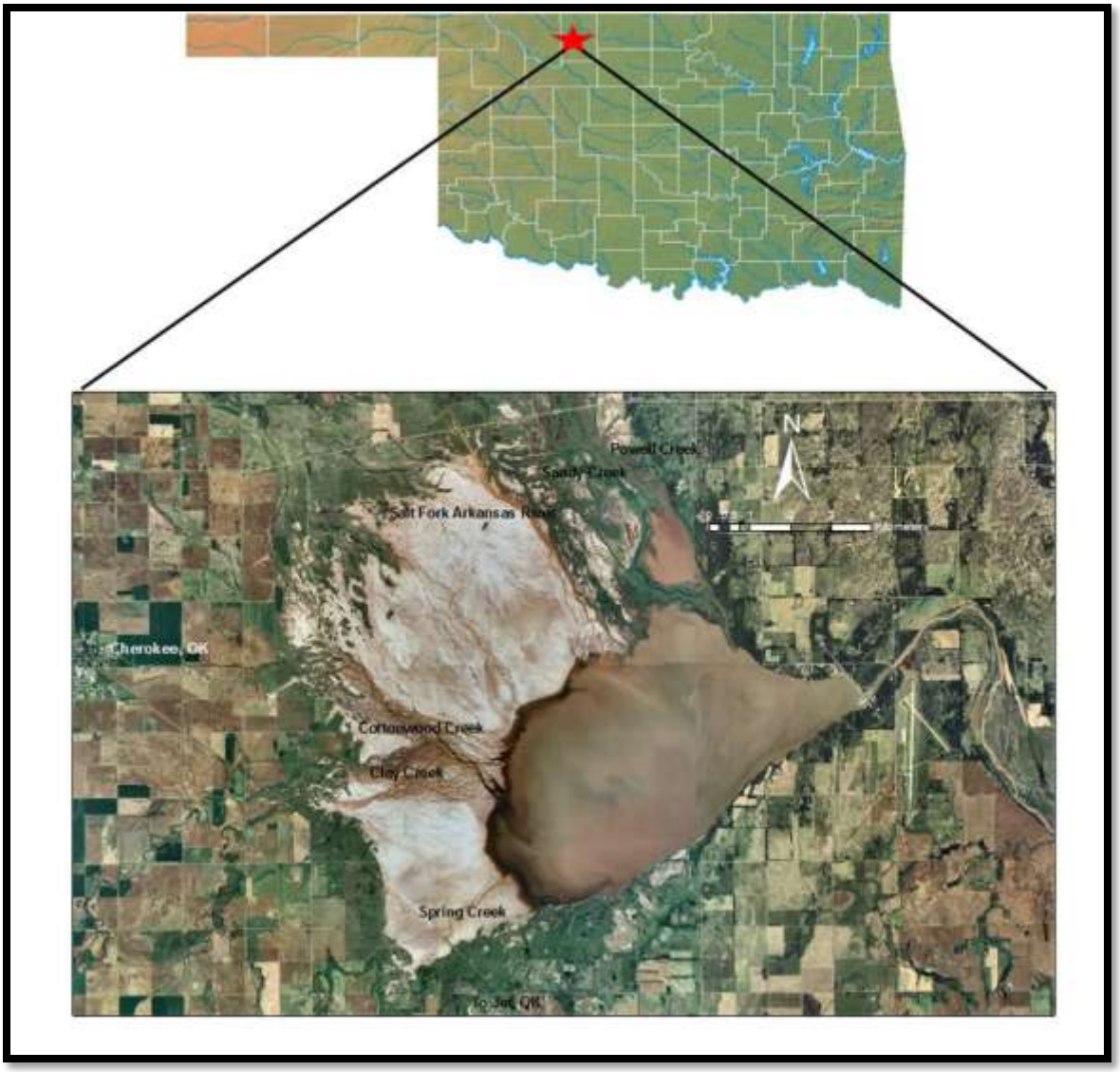

Figure 1: The Great Salt Plains (GSP) location, Alfalfa County, Oklahoma.

The GSP is home to a number of species reliant on its sabkha environments. Whooping cranes pass through the GSP as part of their migratory path in the fall and spring, and the snowy plover nests on the flats (*saltplains.fws.gov/)*. The snowy plover is generally located in coastal habitats, and inland saline environments (Purdue, 1976). Understanding the physical processes that control the development of the snowy plover's will allow the National Wildlife Refuge to maintain a safe haven for their livelihood.

Other studies of continental sabkhas include that of the Moknine continental sabkha (Chairi 2010). This continental sabkha in Tunisia (Northern Africa) provided important analysis on the nature of organic matter sources to salt pans (Chairi 2010). Chairi (2010) found that bacteria, cyanobacteria and microalgae were the primary sources of organic material in the system. This study provides an important modern examination of organic matter which can be analyzed for hydrocarbon potential of ancient sabkhas. Further research in continental sabkhas may prove useful not only for their proper identification in the ancient rock record, but their potential as hydrocarbon sources.

Creating a comprehensive depositional model for the GSP requires the classification of the modern sub environments by means of facies characterization. In order to create a comprehensive depositional model, I will address the Following questions:

1) What are the dominant processes controlling sedimentation?
2) Can the eolian and fluvial sedimentary contributions be distinguished?
3) Where would the optimal location be for a paleoclimate record?

In order to answer these questions, I collected cores, topographic profiles, resistivity profiles and descriptions of surface and shallow trenches.

CHAPTER II

GEOLOGIC BACKGROUND

The GSP of Alfalfa County is located in north central Oklahoma just east of Cherokee, OK and north of Jet, OK (Figure 1). The underlying rocks are Lower-Middle Permian clastic beds of the Hennessey Formation, which is around 200 m thick. Siltstone and sandstone beds of the Cedar Hills member comprise the upper 60 m of the Hennessey Formation. Beds of halite and anhydrite in the Permian rocks from the Wellington up through the Hennessey Formations occur at depths as shallow as 92 meters (Slaughter, 1989). These beds dip gently 3 – 10 m per km to the south and west and are thought to be the primary source of brine migrating through the porous intervals of the Hennessey Formation (Johnson, 1972) (Figure 2).

The water table beneath the salt plains is approximately 0.5 m to 1.2 m below the surface. Brine migrates laterally and upward by capillary action through the Hennessey Formation into the Quaternary deposits (Figure 2). The fluids are saturated with chloride, sulfate, sodium and calcium and cause the precipitation of halite at the surface with gypsum just below the surface (Johnson, 1972). One common gypsum variety found on the flats is Selenite, which contains distinct sand inclusions (Johnson, 1972).

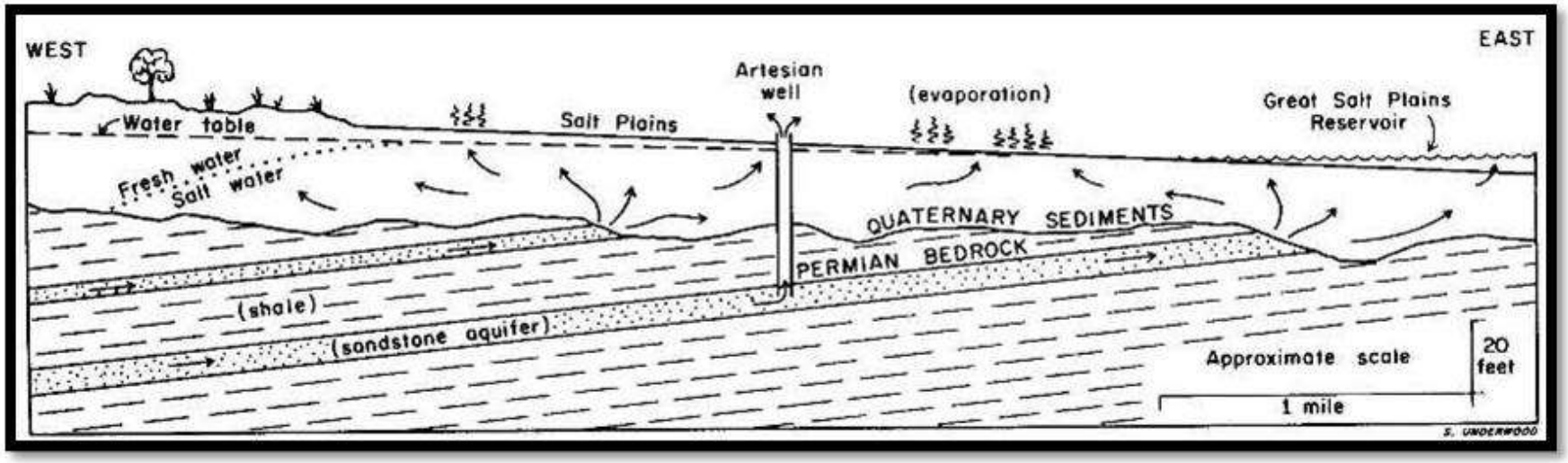

Figure 2: Generalized cross section of GSP. (Johnson 1972)

The barren salt flats cover approximately 65 km^2 (Figure 1) and range from 3 to 8 meters in thickness (Johnson 1972). A dam across the Salt Fork of the Arkansas River was constructed from 1936 to 1941. A reservoir approximately 37 km^2 formed behind the dam and is on average 4.5 m to 7 m deep. The overall shallow slope of the flats is roughly 2.7 meters per kilometer. The Salt Fork of the Arkansas River flows onto the north side of the flats (Figure 3). The GSP is chiefly dominated by the Salt Fork of the Arkansas and other minor creeks: Clay Creek, Sand Creek, Powell Creek, Spring Creek and Cotton Wood Creek (Figure 1). Sediments are transported onto the flats by either fluvial processes, which tend to distribute sediment in a fan-like manner, sheet-wash/flood events, or eolian mechanisms. Elevations of the conservation pool (GSP reservoir) records have been kept since November of 1994 (http://www.swt-wc.usace.army.mil/GSAL.lakepage.html). The maximum elevation of the conservation pool recorded to date is 1135.03 ft above sea-level (345.96 m) in November of 1998. That particular elevation occurs across the middle of the GSP running north to south and it is unlikely that the conservation pool completely flooded all of the GSP.

Alfalfa County is in a sub-humid environment with mean annual rainfall at 78.7 cm (2002 Oklahoma Climatology Survey). Most precipitation for the area occurs between the months of March and October. The potential annual evaporation is approximately 239 cm (2002 Oklahoma Climatology Survey). The predominant wind directions range from a northerly direction for the late fall, through winter months (November – March) and a south-southeasterly wind for the spring and summer months (April – October). In Fairview of Major County (52 km southwest of GSP), climate records were held from 1932 to 1962. The mean annual temperature was 61.6 °F (Brady, 1989). January was the coldest month with a mean temperature of 38.2°F and the warmest month was July with a mean temperature of 83.5°F (Brady, 1989). The average hourly wind speed is 21 kph (13 mph); however during the months of March and April it increases to 24 kph (15 mph) (Soil Conservation Service, 1968).

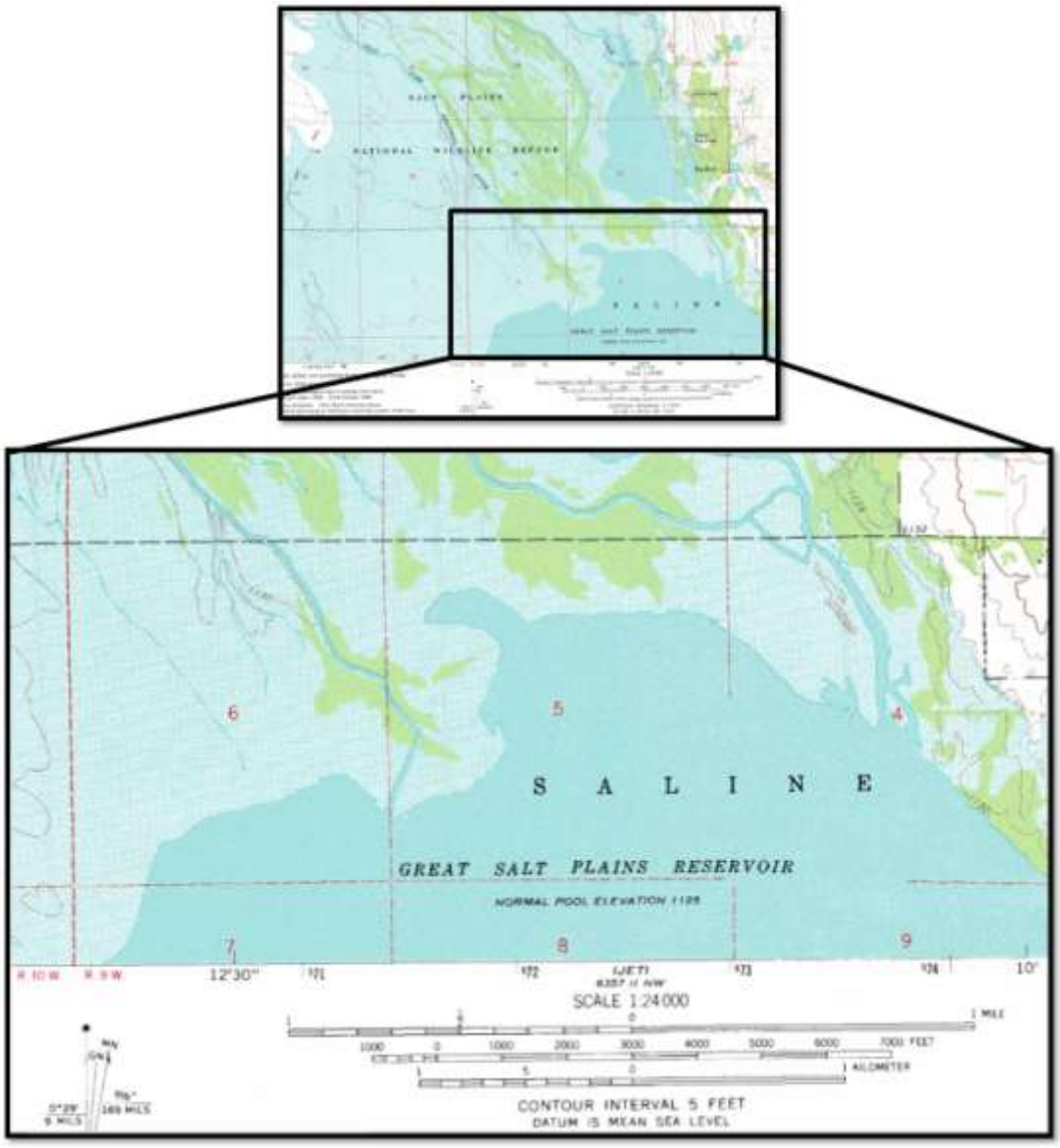

Figure 3: Topographic map illustrating the low relief of the Salt Fork of the Arkansas River delta. (*http://www.topozone.com/states/Oklahoma.asp?county=Alfalfa*)

Eolian dunes line much of the perimeter of the GSP and blanket many of the fluvial terraces found along major rivers in Alfalfa and surrounding counties. The dunes are hummocky or lumpy in appearance and typically line the north sides of major rivers in Oklahoma (Johnson, 1972; Lepper and Scott, 2005; Cordova et al., 2005; Forman et al., 1995). The dunes lining the GSP are sourced from the modern flood plains of The Salt Fork of the Arkansas and are stabilized by vegetation with only a few barren dunes still active (Johnson, 1972). Lepper & Scott (2005) used OSL and ^{14}C dates to constrain late Holocene dune activity in the Cimarron river valley of Oklahoma and found evidence for extensive drought between 1100 and 1250 AD. Dune activity was determined to be episodic based on eolian sediments interbedded with paleosols representing stabilized dunes during intervening periods. Cordova et al. (2005) also found evidence of late Holocene (1100 – 1250 AD) dune activity. Reactivation of dunes also occurred during the arid Altithermal interval between 8,500 to 4,000 yrs. B.P. Evidence for earlier dune activity between 20,000 – 12,000 and 11,200 – 8,000 yrs. B.P. was presented by Forman et al. (1995). Holliday (1999) also found evidence for dune reactivation at 6000, 4500, and 1000 yrs. B.P.

Another useful tool for determining paleo-climate is cycles of pedogenesis and loess deposition. These pairs reveal cyclicity between dry periods marked by sparse vegetation and loess transport while humid periods are marked by soil formation. Two members, the Tertiary Ogallala (Miocene – Pliocene) and Quaternary Blackwater Draw (Pleistocene) formation were interpreted to show climatic variations (dry to wet) on the order of 30,000 – 100,000 year cycles (Gustavson and Holliday, 1999).

Additional paleoclimate records for the region were reconstructed from a site in nearby Harper County. Here paleoclimate reconstructions are based on fauna in the Doby Springs area during the Pleistocene (Stephens, J.J. 1960). At this point in Western Oklahoma's climate, the Illinoian stage (300 – 130 ka) represented a colder climate similar to the present day climate of South and North Dakota with a mean annual temperature of 42°F (Stephens, J.J. 1960).

Previous work on the GSP has concentrated on the geochemistry and hydrogeology rather than the sedimentology, geomorphology or its potential to contain paleoclimatic data. However, the sedimentology and geomorphology of the GSP may provide an important analogue for ancient deposits and characteristics for distinguishing between continental and marine in origin. Both modern marine and continental sabkhas contain similar features such as, desiccation polygons, deflation pits, salt karst depressions, salt hoppers/syntaxial overgrowths, dunes, algal mats and many other features (Hussain 1988). The origin of continental and marine sabkhas differ though, as continental sabkhas are geometrically defined by their intersection with the capillary fringe of a shallow water table rather than the direct interaction of the sea water of a marine sabkha (Warren 2006).

Insights into the processes and sediments of the GSP may be gained by studying analogous settings, such as the ephemeral dryland river system of Fowlers Creek in southeast Australia where ripples, scours, clay layers, laminations of fine grained material and sheet flow deposits are documented (Wakelin-King et al. 2007). Depositional models for similar complexes have been documented by shallow coring, trenches and GPS measurements (Benison et al., 2007; Fisher et al., 2008; Tooth 2005; Wakelin-King et al., 2007) . Three specific terminal splay complexes (TSC) on the shoreline of Lake Eyre in Central Australia have been categorized based on their facies architecture: the modern Neales, Umbum and Douglas TSC's (Rielly et. al 2006). The modern Neales TSC is considered fluvial dominated, is highly constructive and triangularly lobate while the Umbum TSC is noted for its multiple avulsion distributary channels (Rielly et. al 2006). The Douglas TSC is characterized by two avulsion distributary channels causing propagation through sheetfloods (Rielly et al., 2006). Multiple factors can influence splay development such as: the size of the TSC, discharge, vegetation, grain-size distribution, composition and the influences from the reservoir it empties into (Fisher et. al, 2008). Each terminal splay complex or terminal fan is considered to be unique from one another and no single

model is thought to fully capture the variability found in the TSC (Fisher et al., 2008, North and Warwick, 2007).

The low gradient of the GSP also plays a role in the morphology of the landforms. Low stream gradients promote anabranching since they lead to the deposition of fine cohesive sediment and to lower erosional energy (North et al. 2007). Judging from the available aerial photographs and topography maps available, such bifurcation and anabranching-braided networks are present within the Clay Creek, Cotton Wood Creek and The Salt Fork of the Arkansas River in the central and northern portions of the flats.

Another extreme environment that resembles the GSP are the acid saline lakes in Yilgarn Craton of Australia. Several of the lake environments present in the craton undergo extreme processes of evaporation, high winds and flooding (Benison et at. 2007). Sedimentary processes were well documented during flooding, evaporation concentration and desiccation stages of these acid saline lakes (Benison et al. 2007). The unique surface features found in the Yilgarn Craton closely resemble those of the GSP.

In general, the term sabkha (Arabic) i.e. salt flat is generally associated with the marginal marine environment. There are only minor differences between the continental sabkha and marine sabkha: their origin and geochemistry of the evaporite-forming brines (Handford 1982). Another explicit way to describe their differences is that marine sabkhas are depositionally offlapping from marine sediments from which the evaporite precipitates from; while continental sabkhas are derived from the evaporation of continental waters whose evaporites may originate from either previous marine cycle evaporites or continental evaporites (Kinsman 1969, Amiel 1971). Both environments undergo similar physical and chemical process such as, intense evaporation, wind deflation, subaqueous and intrasedimentary precipitation of evaporites and ground water discharge (Handford 1982 & 1981). Both marine and non-marine Holocene sabkhas have been examined by Lowenstein et. al (1985) and can be characterized by three different alternating periods of deposition: flooding, evaporative concentration and desiccation (Lowenstein 1985,

Figure 4). Similar facies architectures between marine and continental sabkhas may be the culprit for the absence of continental sabkhas in the rock record, as many of them may be interpreted as marine sabkhas.

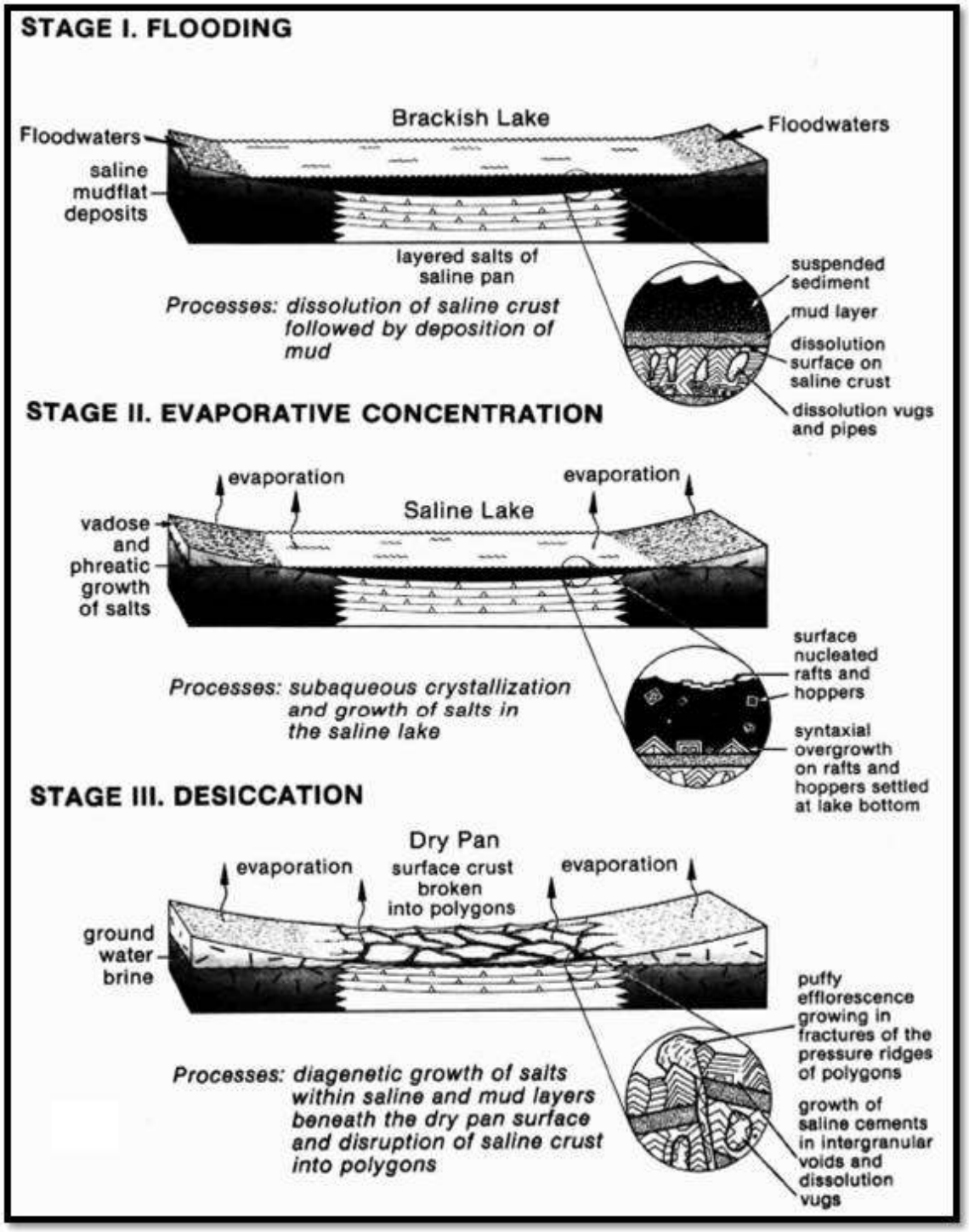

Figure 4: Stages of deposition for salt pan/sandflat, Lowenstein 1985.

CHAPTER III

METHODOLOGY

Multiple methods will be utilized for characterizing the GSP. These methods include field studies involving the collection of surface observations, and subsurface data as well as lab analysis of field samples. The field methods used for the collection of surface data include: sediment traps, GPS (Global Positioning System) surveying, aerial photography and surface observations. All surface and surface observations are presented in Figure 5.

Sediment traps were constructed from Rubbermaid Tupperware (9 cm diameter lids), filter paper, rubber bands and a stake through the middle of the receptacle (lid) to hold it in place (Figure 6). These traps were placed in 9 locations in order to determine the rates and sources of sediment transport as well as distinguishing between depositional and erosional surfaces. The lids were slowly imbedded into the surface with the filter paper wrapped on top until level with the surface. A hand-held Garmin GPS was used to place all sediment traps and surface pits into a spatial reference frame. The first round of sediment traps were deployed for a two week period between 09/27/2009 – 10/09/2009 and a two month period between 10/09/2009 – 12/10/2009. GPS surveying was utilized to delineate the dimension of the channels from proximal to distal reaches of the GSP. Since the Salt Fork of the Arkansas is not the only fluvial influence, examination of the other channel environments was conducted. Dryland river environments similar to that of the GSP display a great variety of forms and processes thus; a GPS survey is necessary in order to illustrate the differences between the scale

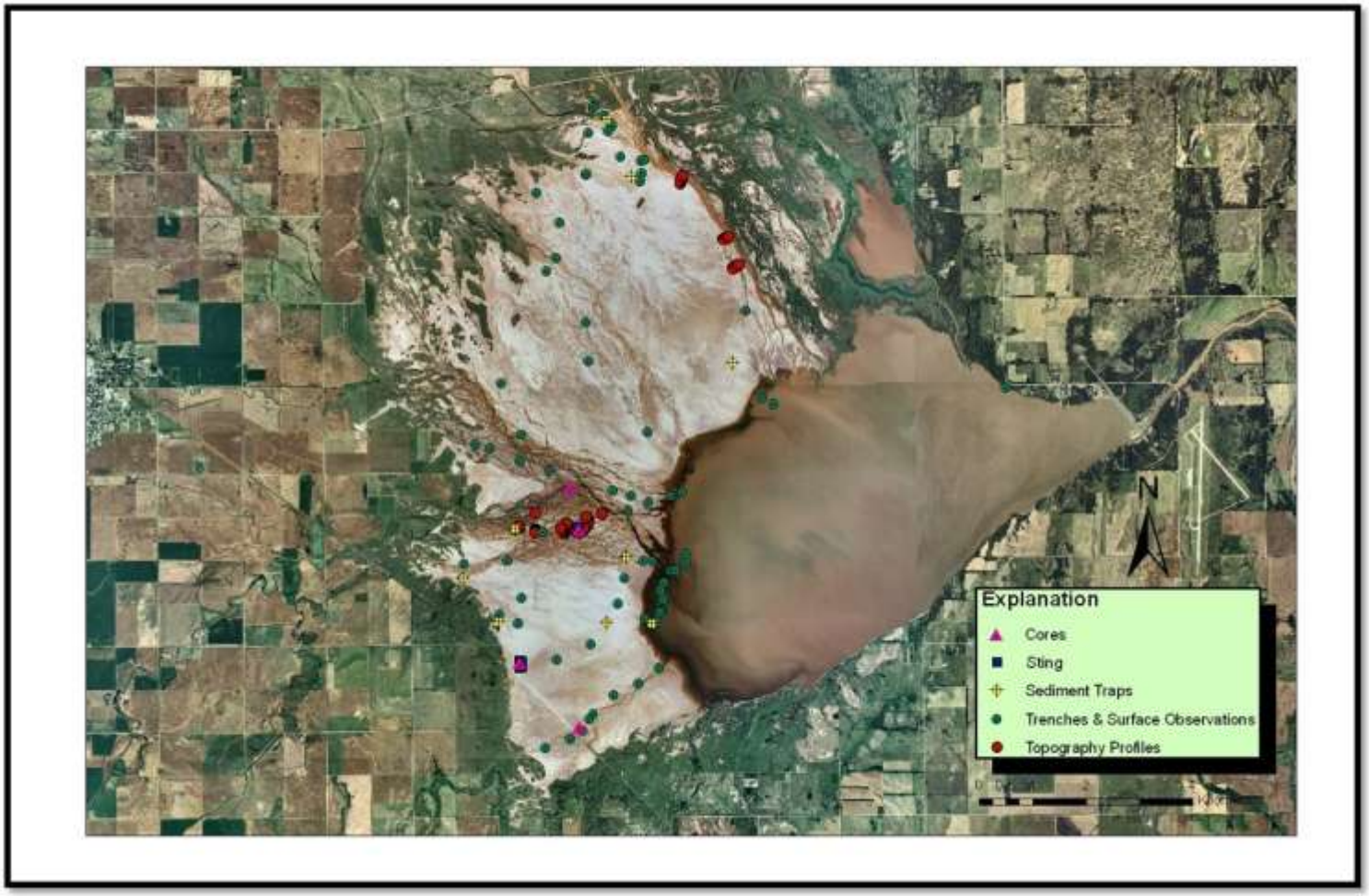

Figure 5: All surface and subsurface locations.

Figure 6: Sediment trap apparatus.

of the features produced by the Salt Fork of the Arkansas and other creeks (Wakelin-King, 2007). A RTK-GPS TopCon system was used for the topography acquisition of the channels. Raw GPS data (ellipsoidal height) was corrected by OPUS: Online Positioning User Service. GPS topography profiles have an accuracy of approximately 3 cm. Spacing for the topographic profiles was paced approximately 2 meters between each way point. Aerial photography was used to study the geomorphic changes of the GSP over time (approximately 70 year time span, beginning in 1941). Surface observations were also implemented for documenting modern environment and deciphering sedimentation processes.

The methods used to collect subsurface data included: trenches, ERI (Electrical Resistivity Imaging) lines, and vibra-cores. 60 trenches were dug to a depth of 25-45 cm or until reaching the ground water table in order to document sedimentary structures and grain sizes. The position of all trenches and other observations were recorded with a GPS unit. An AGI Super Sting resistivity imager was used to image the depth of the Quaternary sediments. The resistivity acquisition was used to gain a further understanding of the three-dimensional architecture of paleo-environments preserved in the Quaternary subsurface of the flats. Processing of the resistivity data was completed with AGI EarthImager 2D software. This software is designed to process resistivity inversions of AGI Supersting data sets and create 2D sections for interpretations. Eight (8) separate lines were processed with this software, with 5 specific lines utilized for paleo-environment interpretation. Electrode spacing was 2 meters (4 meter dipole length) with 7 of the ERI lines and 1 meter electrode spacing for GSP08NA which was also a topographic profile line in the center of the Clay Creek system (central portion of the GSP). Due to the low resistivity values for the GSP, the reciprocal of the data was taken (1/ohm-m) for the purposes of discussing the data in conductivity, S/m (*Siemens per meter).* A tripod vibracore apparatus was used to collect 5 7-cm diameter cores from across the flats. 4 cores in 2010 and 1 core was collected in 2006. GSP06-01 reaching a depth of 273 cm was collected in the sand flat

environment at the time (2006) between the Salt Fork of the Arkansas River and Clay & Cottonwood Creeks. Two of the cores collected were exclusive to two of the resistivity lines acquired. Core GSP10-01 reached a depth of 280 cm and was collected along resistivity line GSP02NA, as it had the strongest signature of a paleo-channel deposit. Core GSP10-03 reached a depth of 397 cm and was collected along resistivity line GSP08NA (modern channel area). Core GSP10-02, was the shortest core reaching a depth of 74 cm and was collected in the southern part of the GSP within the active area of Spring Creek. Core GSP10-04 was 237 cm long and was collected further north of core GSP10-03 (along resistivity long GSP08NA) in an active channel area where Cottonwood Creek and Clay Creek coalesce.

Grain-size analysis component was conducted with a 1180L CILAS Particle Size Analyzer. Grain size analysis was conducted on sediment trap samples, trench samples, core and surface samples. Grain size analyses for all of these samples are fundamental for distinguishing between facies and possibly detecting sediment contribution within the entire depositional system (Cheetam et al., 2008). All samples were treated with Hydrogen peroxide (H_2O_2) to remove organic materials, but not treated with acid (such as HCl) to remove carbonates as these grains could have potentially been allogenic and deposited via fluvial and/or eolian processes across the GSP. The dispersing agent to prevent flocculation was a 10% concentration of sodium hexametaphosphate [$(NaPO_3)_6$].

CHAPTER IV

RESULTS

5 depositional environments were identified with in the GSP. These environments include: channel, sand flat, mud/algal flat, dune and delta. Each environment is marked by at least one characteristic sedimentary facies. Each environments exhibited changes from proximal through medial and distal zones of the GSP.

Environments:

Channel

The channel facies is composed of a 500 – 800 m wide of anabranching-braided stream channels containing relatively the coarsest of the deposits. The most common facies preserved in cores and trenches of the GSP is the channel facies. The grain size of this faces ranged from granule to clay size. Most of the channel facies deposits were tan-brown to red medium to coarse grained sand. This facies has a mean grain size of 2.85 **Φ** with an average moment standard deviation of 1.49 **Φ** and an average moment skewness of 2.11 **Φ**. Multiple sedimentary structures are found in the channel facies including small scale trough cross bedding, parallel laminations, clay drapes, rip up clasts, starved ripples, lenticular bedding, cut and fill structures, isolated clay stringers, clay beds, and climbing ripples. Topographic profiles were collected from two of the fluvial channels delivering sediments and water to the GSP: a splay of the Salt Fork of the Arkansas River and Clay Creek (Figure 1).

Profiles A-J were collected as a series of strike profiles along the Clay Creek system at 0.1 and 0.6 km spacing downstream (Figures 7 & 8). Profiles L-M were also collected along strike along a splay of the Salt Fork of the Arkansas River (Figures 9 & 10). The Salt Fork splay is much larger than the channels of Clay Creek as seen in the channel depths and widths of profiles L-M. Though the dimensions of these channels differ greatly, both fluvial systems decreased in channel depth downstream. The other two dimensions, width and length did not exhibit any clear trends from proximal, medial and distal portions of the GSP. These topographic profiles are taken from channels present at the time of field inspection. Aerial photos do not always reflect current channel locations as these channels change every rain storm locally. Therefore, some of the topographic lines on the aerial photography may appear not to have been collected along strike across a channel, but the location is accurate for a channel at the time of collection.

At the surface, unique scour pits are present in the active flood plain (Figure 11-B). These scours were most common in the proximal portion of the Salt Fork of the Arkansas River in association with a very thin algal mat layer. This thin algal mat layer rapidly disappears downstream, but another thicker and more widely distributed algal mat is encountered more distally (Figure 12). Additionally, an array of sedimentary features such as: armored clay balls, transverse-catenary ripples, isolated pools (some with halite hoppers & rafts), crevasse splays, and contorted over-bank deposits are present (Figures 11-D). Bedforms at the surface and sedimentary structures in the subsurface were observed to decrease in size distally (Figure 13). Trenches in the channel facies revealed an overall decrease in grain size and bed thicknesses from proximal, medial and to distal portions of the GSP. The sand flat facies also exhibited a similar trend as revealed by the trenches. Figure 12-A illustrates large asymmetrical dunes and ripples found in the proximal portion of the Clay Creek splay. The larger asymmetrical dunes are 10-13 cm deep, 0.6 to 1 m wide and 1 to 1.5 m long. Figure 8 12-B provides an example of traverse-

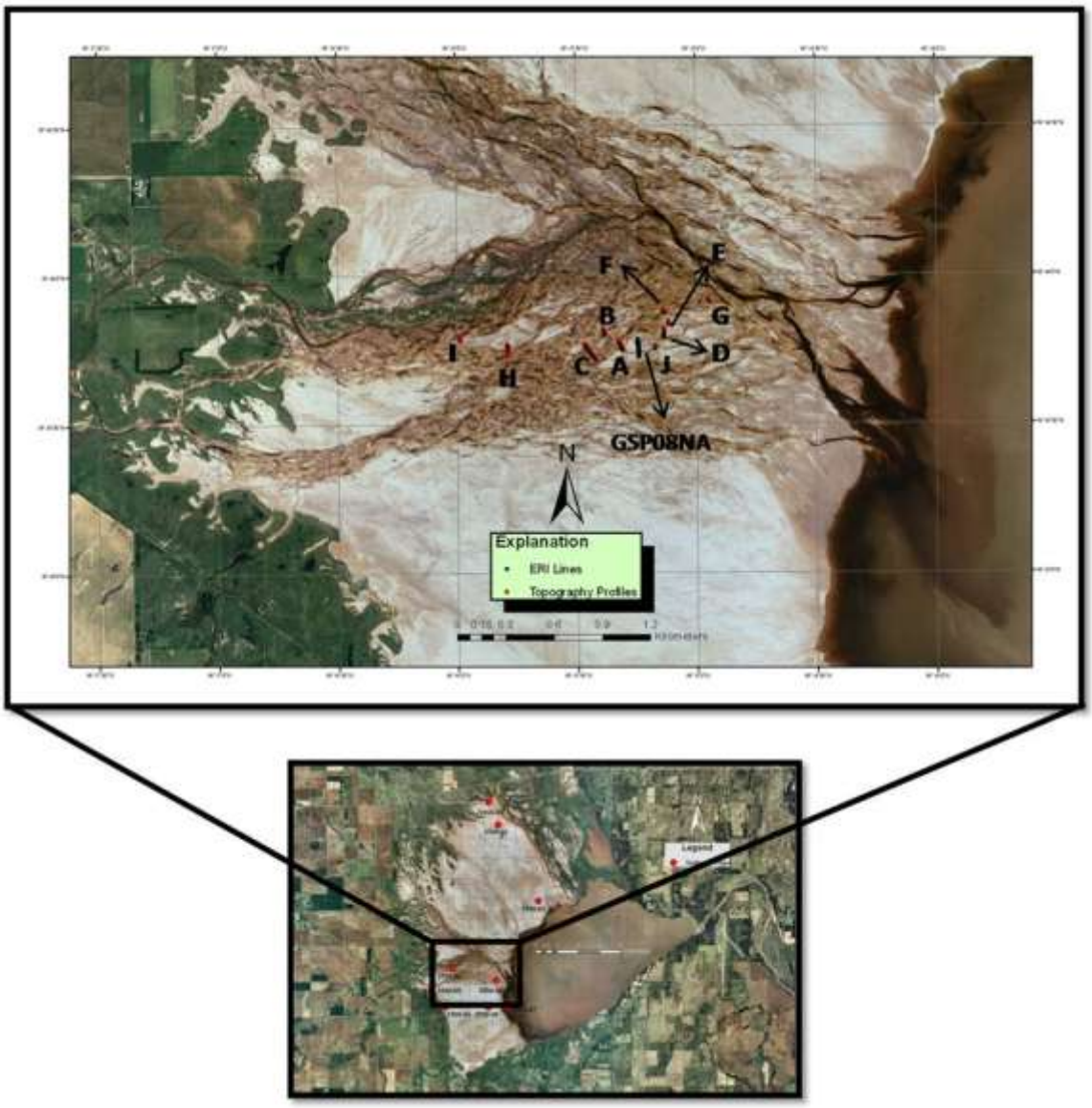

Figure 7: Location of GPS topography profiles I – G, Clay Creek System.

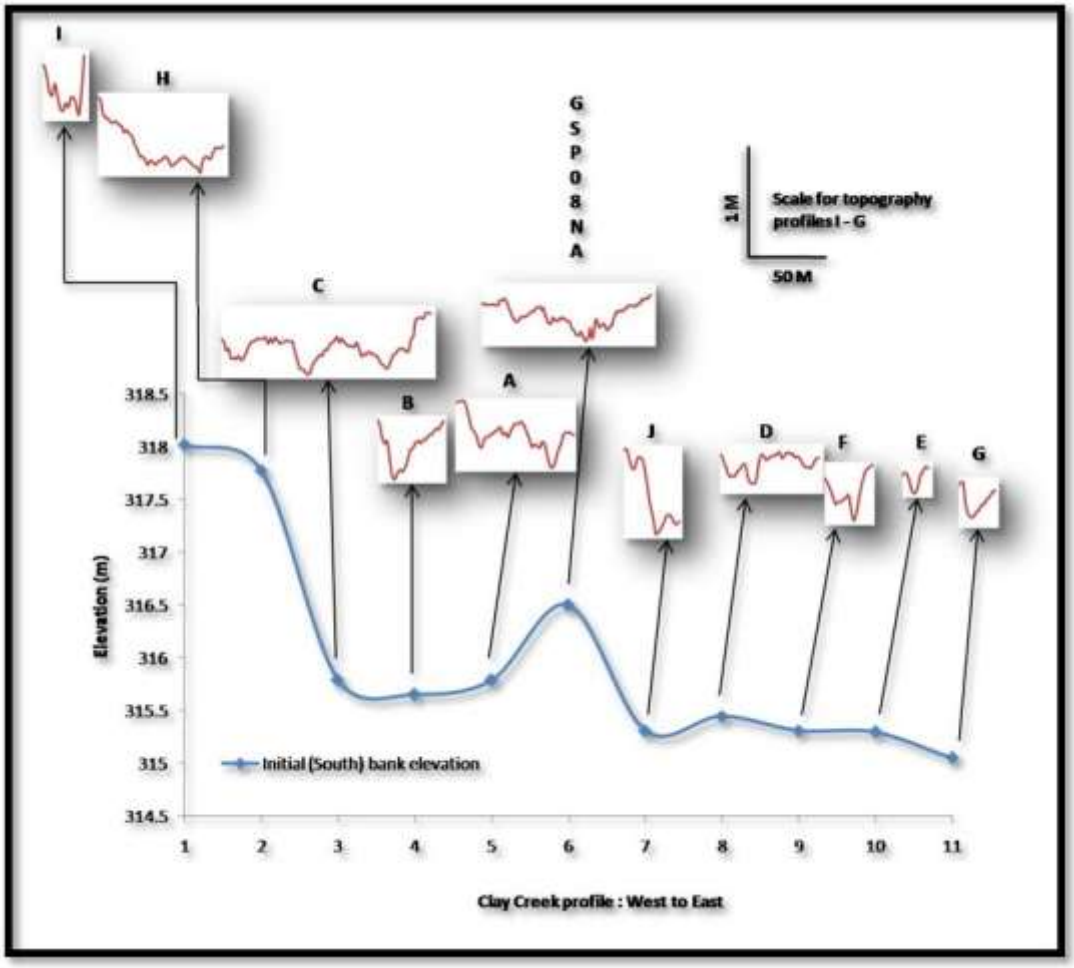

Figure 8: GPS topography profiles: Clay Creek (W-E, proximal to distal).

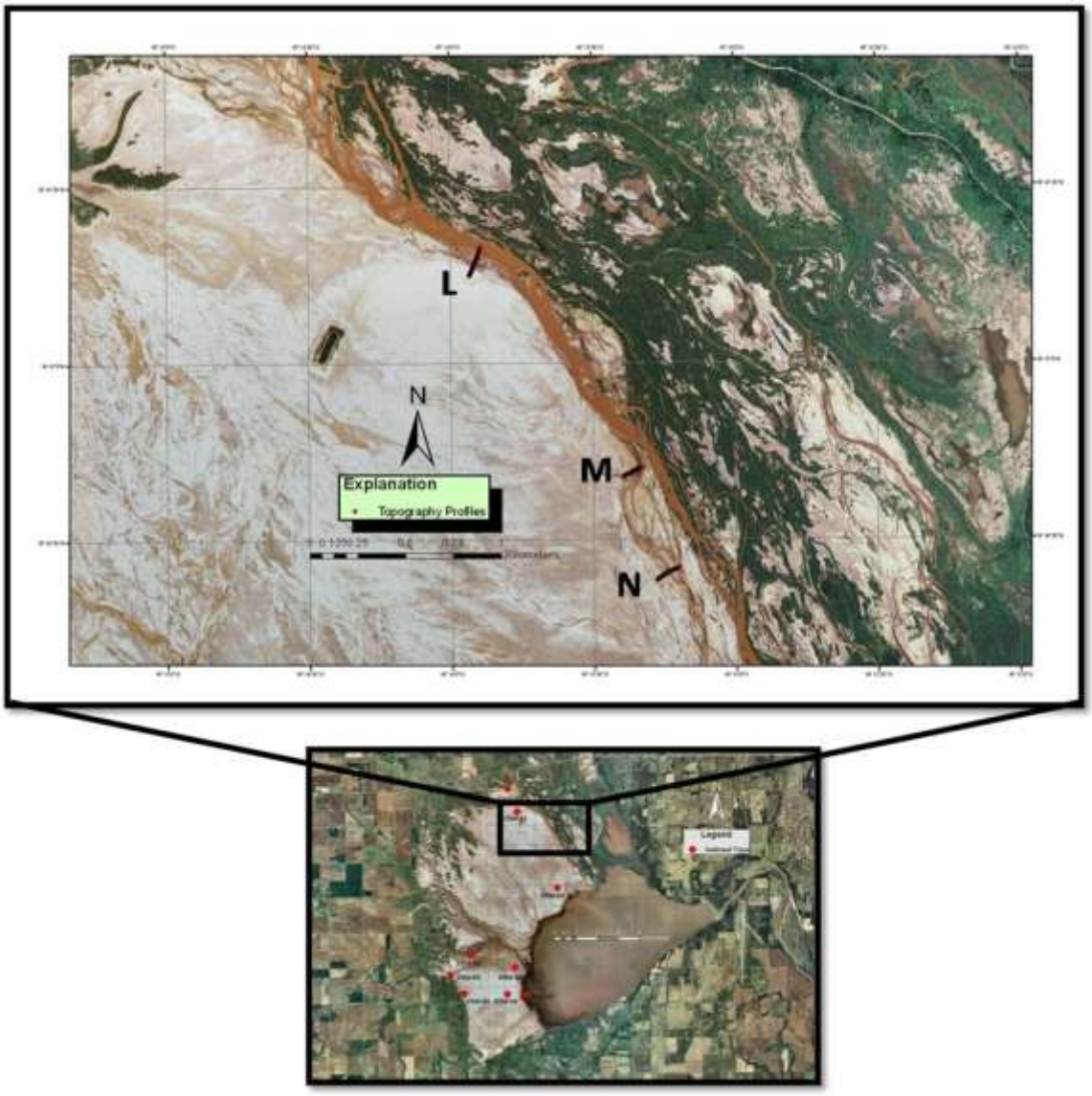

Figure 9: Locations of GPS topography profiles L – N, Salt Fork of the Arkansas River.

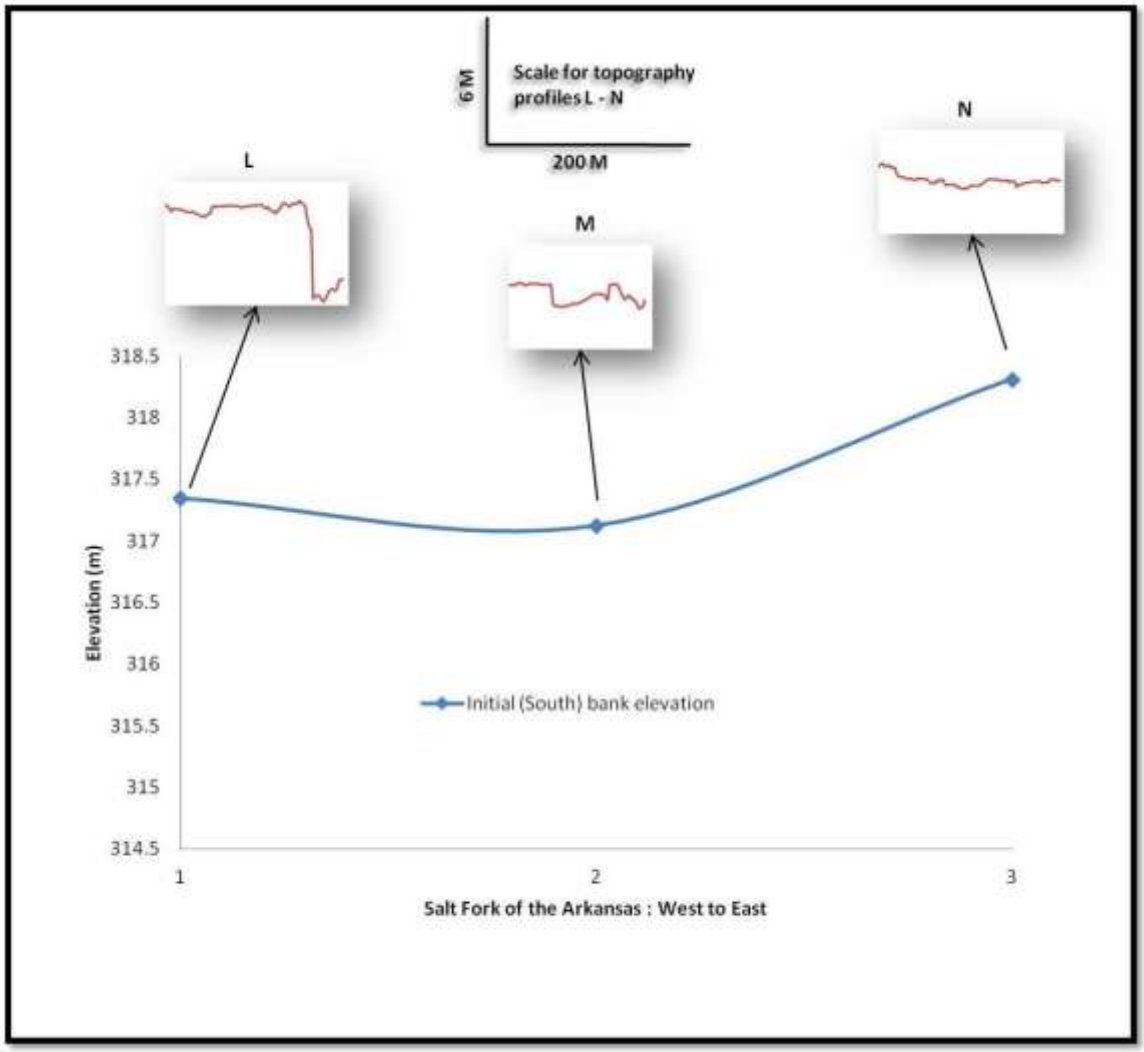

Figure 10: GPS topography profiles: Salt Fork of the Arkansas (W-E, proximal to distal).

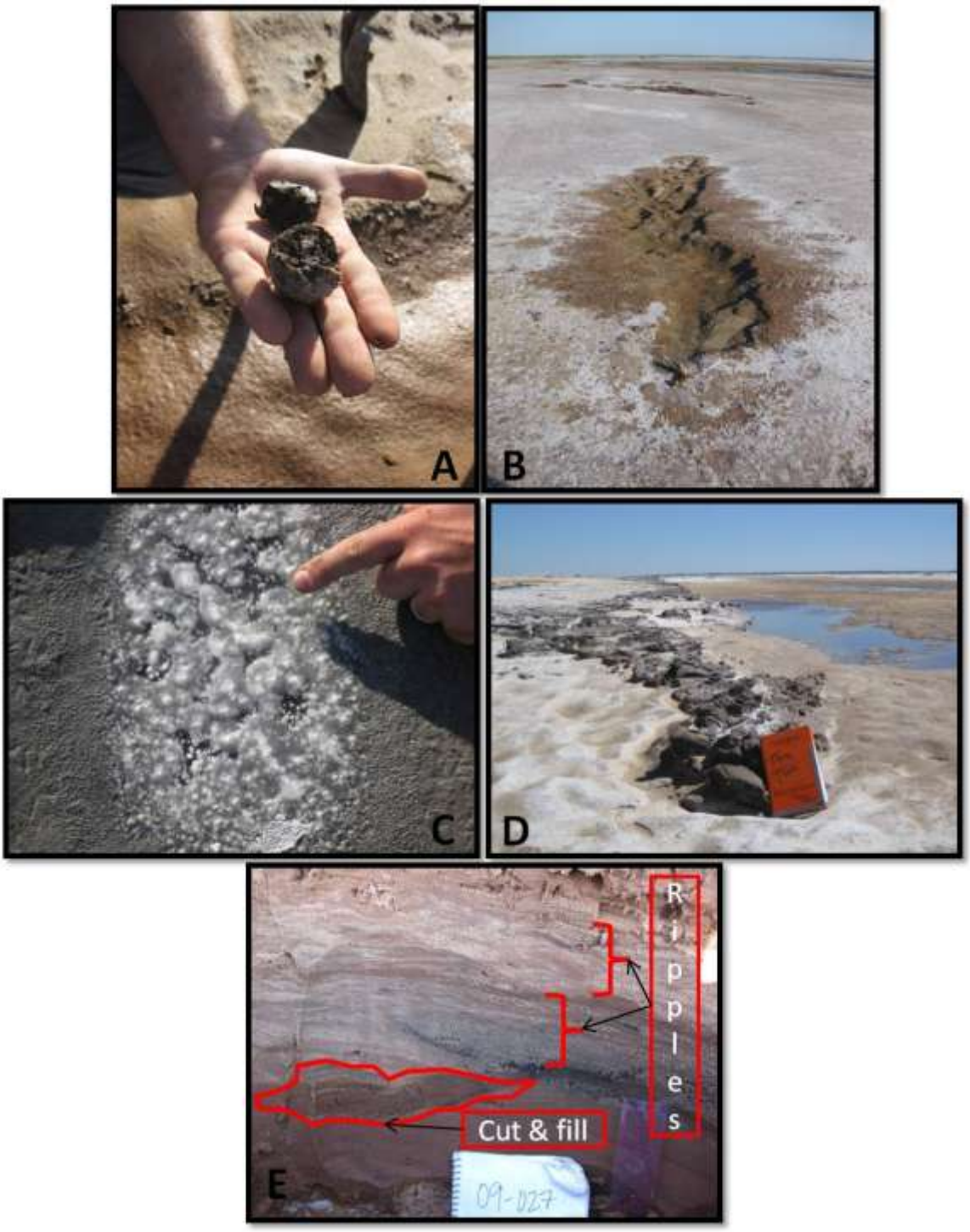

Figure 11: Channel environment observations. A: Armored clay ball. B: Scour in flood plain. C: Cubic halite crystals precipitating in an isolated pool. D: Collapsed bank from channel avulsion. E: Cut and fill structure and ripple cross lamination.

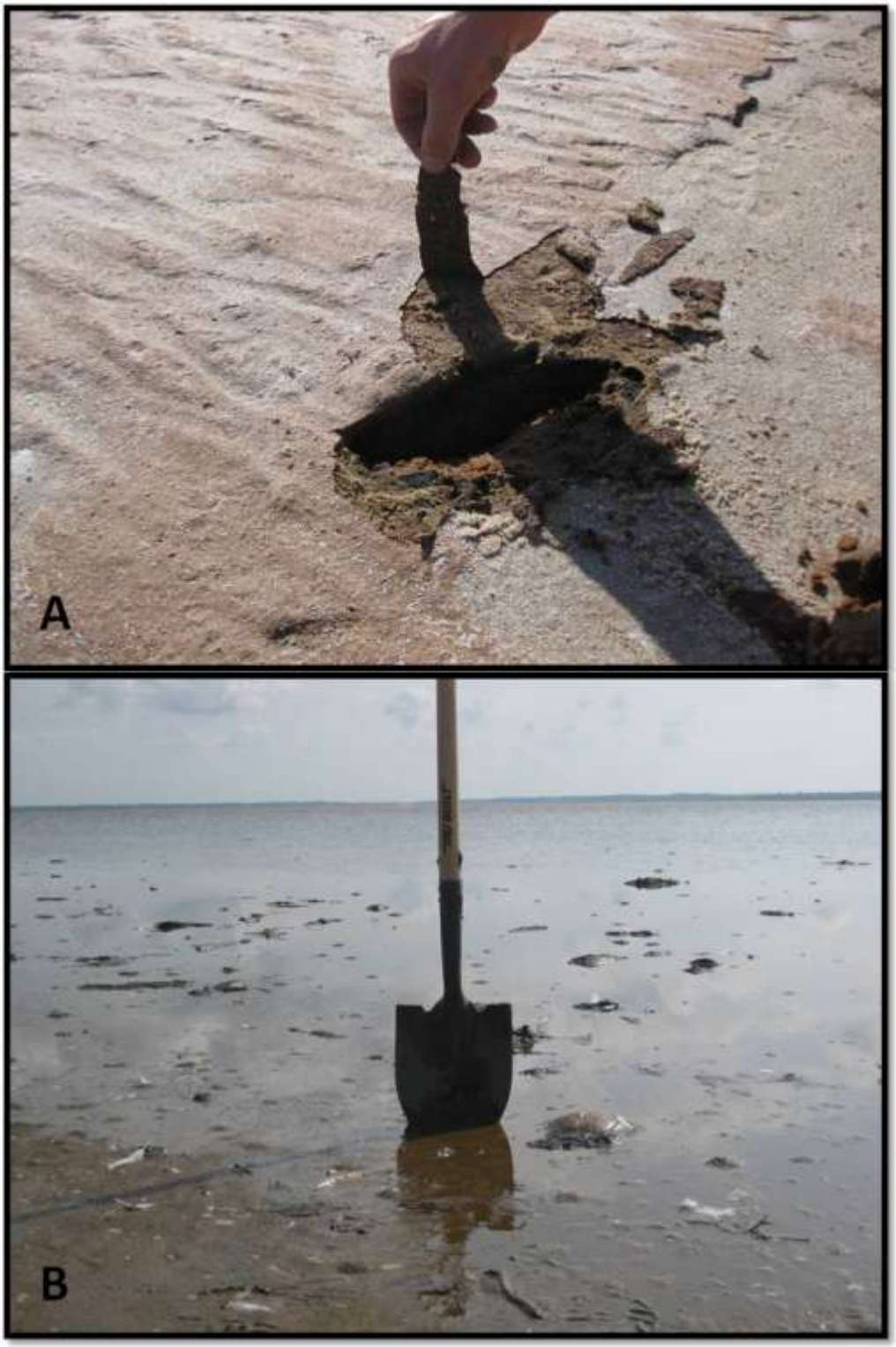

Figure 12: Algal mat. A: Proximal flood plain of the GSP channel: Salt Fork of the Arkansas River. B: Distal zone, gas dome present just to the right of shovel.

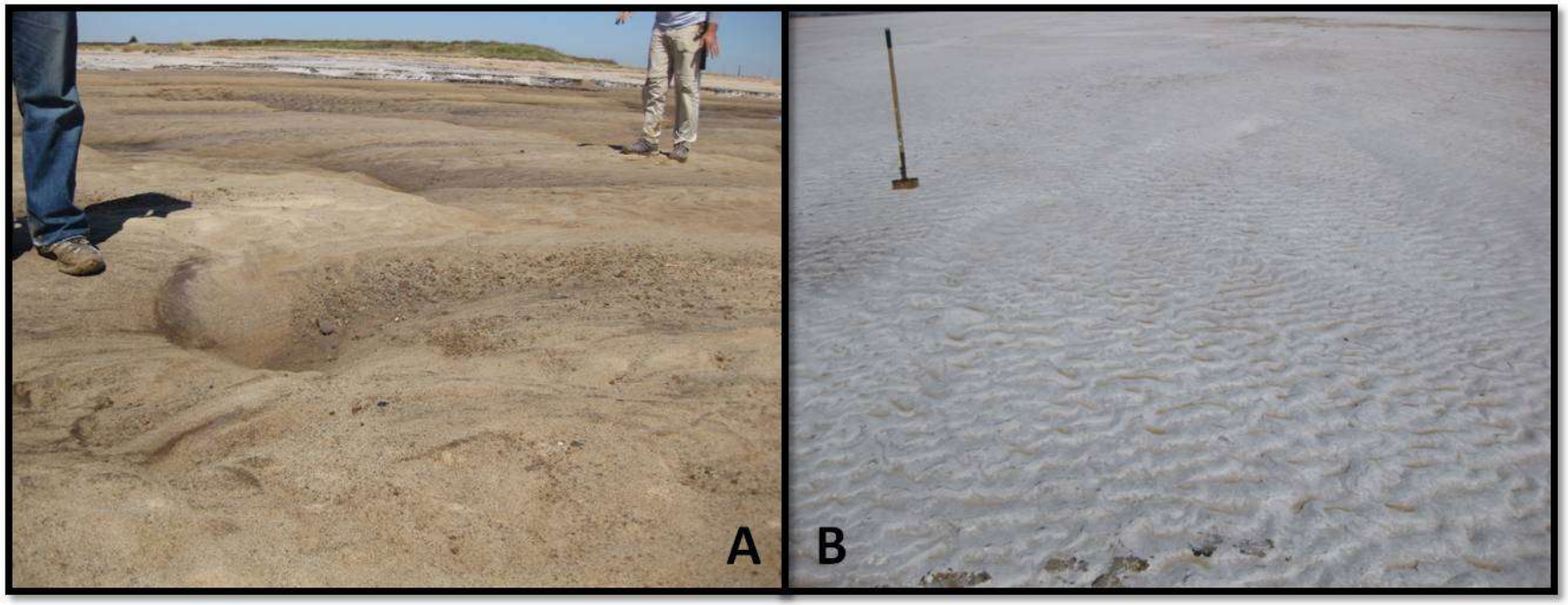

Figure 13: Reduction in the size of bedforms across the channel environment. A: Anti-dunes and transverse-catenary ripples (proximal). B: Transverse-catenary ripples downstream (distal)

catenary ripples down-stream that is much smaller in dimension: 0.5-2 cm deep, 8-20 cm wide and 2-5 cm long. Sediment is sourced from the creeks and rivers that flow onto the flats. In addition to this source, eolian processes provide a minor source from nearby dunes. Eolian processes also re-work the channel sediments in flood plains and redistribute channel sediments onto the sand flats.

Three sub-facies were identified within the channel facies: sub-facies 1 (coarse – granule sands), sub-facies 2 (fine – mud sized grains) and sub-facies 3 (medium – coarse sands). Identification of sub-facies 1 was primarily based on grain size. Sub-facies 1 is coarser material ranging from coarse-upper, to very coarse and granule size. Grain size samples from this sub-facies include: G.S. 01E & F, G.S. 03A-G and G.S. 04B-D (Figures 14-17). The mean grain size for these samples ranged from 0.5 **Φ** to 4.8 **Φ**. The bed thicknesses of this facies ranged from 20 – 50 cm. The sub-facies is tan-light brown to orange in color (Figures 18& 19). Beds are dominantly massive and structureless, and contained minor amounts of clay drapes, rip up clasts and cross bedding.

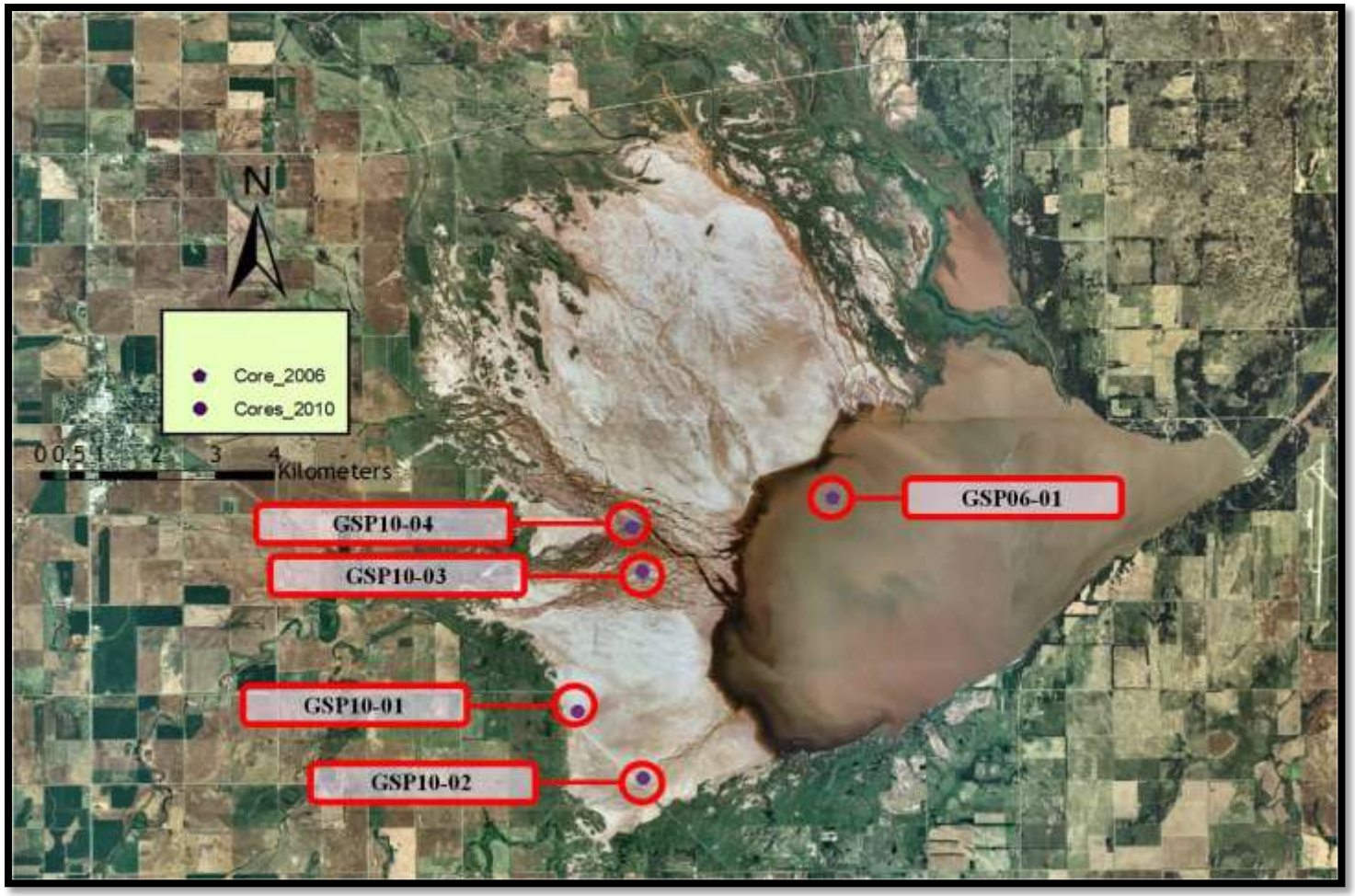

Figure 14: Vibra-core locations.

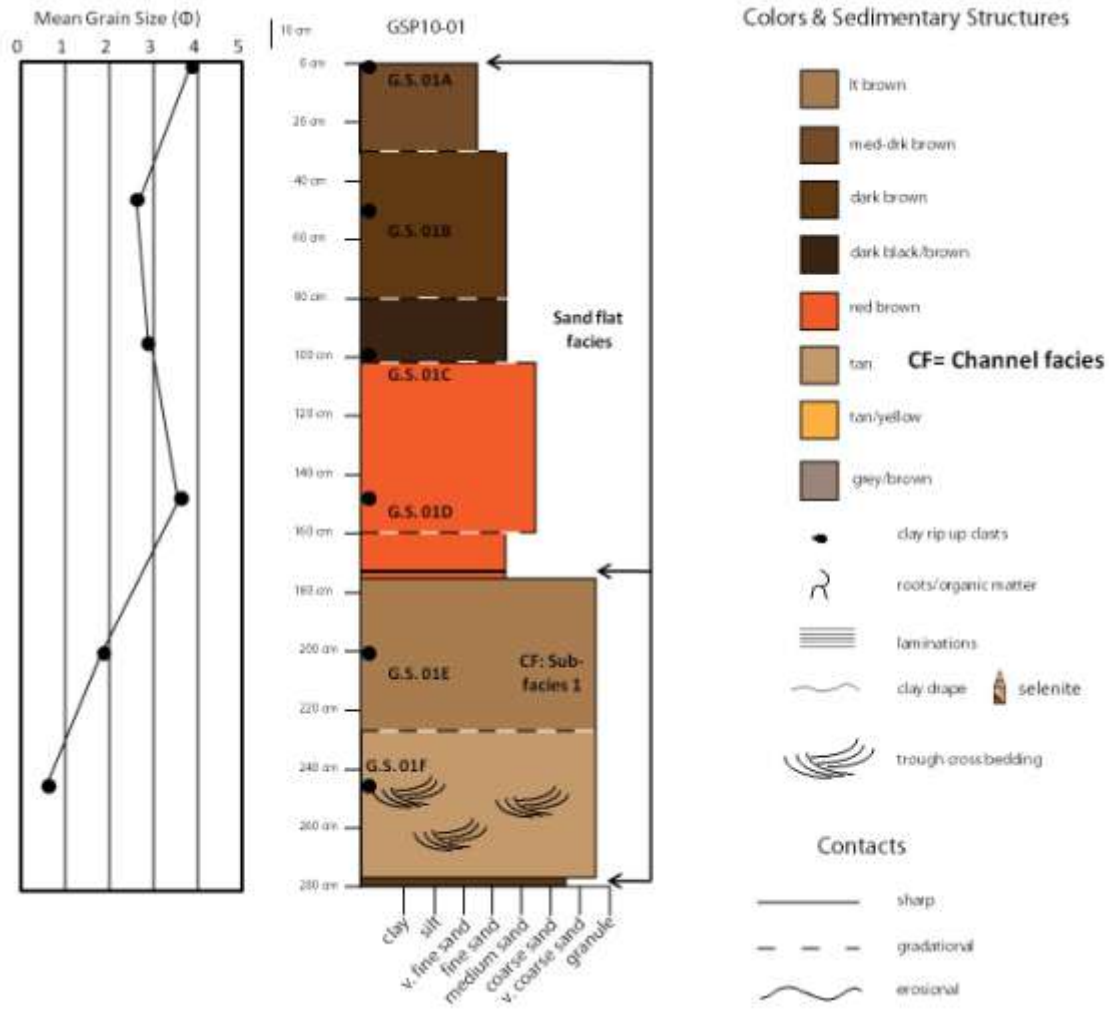

Figure 15: Core GSP10-01.

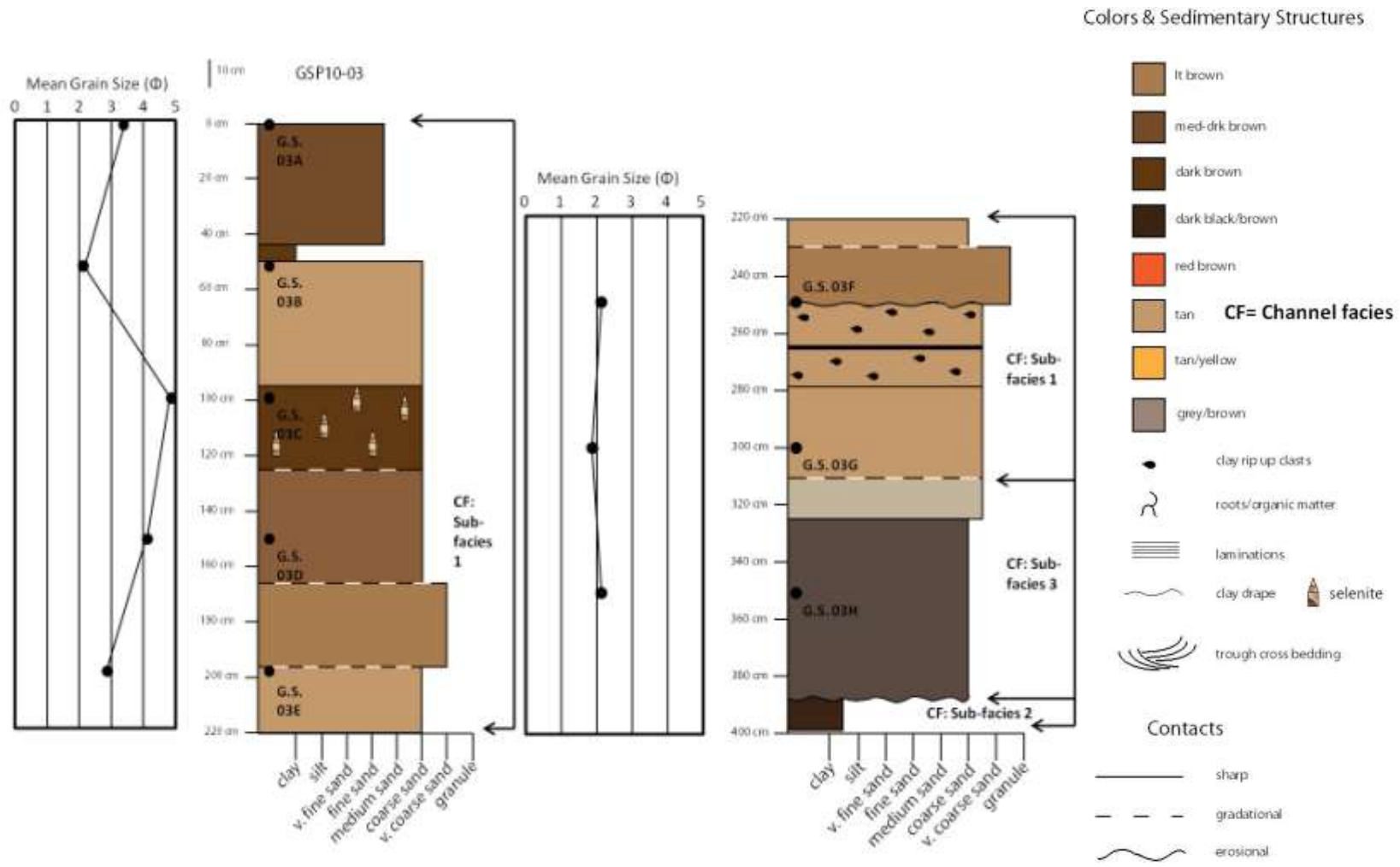

Figure 16: Core GSP10-03

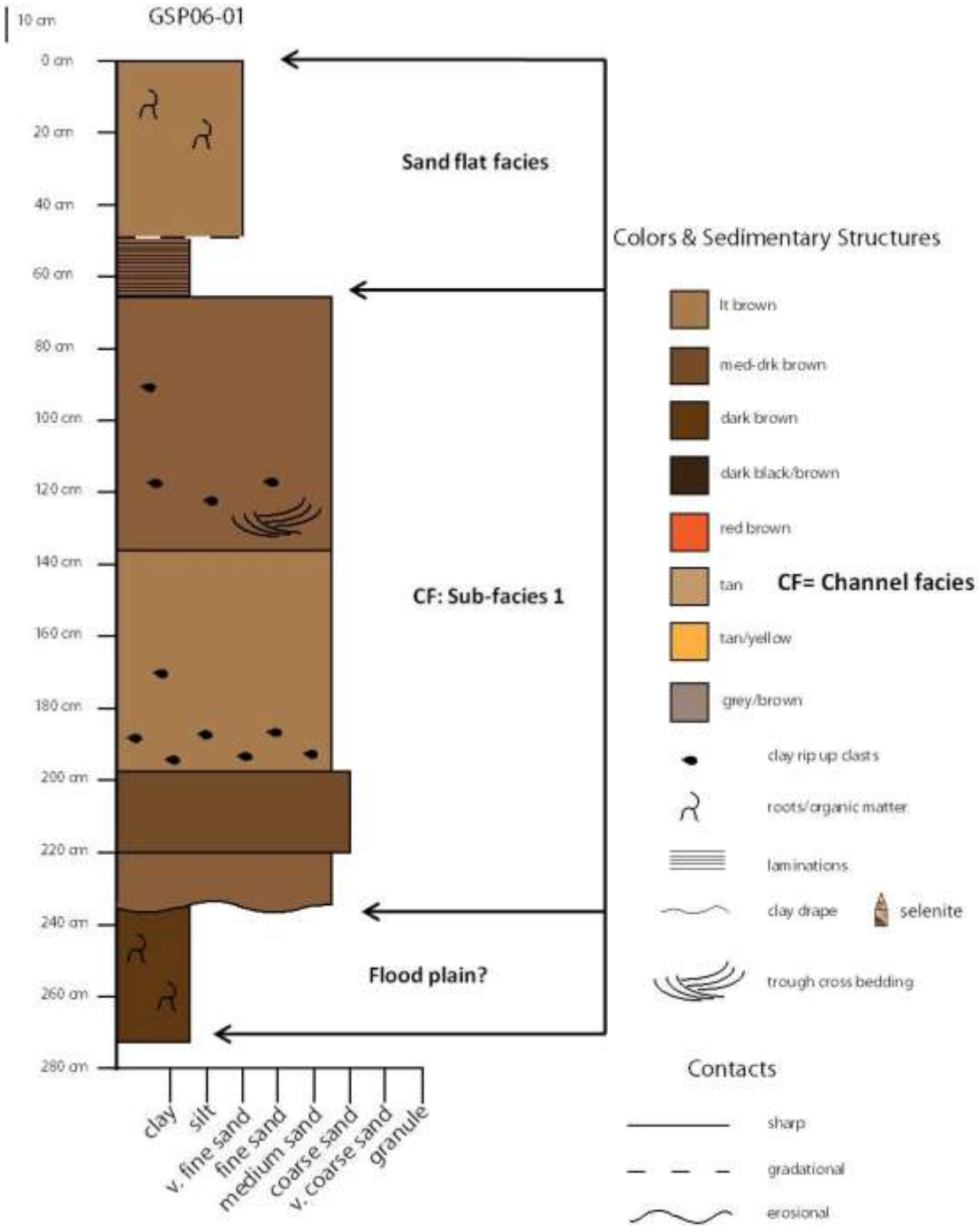

Figure 17: Core GSP06-01.

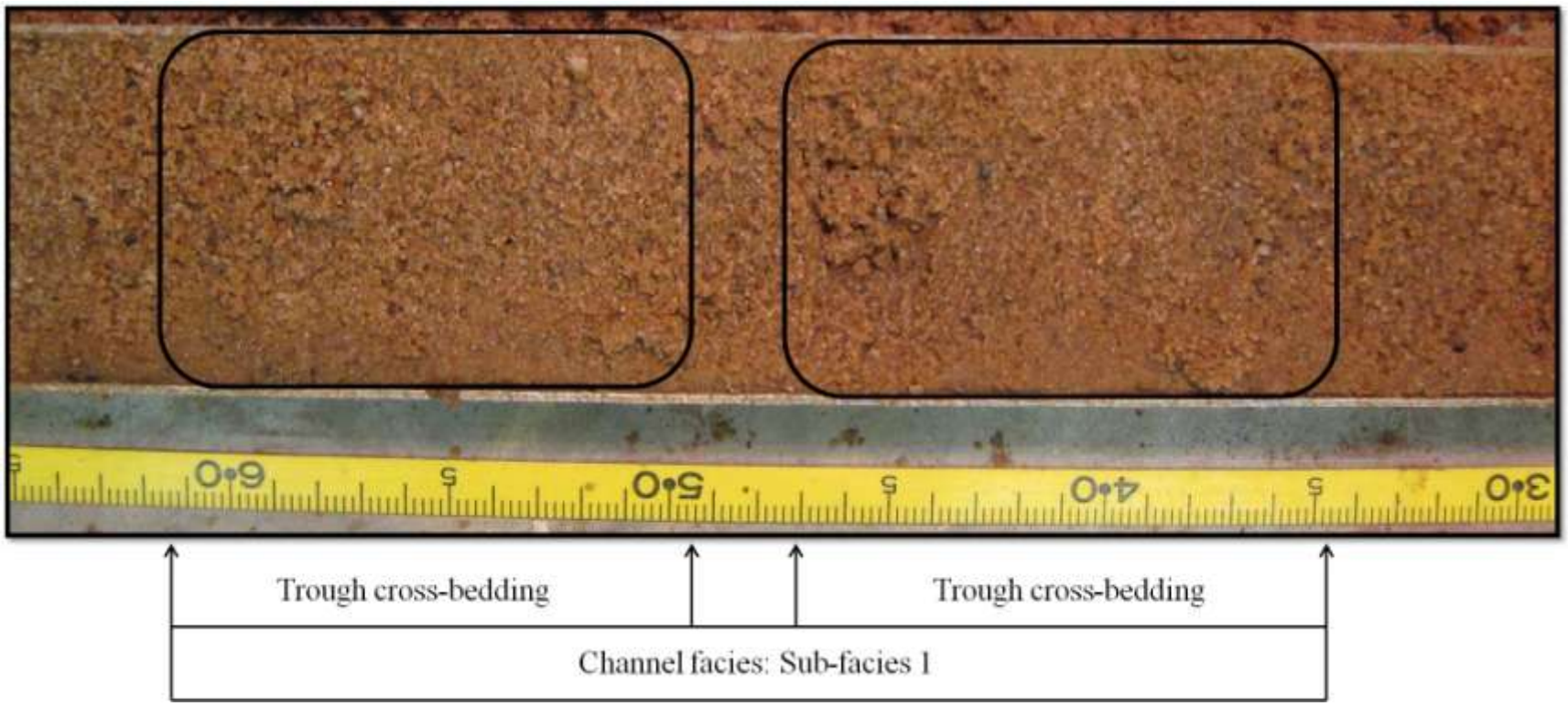

Figure 18: Trough cross-bedding in channel sub-facies 1: Core GSP10-01, 229 – 265cm.

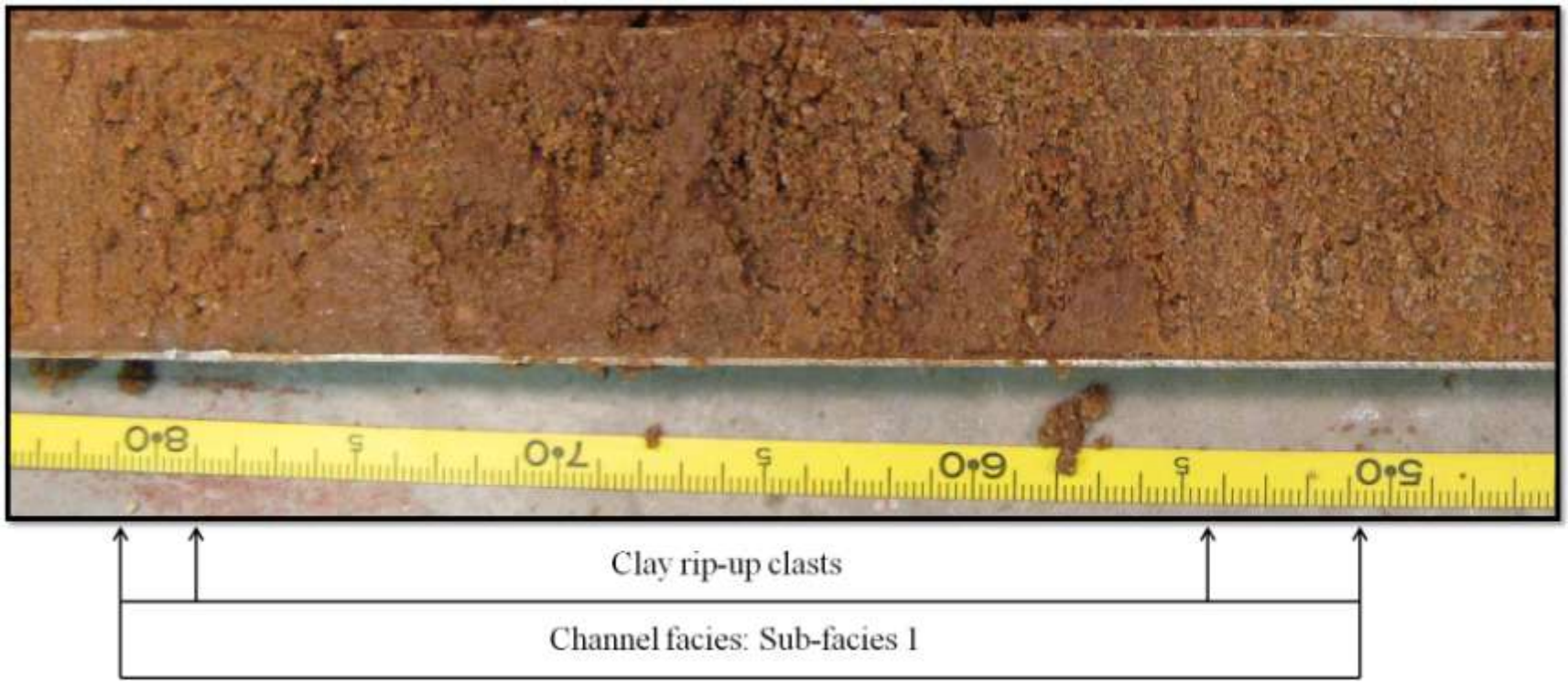

Figure 19: Clay rip up clasts in channel sub-facies 1: Core GSP10-03, 246 – 283 cm.

Sub-facies 2 contain finer grained sediments ranging from mud to fine grained sands. This facies contains the most plant fragments and trough cross bedding. Grain-size measurements taken from this sub-facies within trenches and core (Figures 16 & 21): G.S. 02 and G.S. 04-A-C had a mean grain size of 2.07 **Φ**. The color of this sub-facies is typically much darker, likely due to the higher organic content and ranges between brown-dark brown to black (Figure 22 & 23). Lighter colored sediments are found as very fine to medium sands inter-laminated with darker mud. One unique trait of this sub-facies was the thin fining upward sequences. Though most trenches and core data contain fining upward sequences, the packages of fining upward sequences within this particular sub-facies were thinner, 10-12 cm and 6-4 cm thick. Sub-facies 2 also contains horizons of precipitated selenite. When present, the selenite crystals destroyed original bedding and other sedimentary features.

Sub-facies 3 contained medium to coarse grained sands that have a distinct tan, to grey and rusty yellow color. Two grain size samples from this facies were collected from core (Figure 18): G.S. 03H and samples from trenches. The mean grain size of the samples was 2.88 **Φ**. This particular sub-facies also contained selenite horizons. However, as the bedding of this sub-facies was much thicker than sub-facies 2, precipitates did not destroy all bedding and sedimentary structures. Clay drapes and minor plant and wood fragments were often encountered within this facies, as well as flaser bedding and minor starved ripples (Figures 23 & 24-I). A repeated pattern of fining upward sequences was also found in core, but not as common as seen in sub-facies 2.

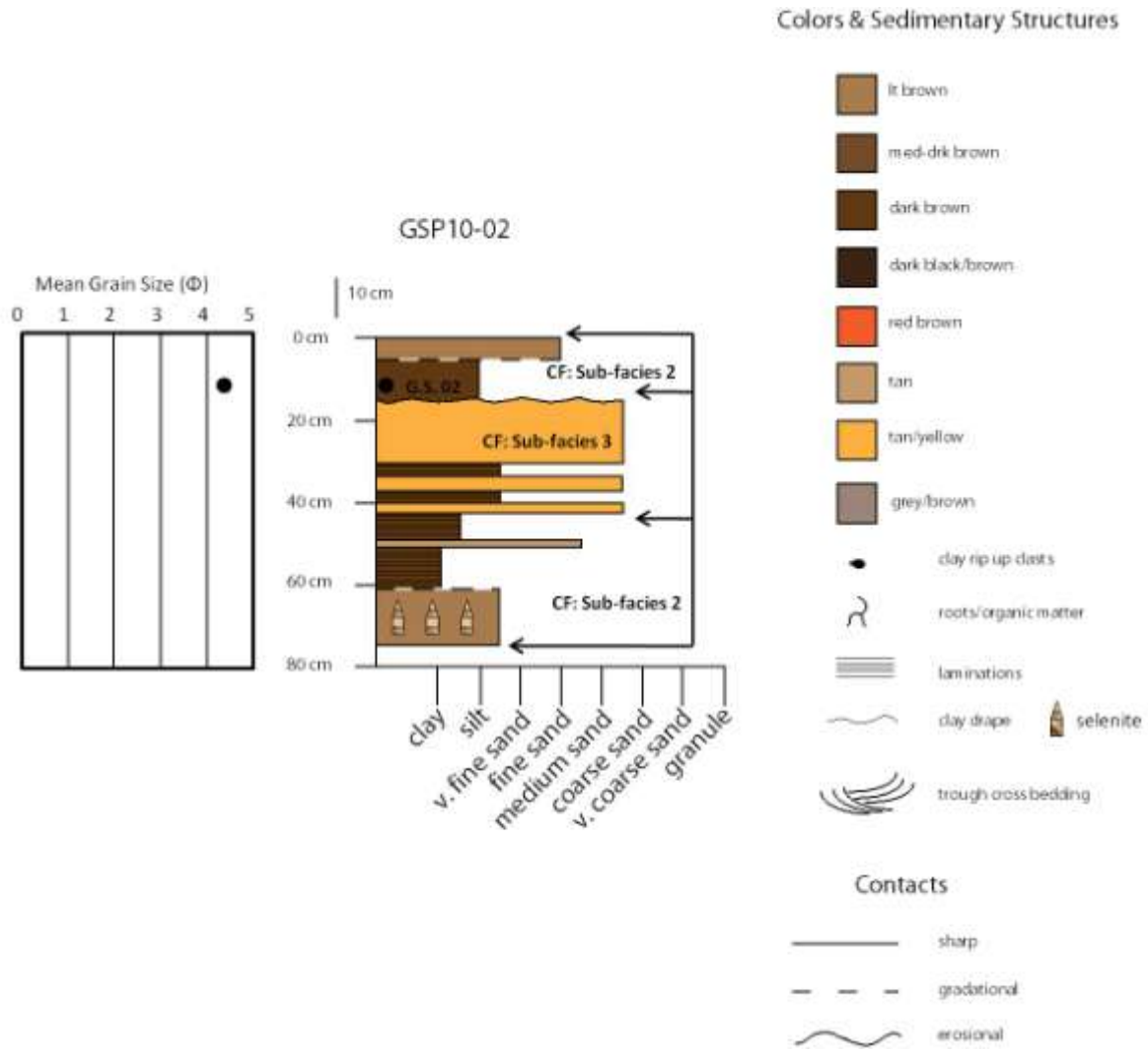

Figure 20: Core GSP10-02.

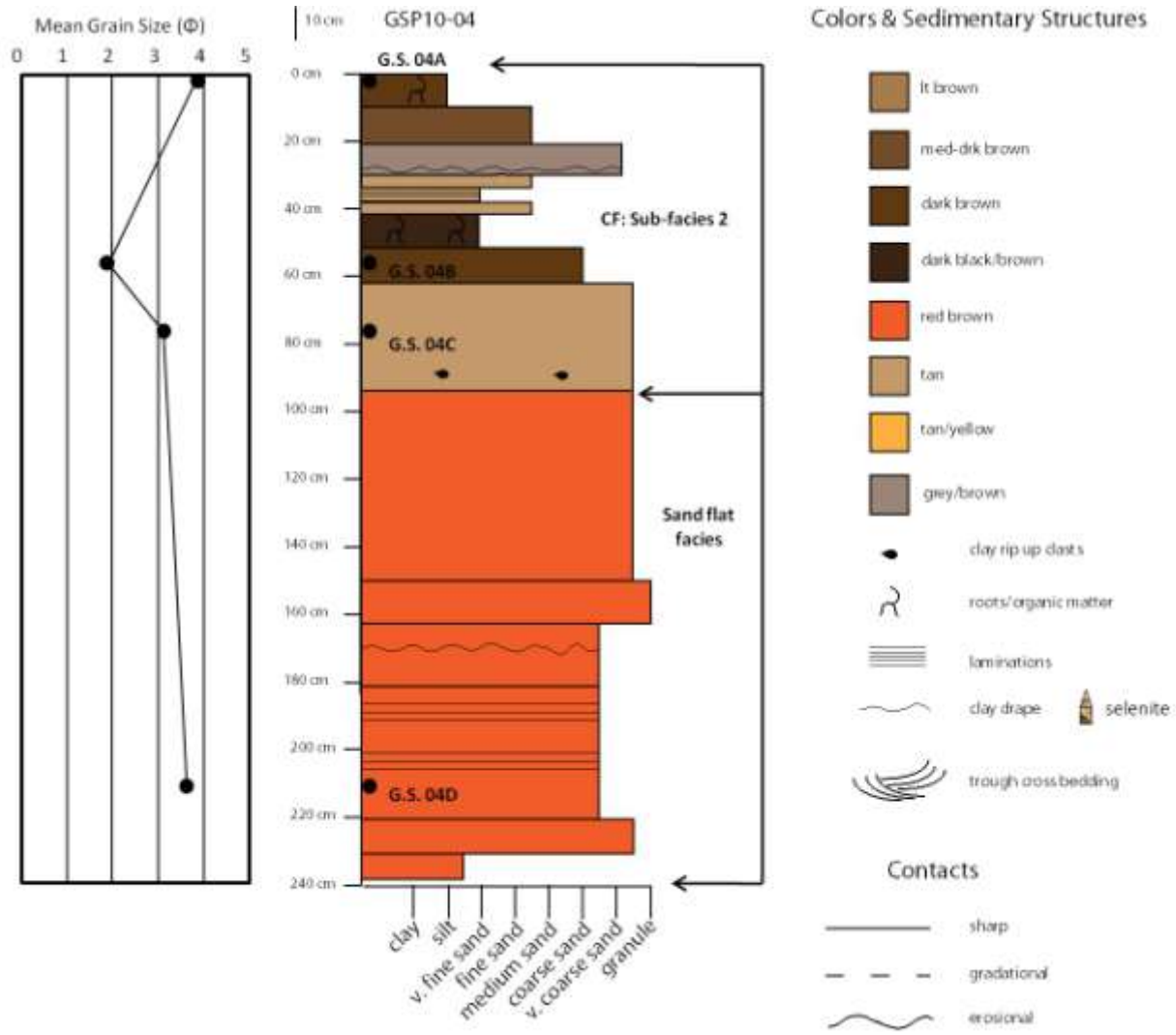

Figure 21: Core GSP10-04.

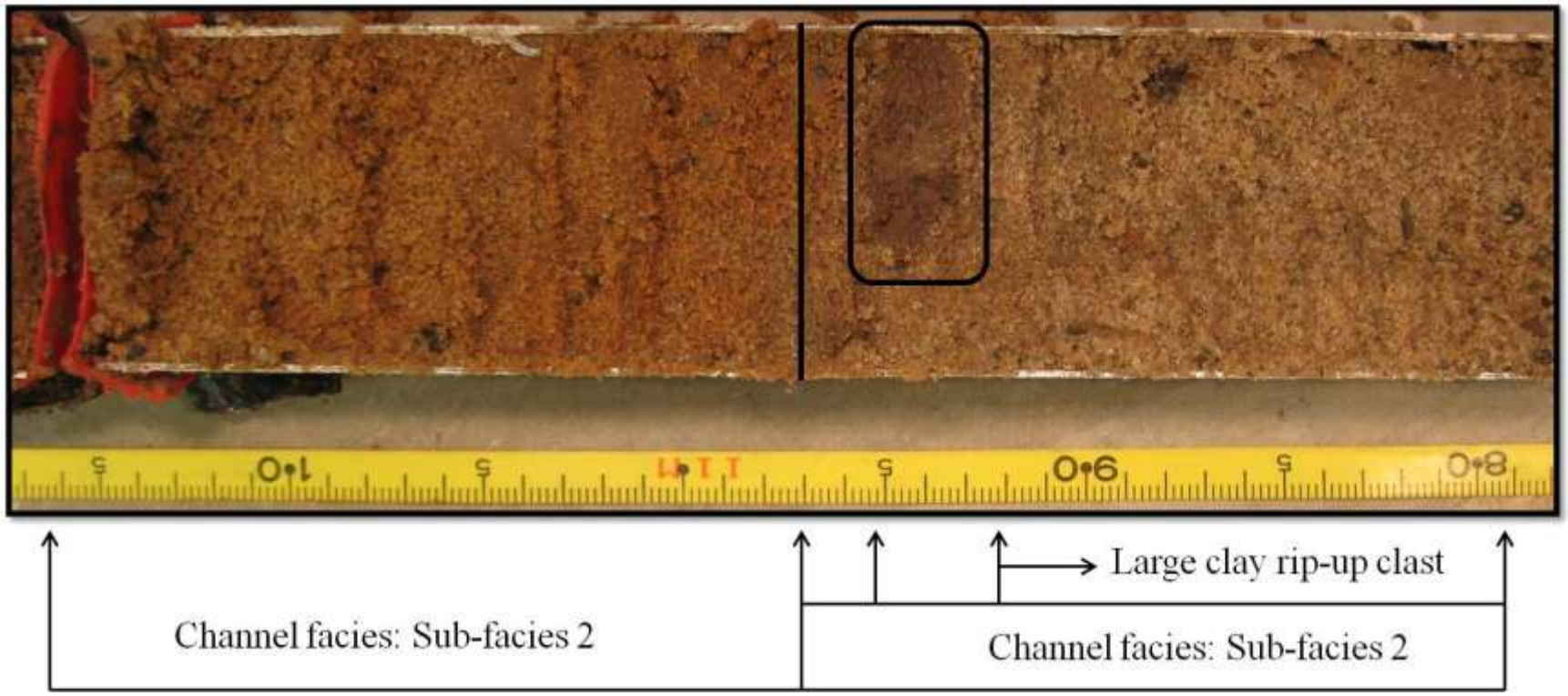

Figure 22: Channel sub-facies 2: Core GSP10-04, 78 cm – 105 cm.

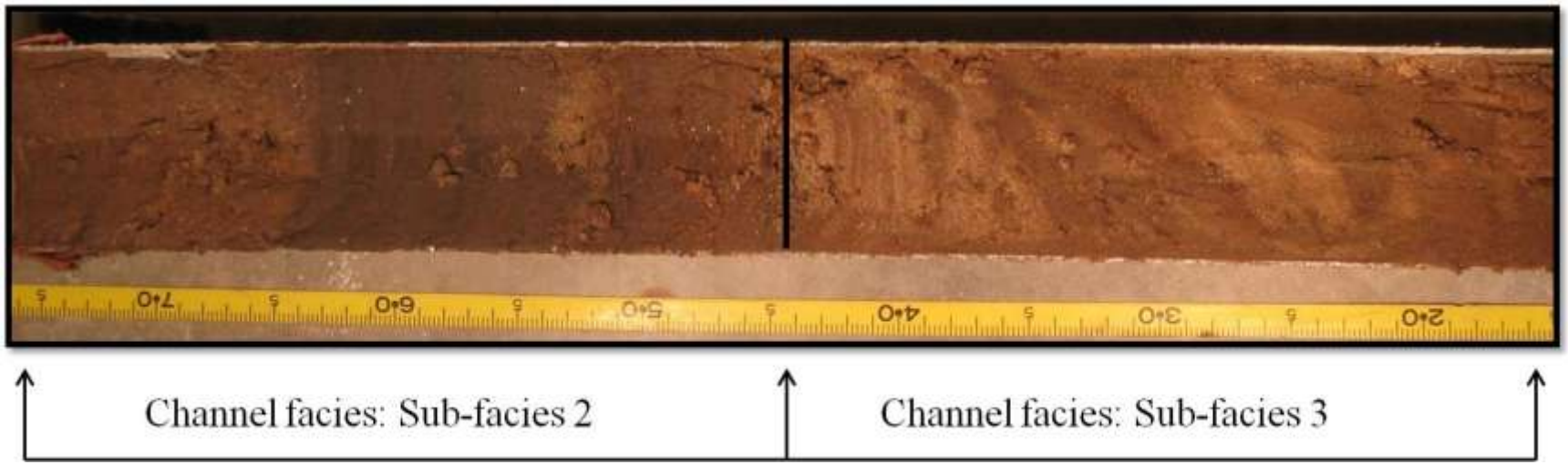

Figure 23: Contact between sub-facies 3 & 2, selenite precipitation from 64 – 74 cm and sand to silt laminations 35 – 44 cm: Core GSP10-02, 15 cm – end of core (74cm).

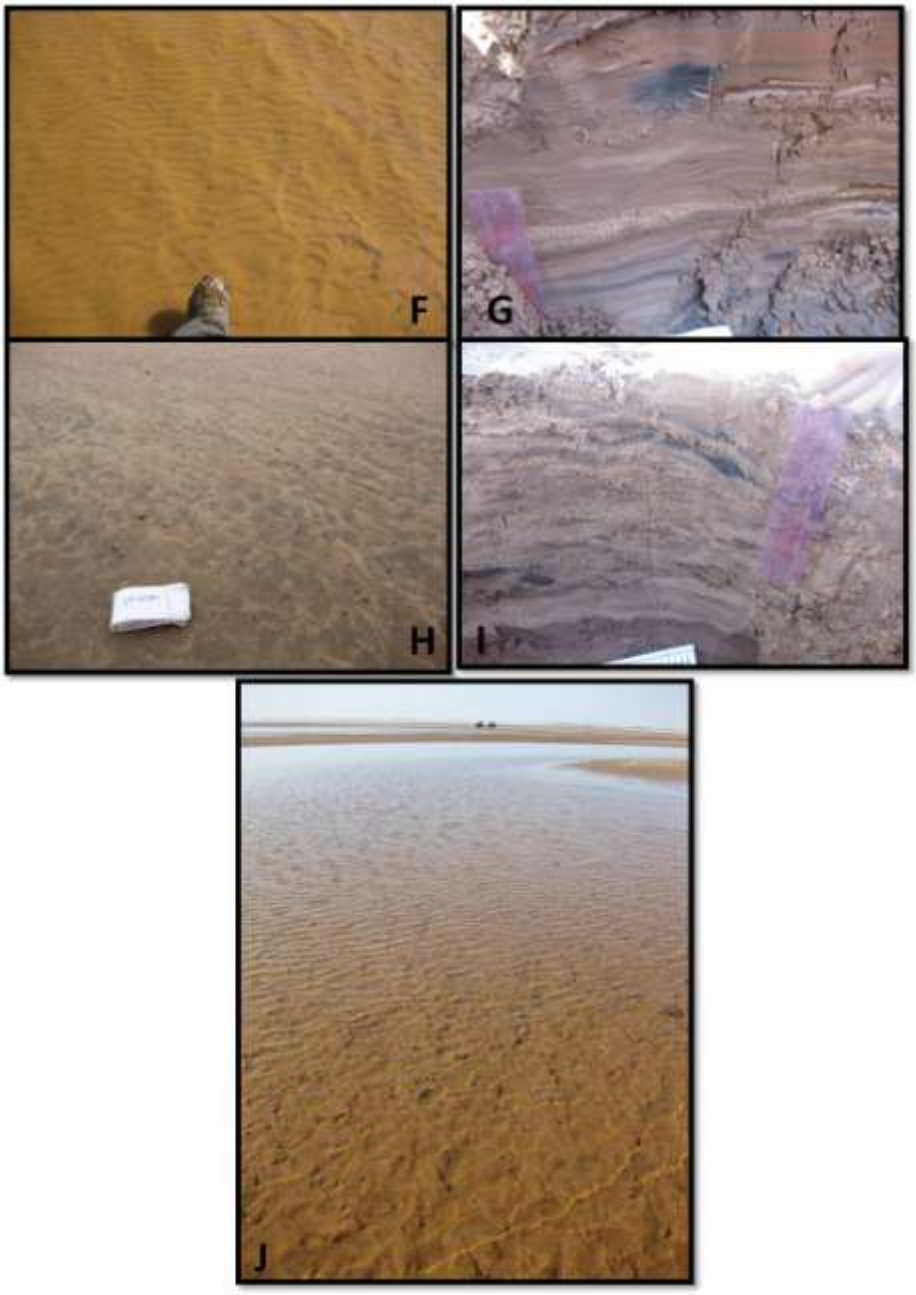

Figure 24: Facies. F: Oscillation ripples in delta of the Salt Fork of the Arkansas. G: Sand, silt and clay lamination with clay layer, within channel facies transitioning from medial to distal sub-environments H: Swept catenary ripples of the sand flat environment post flooding stage transitioning into evaporation-concentration stage. I: Flaser bedding and organic matter fragment within channel sub-facies 3. J: Reworked asymmetrical ripples in delta of the Salt Fork of the Arkansas River.

Sediment traps ST09-01, 02, 05, 08 and 09 were deployed within the channel environment. Table 1 gives the textural characteristics of the sediments captured in the traps. These traps contained moderately to well sorted fine to coarse grained sands. Table 2 shows the total mass accumulation for each trap. Traps ST09-01A and 08A retained the highest mass of sediments over the two week period, with 49.17 g and 49.76 g, respectively. However, over a 2 month period, traps ST09-06B and 08B had the highest mass accumulation rates with 265.69 g and 134.76 g, respectively (Figure 25). Locations for all sediment traps are depicted in Figure 26.

Sand flat

The sand flat environment is one of the most widespread and covers most of the modern surface of the GSP. It is a broad nearly flat and featureless plain with a gentle lake-ward dip. The facies comprising the deposits of these environments consists of dark brown-black to light brown fine to medium sand (Figure 27). This facies had samples collected from trenches and core: (Figures 15 & 21) G.S. 01 A-D and G.S 04 D; a mean grain-size of 3.1 **Φ** and a mean moment skewness of 2.10 **Φ** and a mean moment standard deviation of 1.55 **Φ**. At the surface this environment exhibits: transverse-catenary ripples, oscillation ripples (cross hatched pattern), isolated pools, concentrated selenite precipitates, syneresis cracks, flood wash lag deposits, obstacle scours, linguoid ripples, adhesion structures (Figure 28), dead wood debris, anthropogenic debris, efflorescence surfaces (Figure 28-E) and sand filled troughs. Some of the surface features seen in Figure 21 are defined as evaporitic-adhesion structures that form with surface salt growth (Kocurek & Fielder, 1982, Olsen et al., 1989). Ripples form when windblown sediment adheres to a moist surface and adhesion ‘warts’ form when moisture is lost by the upwind migration of small protuberances on the adhesion ripples (Olsen et al., 1989).

Trenches through this environment revealed: parallel laminae, rip up clasts, plant fragments, ripple cross lamination, flaser bedding, lenticular bedding, clay layers, black organic

Two (2) Weeks: 09/27/2009 - 10/09/2009					
	Field		Lab		
Sample	**Grain size**	**Texture**	**Mean Φ**	**Std Deviation Φ**	**Skewness Φ**
ST09-01A	mU	ms, sub-r	2.397162117	1.754893681	1.906094157
ST09-02A	mL	ws, w-sub r	2.817628073	1.087317508	2.658311237
ST09-03A	mL	ws, wr	2.662444913	1.239367373	0.164537934
ST09-04A	cU	ms, sub-r	3.433998443	1.455942083	1.484771696
ST09-05A	mL	ms, sub-r	2.540224864	0.912253122	3.65205228
ST09-08A	fL	ws, wr	3.380176982	1.182240715	2.221694365
ST09-09A	cL	m-ps, sub-r sub ang	1.76202127	1.287218807	1.529093195
lost 07a and 06a					

Two (2) Months 10/09/2009 - 12/10/2009					
	Field		Lab		
Sample	**Grain size**	**Texture**	**Mean Φ**	**Std Deviation Φ**	**Skewness Φ**
ST09-01B	mU-cL	ms, r-subr	2.189956177	1.425664623	2.583017518
ST09-03B	mL	ms, r	3.643515549	1.831985021	1.219313596
ST09-04B	cU-vcL	ps, ang-wr	3.456884658	1.513022871	1.381911332
ST09-05B	cL	ms, r-subr	2.759644665	0.984648664	3.154342831
ST09-06B	cL	ms, r-subr	2.531230393	0.912799187	3.624153099
ST09-08B	mL	m-ws, wr	3.086824406	1.12988638	2.793277841
lost 09b, 02b, and 07b					

Table 1.

Field Legend				
Grain size		mm	Texture	
vcU	Very coarse upper	1.41 - 2.0	ws	well sorted
vcL	Very coarse lower	1.0 - 1.41	ms	moderately sorted
cU	Coarse upper	0.71 - 1.0	ps	poorly sorted
cL	Coarse lower	0.5 - 0.71	wr	well rounded
mU	Medium upper	0.35 - 0.5	sub-r	sub rounded
mL	Medium lower	0.25 - 0.35	ang	angular
fU	Fine upper	0.177 - 0.25		
fL	Fine lower	0.125 - 0.177		
vfU	Very fine upper	0.088 - 0.125		
vfL	Very fine lower	0.062 - 0.088		

Mass Accumulation Rates					
Two (2) weeks	Mass Accumilation (g)	Rate (g/day)	Two (2) months	Mass Accumilation (g)	Rate (g/day)
ST09-01A	49.17	3.51	ST09-01B	94.87	1.51
ST09-02A	6.49	0.46	ST09-02B	N/A	N/A
ST09-03A	18.41	1.31	ST09-03B	50.51	0.80
ST09-04A	7.64	0.55	ST09-04B	121.14	1.92
ST09-05A	21.12	1.51	ST09-05B	64.72	1.03
ST09-06A	N/A	N/A	ST09-06B	265.69	4.22
ST09-08A	49.46	3.53	ST09-08B	134.76	2.14
ST09-09A	5.05	0.36	ST09-09B	N/A	N/A
* ST09-07A & 07B lost both periods					

Table 2.

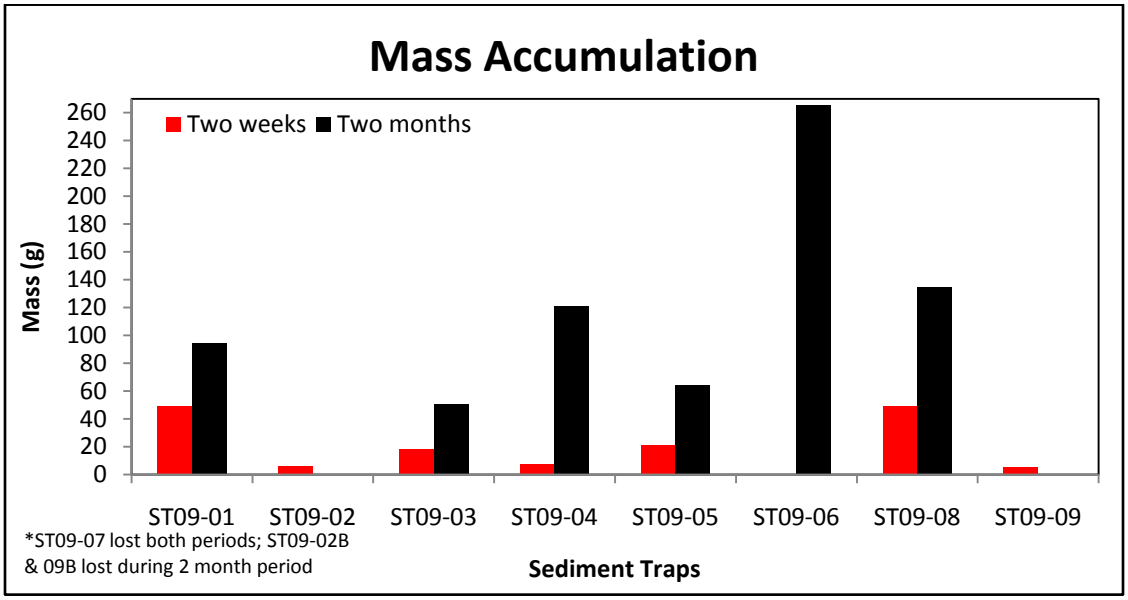

Figure 25: Mass accumulation results for sediment traps.

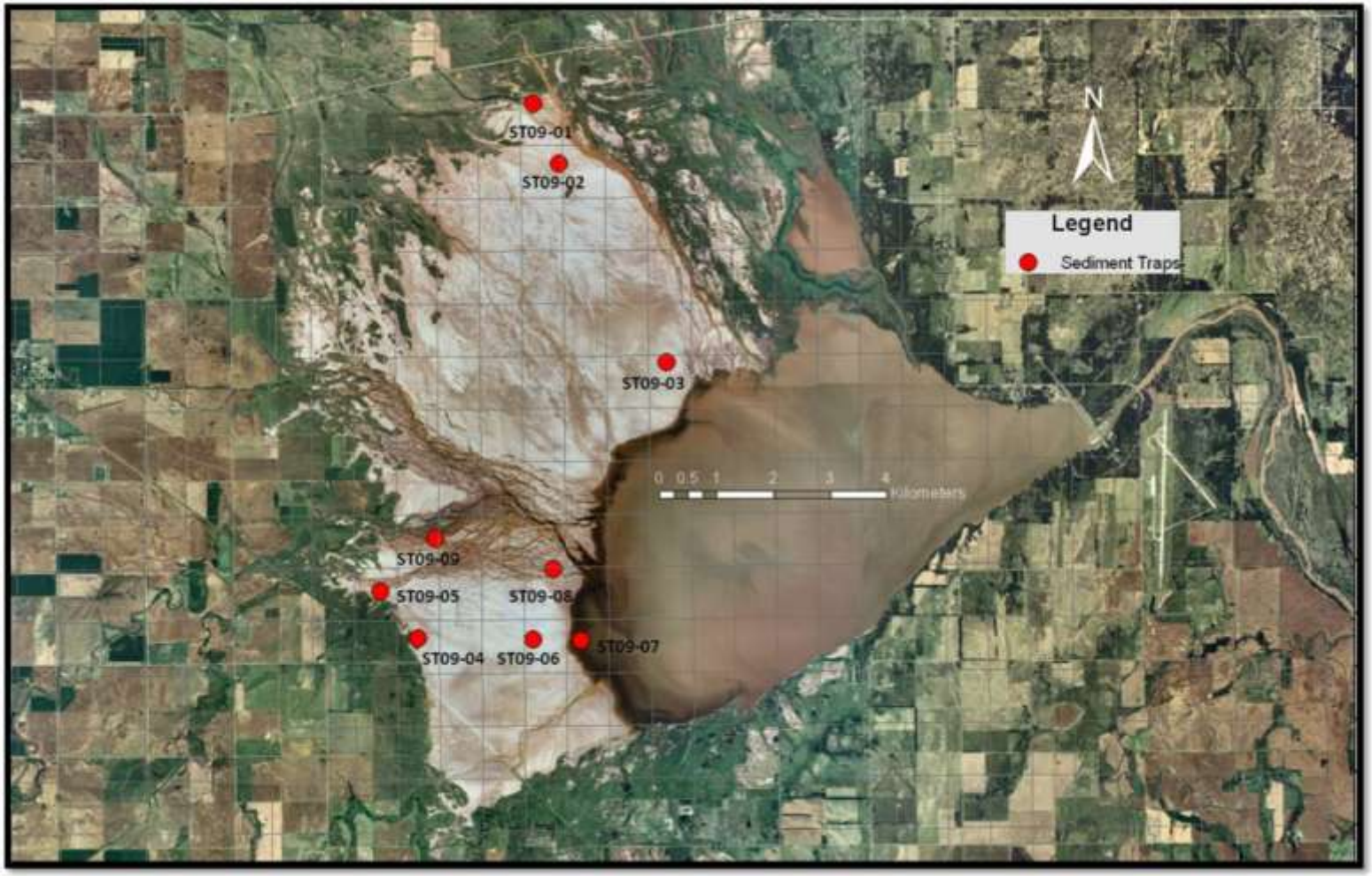

Figure 26: Sediment trap locations.

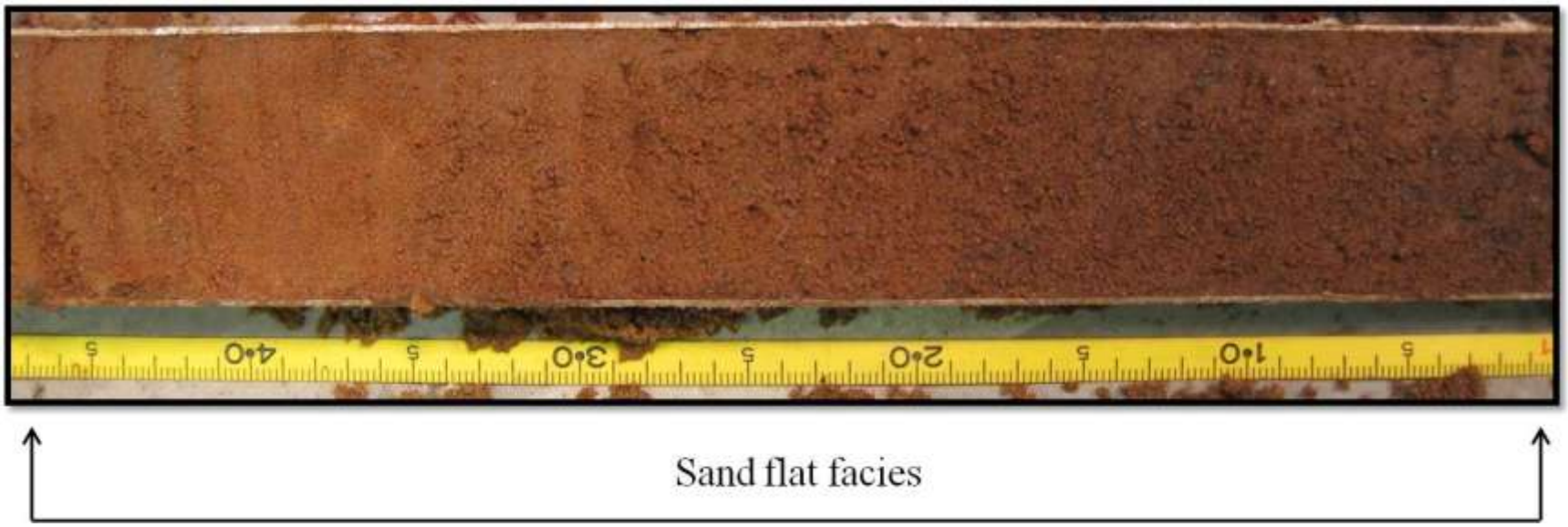

Figure 27: Sand flat facies: Core: GSP10-01, 100 cm – 147 cm.

Figure 28: Sand flat bedforms & surface features. A: Adhesion structures, gas escape pores. B: Raindrop imprints. C: Adhesion structure, ‘warts’. D: Adhesion textured surface; ripples. E: Efflorescence surface.

rich sands and isolated sand lenses. Sediment sources for the sand flat facies included both eolian and fluvial processes.

Sediment traps ST09-03, 04 and 06 were located in the sand flat environment. For the 2 month deployment, trap ST09-06B had the highest mass accumulation rates and the third highest was trap ST09-04B with 265.69g and 121.14g, respectively (Tables 1 & 2, Figure 25). The second highest mass accumulation rate was trap ST09-08B with 134.76 g. It was located in the channel environment in close proximity to the sand flat, and channel environment boundary. Field observations did reveal that some debris such as grass and plant fragments were caught in trap 06B, which probably aided in capturing sediments leading to higher mass accumulation rates.

Mud/Algal flat

The algal mat/mud flat environment closely resembles the surface morphology of the sand flat environment. Finer grain sizes distinguish the facies deposited within this environment from the sand flat facies as does the presence algal mats. Mean grain size for this facies was a 3.22 **Φ.** The moment standard deviation is 1.03 **Φ** and the moment skewness is 2.85 **Φ**. Sedimentary structures are not as well preserved or developed in comparison to the sand flat facies. However, some sedimentary structures such as ripples can be found. The algal mat environment is only found along the reservoir shores and thus is an anthropogenic environment. The extent of the mud/algal flat facies is subject to the extent of water levels within the reservoir. One sediment trap was placed in the mud/algal flat environment, ST09-07; however, in both the two week and two month deployments, it was washed away (Figure 29). This was probably due to the wave action along reservoir shoreline. Any precipitation on the flats would cause the reservoir to transgress rapidly as the slope of the GSP is extremely shallow. During the 2 week deployment (9/27/2009-10/09/2009) one substantial rainstorm occurred which most likely removed the sediment trap. A cold front passed through and delivered 2.4 inches of rain within a

Figure 29: Sediment trap ST09-07, post 2 month deployment during retrieval.

24 hour period on 10/08/2009. Just one day prior to the sediment trap's extraction. During the two month deployment, multiple storms occurred, which undoubtedly removed the trap again.

Delta

Each of the fluvial systems entering the GSP produced a delta. However, this feature is not related to the GSP, but created by the man-made Great Salt Plains Reservoir. Collecting subsurface data in the delta front and prodelta environment proved difficult as it was submerged during the time of this study. However, slowly using a shovel to scoop up a layer at the surface provided some useful observations (discussed in Ch 5). Ripples were observed in the shallow depths of the reservoir in the delta from environment, from oscillation, transverse, linguoidal, and reworked asymmetrical ripples. These features are created by the reservoir wave action as the fluvial systems terminate into the waters.

Dune

Inactive dunes are present in the GSP extending from north to south along its western perimeter. These dunes were observed to act as a source of the surface deposits found on the sand flats on several occasions. The dunes are 10-30 m wide, 25-100 m long and 2-5 m high (Figure 30). The sands within the dunes are much coarser than the sands encountered in the medial and distal portions of the channel facies and across much of the sand flat facies area.

Figure 30: Vegetated dunes, lining the western perimeter of the GSP.

Subsurface observations

Vibra-cores

Five vibra-cores were used to document the stratigraphy of the modern the GSP. Two cores were collected along ERI – Sting lines, one from Spring Creek, one from the Clay Creek system and one from the sand flat near the Salt Fork (Figure 14). Core descriptions are shown in Figures 15-17, & 20, 21. The fifth core was collected prior to this research in 2006 and was used to constrain the subsurface stratigraphy of the northern portion of the GSP. The cores were helpful for determining the facies architecture of the GSP. In general, the three cores collected in the current channel facies environment, cores GSP10- 02, 03 and 04 demonstrated 20-200 cm cycles of fining upward sequences and coarsening upward sequences. Core GSP10-04 contains 1 meter of channel sub-facies 3 overlaying approximately 1.5 m of sand flat facies deposits. This particular core was collected at the confluence of Clay Creek and Cottonwood Creek systems. The presence of the sand flat facies within 1 m of the surface suggests that these two systems have not always coalesced in this location suggesting the systems are prone to avulsion. GSP10-01 was collected in the modern sand flat environment with 1.75 m of sand flat deposits overlaying a little over 1 meter of channel deposits.

Geophysics

An AGI SuperSting was utilized for identifying potential paleo-channels. Aerial photography was used to determine a location without the surface expression of a modern or recent channel avulsion. Seven ERI lines were acquired, seven of which were located in the area free of recent fluvial channeling and one was collected across an active channel of Clay Creek. Five of the seven ERI lines collected across the sand flat aligned parallel to one another from west to east (Figure 31). These lines are GSP02NA, 04NA, 05N, 06N and 07N. All of the 5 ERI lines demonstrated similar visual signatures at the same depths and locations across their respective array, however, GSP02NA demonstrated the clearest signatures. ERI line GSP02NA shows a package approximately 1.75 m thick of a green less conductive unit overlying a 1 m thick unit of red/orange more conductive materials (Figure 32). Another less conductive horizon is seen just below the red/orange more conductive material and is approximately 5-8 meters thick. The bottom unit is blue and even less conductive than any of the overlying units and ranges between 7-10 m in thickness.

The criteria used to identify potential channels were based on the sedimentological/electrical conceptual model shown in Figure 32 (Halihan). The interpreted channel is thought to be electrically more conductive due to the relatively larger pore spaces present then in coarser grained channel deposits compared with over bank-mud flat deposits. This allows for the interpreted channel deposits to have an electrically more conductive signature in-cased by electrically less conductive over bank-mud flat deposits. The conductivity average of the 5 ERI lines show robust deviations in the two locations that line GSP02NA exhibits the isolated signatures. This suggests that these paleo-channels are potentially continuous (Figure 31). The bulk average of the 5 ERI lines (Figure 33) is the horizontal hashed line and illustrates the points at which the robust kicks of the interpreted channels deviate from the average

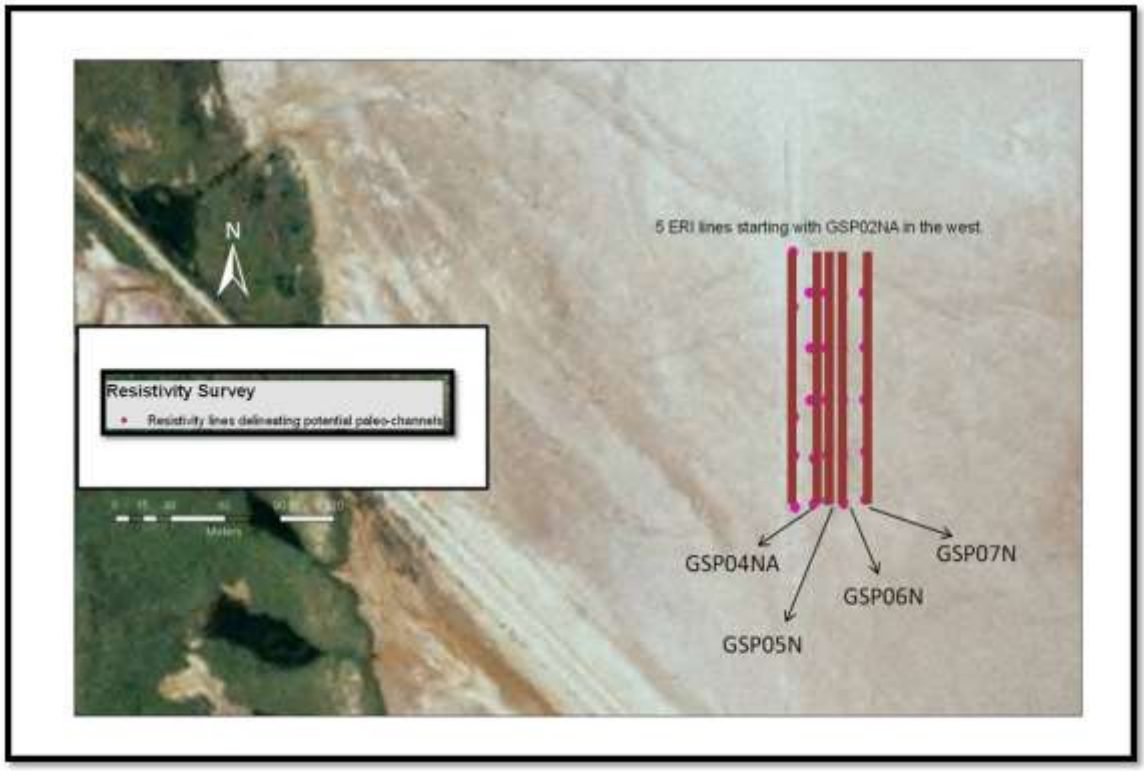

Figure 31: Zoomed in area of ERI lines with channel signature, beginning with GSP02NA (Figure 32).

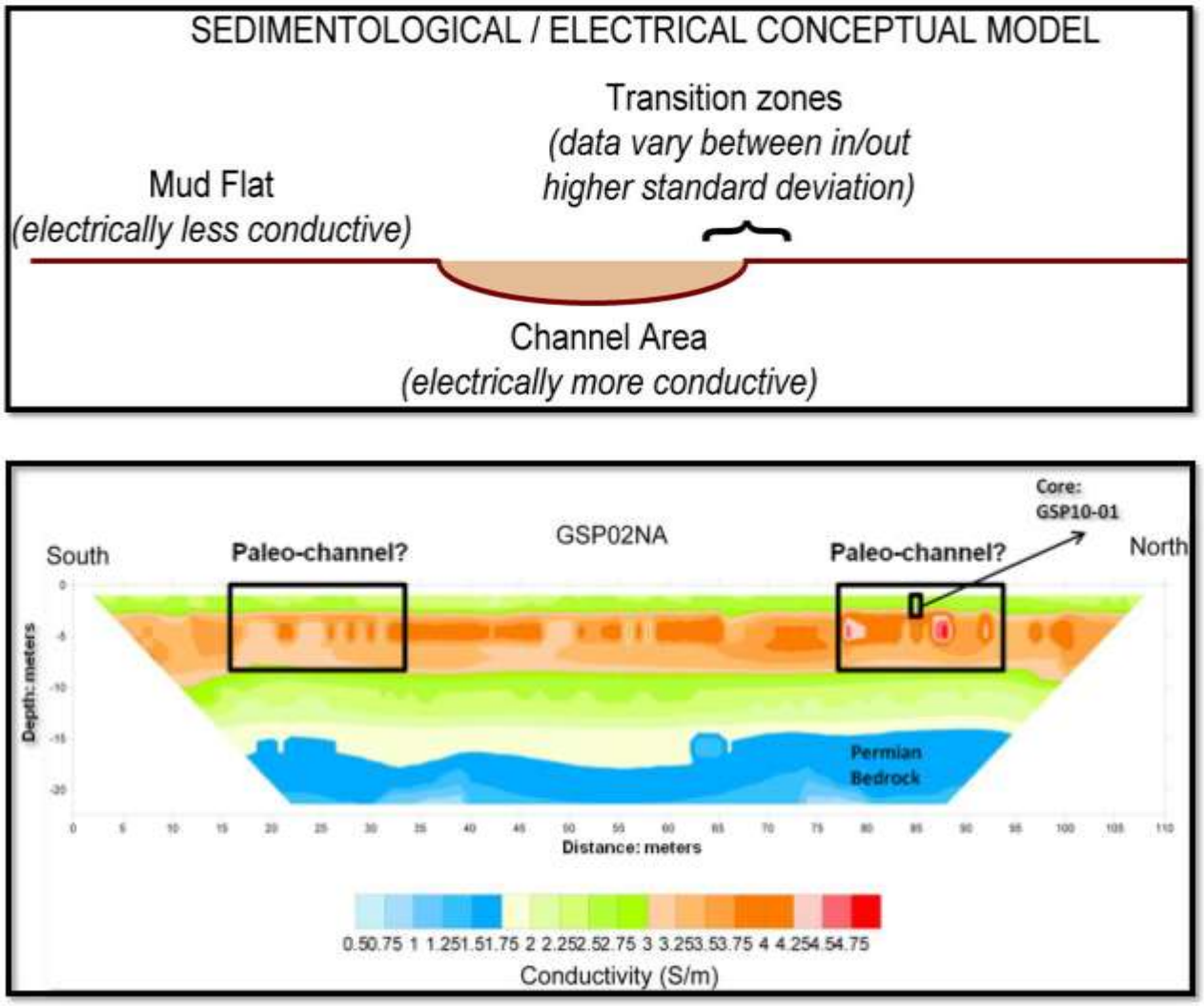

Figure 32: Conceptual channel model (Halihan) and ERI line GSP02NA.

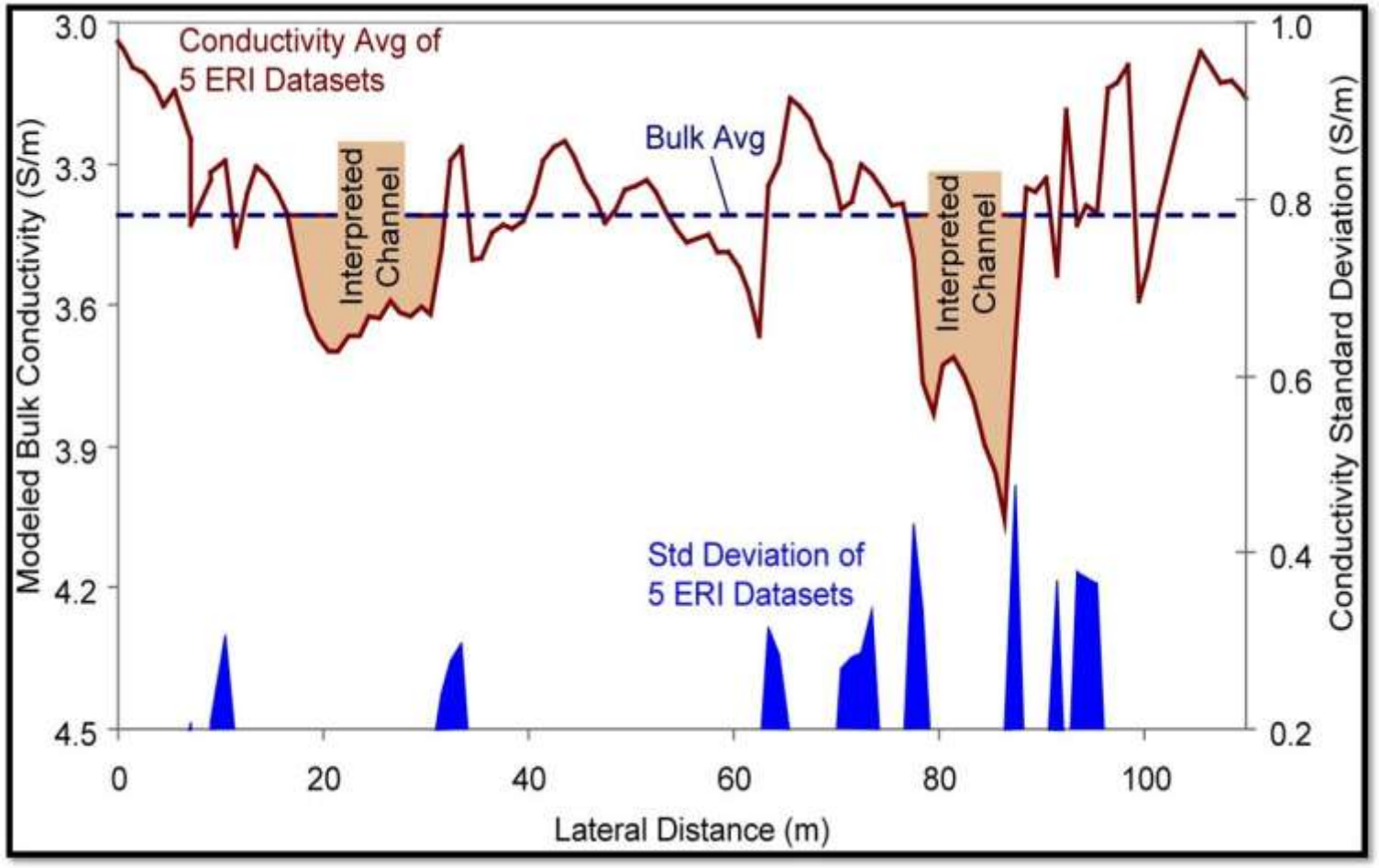

Figure 33: Conductivity results of 5 ERI lines, showing two potential paleo-channels.

(highlighted). Additionally, the standard deviation is plotted at the bottom with its values along the right y-axis. This reaffirms the robust deviations of the interpreted channels as they are both bounded by areas exhibiting relative increases in standard deviations.

The upper 1.75 m green less conductive unit is interpreted as sand flat deposits overlying 5-6 m of a red/orange more conductive unit of channel deposits. Approximately 0.6 – 1 m of the potential channel deposits are captured in core GSP10-01 (Figures 14 & 15). Underlying the red/orange more conductive potential channel deposits is another green less conductive unit 5-8 m thick and is interpreted to be either sand flat deposits or normal fine-grained floodplain deposits of the Salt Fork of the Arkansas River. The bright blue lower 7 – 10 m less conductive unit is interpreted to be the Permian bed rock that is much more consolidated than the overlying deposits and thus, much more resistive. Using Halihan's method in combination with vibra-core GSP10-01 (Figures 14 & 15) proved beneficial for understanding the processed images. Roughly 1.75 m of sand flat deposits are captured in core GSP10-01 (Figure 15). Additionally, the core data exhibited channel sub-facies 3 with trough cross beds at the same depth (2.4 m) of the ERI depicted channel using Halihan's method.

CHAPTER V

DISCUSSION

The GSP can be subdivided into three zones: proximal, medial and distal. Changes with morphology and sedimentological processes occur within each environment zone. Changes occur in three stages of evolution: flooding, evaporation-concentration and desiccation. The relative roles and individual processes operating during each of these stages differ by location.

Morphology

The architecture of the GSP though considered a "featureless surface" (Johnson, 1972) varies from proximal to medial to distal sub-environments. Topographic profiles reveal that there is a trend in channel dimensions, contrary to North et al. (2007) stating that, "there is no systematic variation in channel dimensions". Channel depth does decrease from proximal to distal zones of the GSP as shown in Figure 34. Both charts show maximum incision defined as the difference from the southern bank to the lowest channel depth on the y-axis. The x-axis shows profile names aligned down dip, moving from west to east for Figure 34, Clay Creek and The Salt Fork of the Arkansas, respectively (Figures 7 & 9).

Other trends are formed within the channel environment in which bedform size is observed to decrease from proximal to distal zones (Figure 13). Additionally, riparian vegetation decreases moving from proximal to distal zones of the GSP (Figure 35).

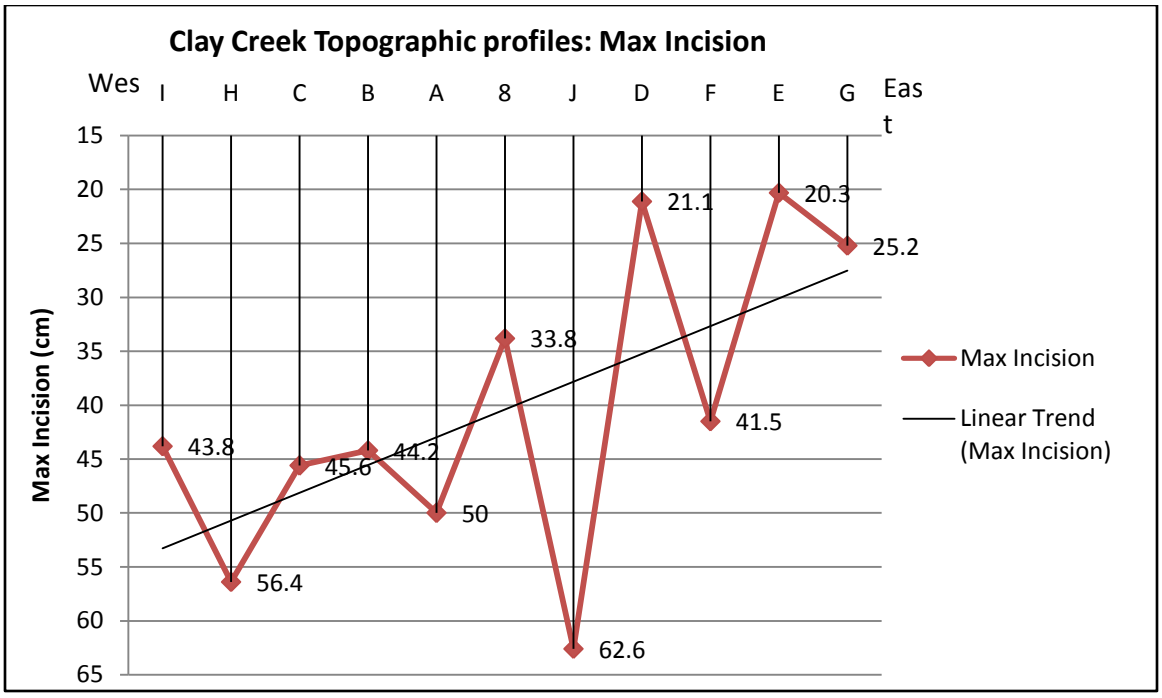

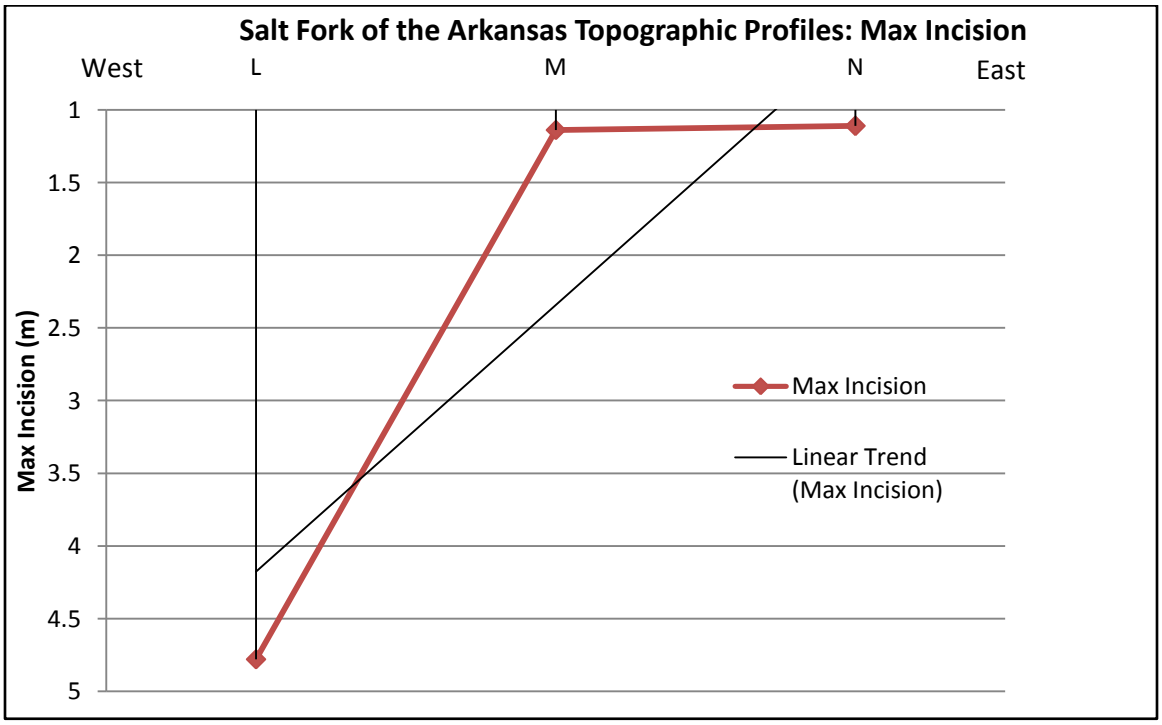

Figure 34: Clay Creek and the Salt Fork of the Arkansas maximum incision of channel profiles, down dip.

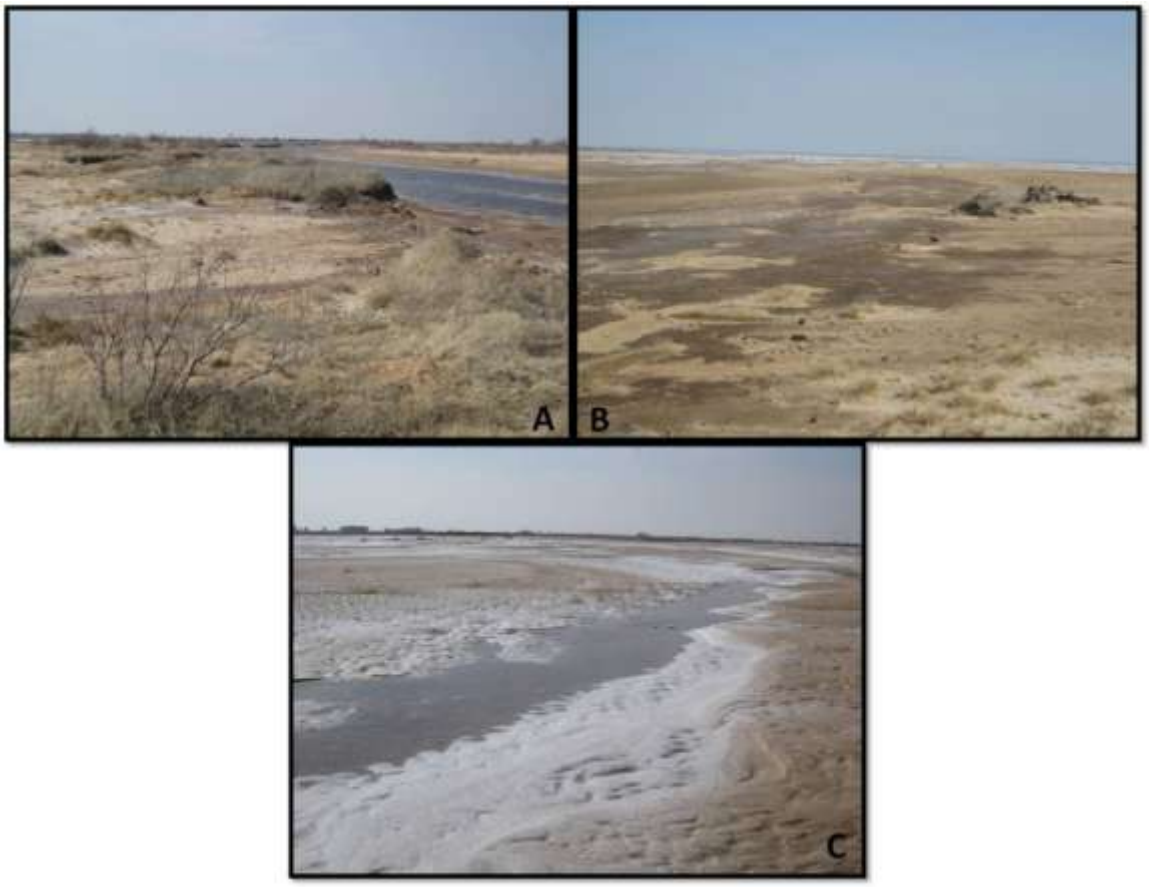

Figure 35: Decrease of riparian vegetation: Clay Creek. A: Looking due west, upstream in the proximal zone. B: Looking due east, downstream in the medial zone. C: Looking due west, upstream in the medial (nearing the distal) zone.

The Salt Fork is more extensive and larger and though it does demonstrate bifurcation in the distal sub-environment, it predominantly has an anabranching style of channel geomorphology in the proximal and medial sub-environments. Clay Creek and other minor creeks demonstrate bifurcation and anabranching, but do not always rejoin the main channel in the distal sub-environment (Figures 36 & 37). This constantly changing spatial distribution of channels in the medial sub-environment is likely partially responsible for the decrease in riparian plant life.

The proximal zone has some of the smallest geomorphic features observed in the field (Figure 13). Additional features were observed in the delta environments produced by the Clay Creek and The salt Fork of the Arkansas delta fronts (Figure 38).

Although it is possible some of the vibra-cores did not retain all of the possible sedimentary structures observed in tranches and at the surface; erosional, gradational and sharp contacts were preserved. These contacts provided information regarding the nature of facies transitions. GSP10-01 & GSP06-01 were the only cores not collected in the channel environment, but were collected within the sand flat environment. GSP10-01 was collected along an ERI line in order to calibrate potential channel signatures. This particular core did preserve trough cross bedding. Cores GSP10-02, 03 and 04 were all collected within the channel facies. Though cross stratification is not preserved in all cores, it was observed in trenches from the same locations. Both cores and trenches show alternating coarse and fine grained lamina (Figure 23). This is representative of the frequent shifts in flow magnitude. This type of sediment delivery is often considered a ‘pulse’ and is generally associated with ephemeral fluvial systems (Nanson et al., 2002). With the exception of Clay Creek, Powell Creek and The Salt Fork of the Arkansas all the fluvial systems of the GSP are ephemeral and only active during flooding stages.

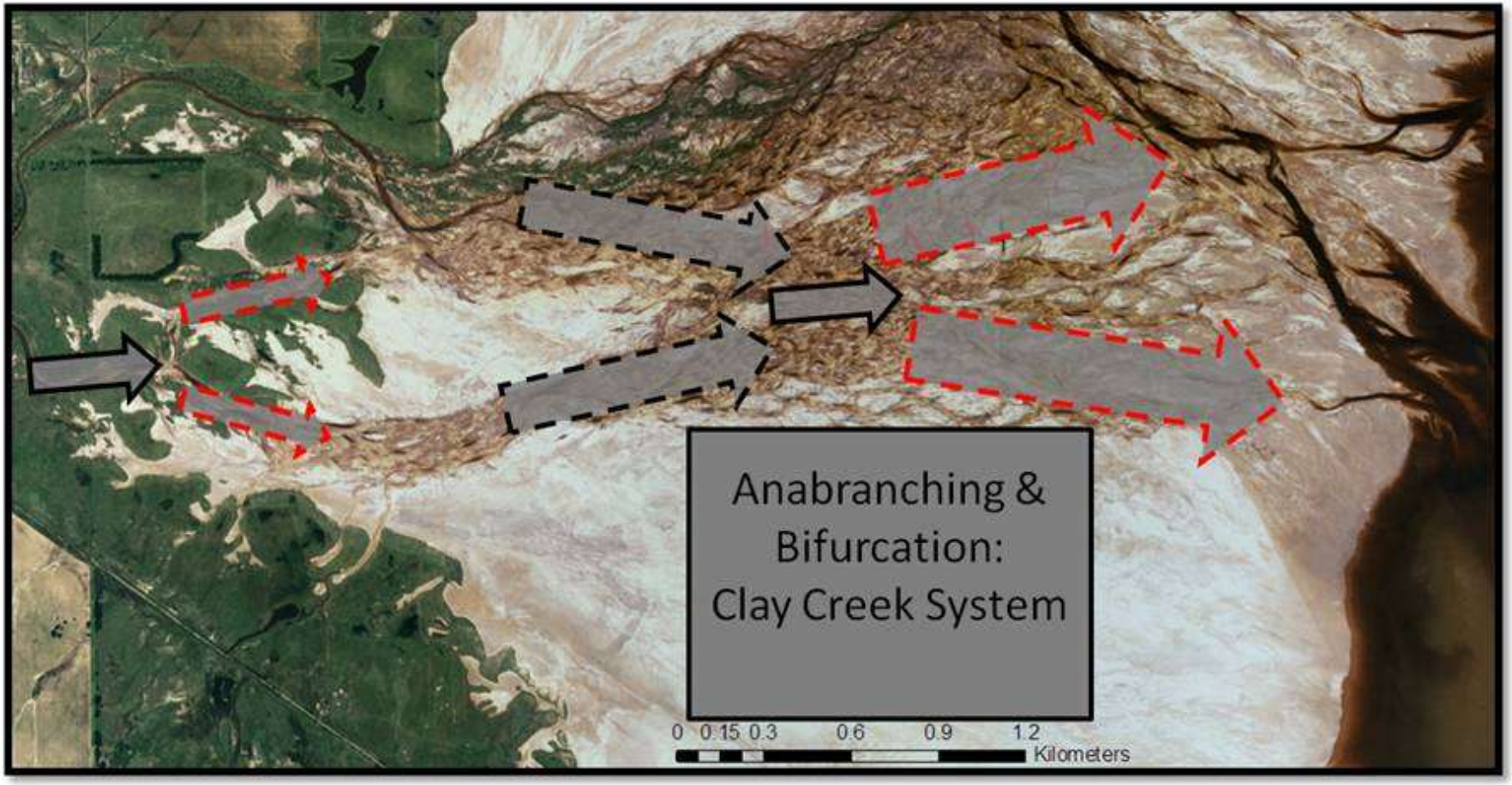

Figure 36: Black solid arrows indicate main channels, red hashed indicate splitting away and black hashed indicate rejoining. Not all channels rejoin in Clay Creek.

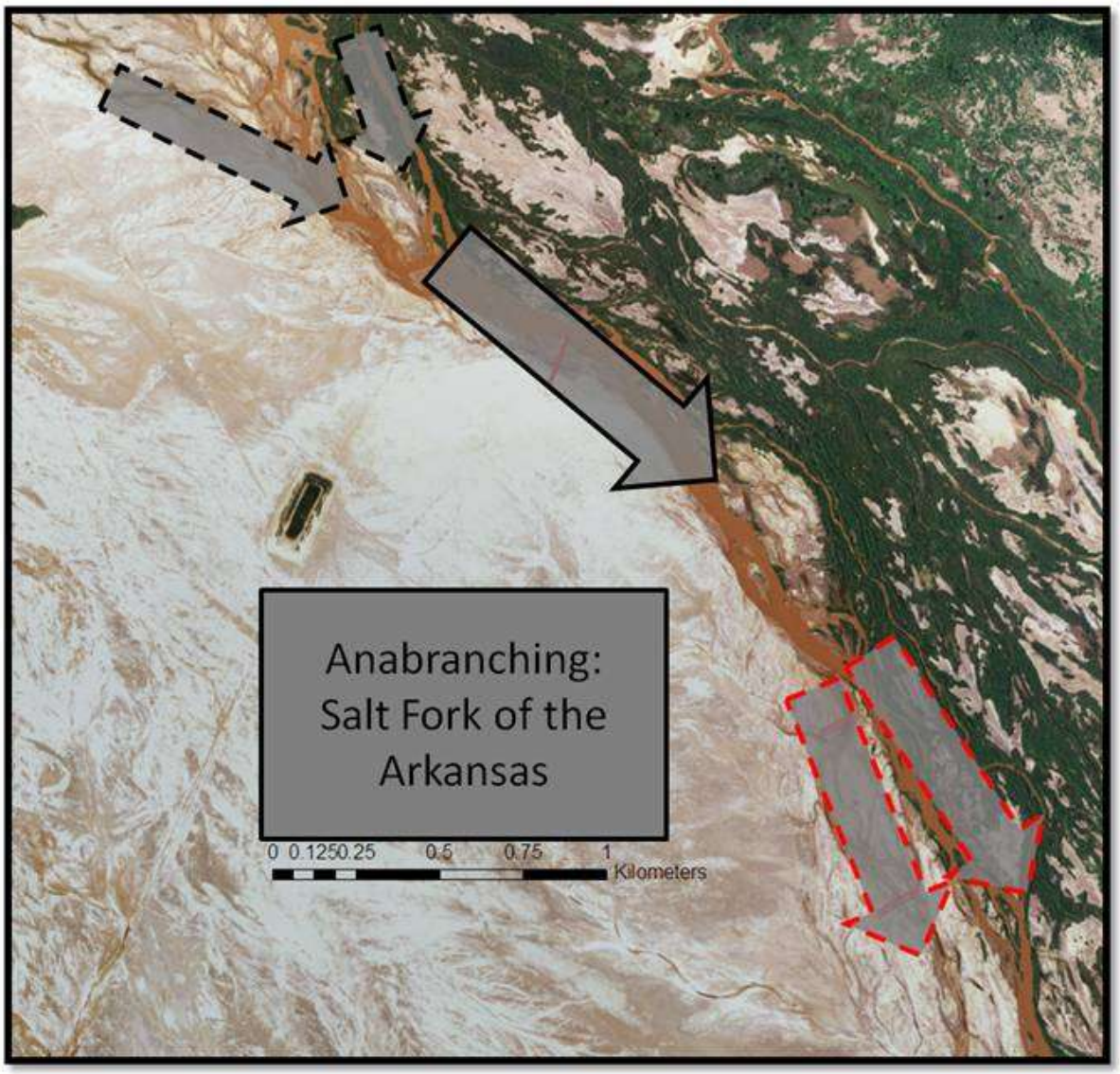

Figure 37: Arrow definition same as in Figure X, however The Salt Fork of the Arkansas is dominated by channels that split and rejoin (anabranching).

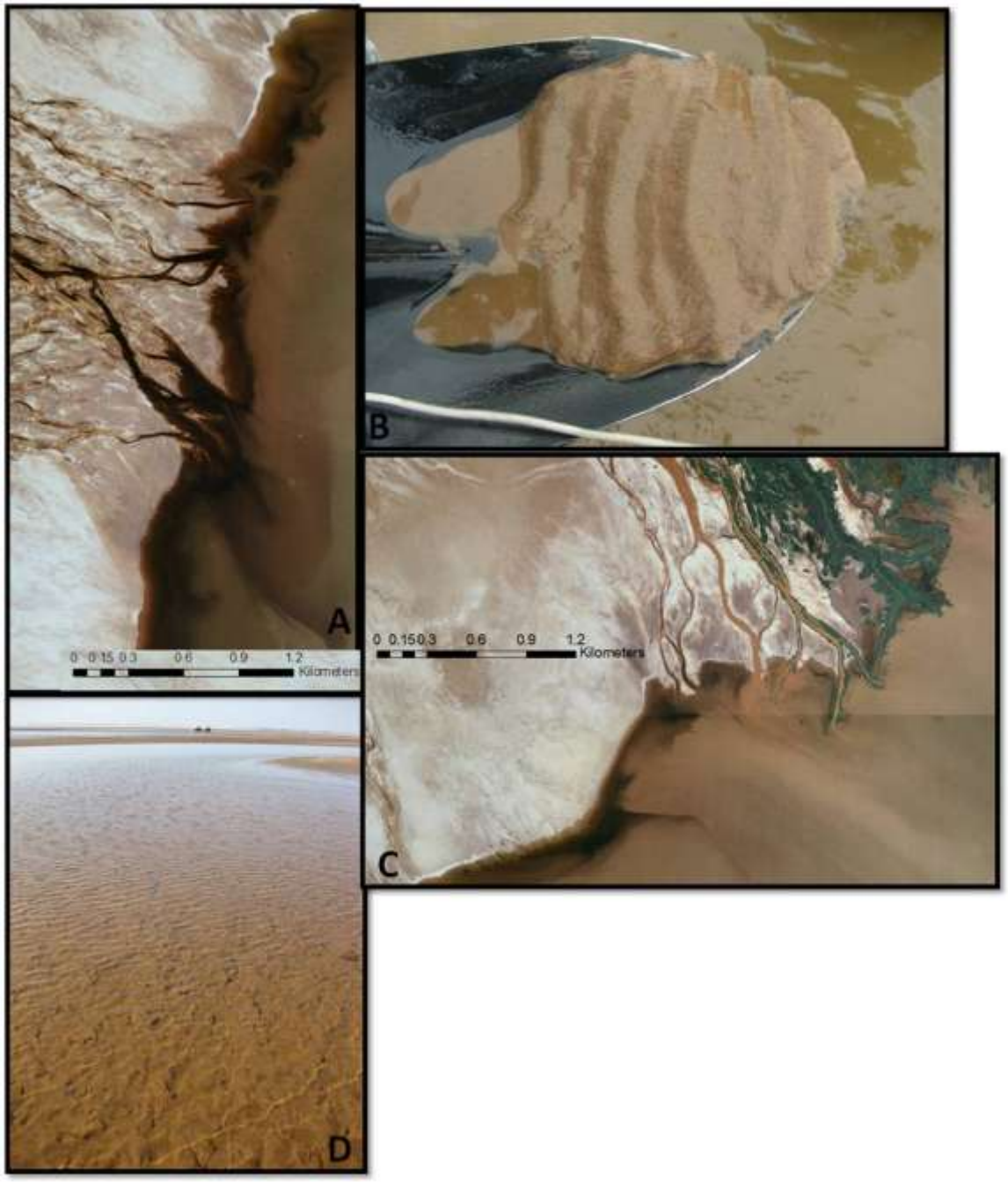

Figure 38: A: Aerial photography of the Clay Creek delta. B: Oscillation ripples submerged in Clay Creek delta front. C: Aerial view of The Salt Fork of the Arkansas delta. D: Reworked asymmetrical ripples submerged in delta front of The Salt Fork of the Arkansas.

Erosional vs Depositional surfaces

The surface of the GSP undergoes both deposition & erosion. Destroyed or missing traps allows for the distinction between depositional and erosional surfaces. Trap 07(A & B) was never successfully retrieved after deployment for either time periods (Figure 25). This is an indication of a highly erosive surface near the shoreline of the southern portion of the GSP where ST09-07A&B were deployed. In times of rain, the GSP is highly susceptible to flooding beginning at the shoreline as the reservoir quickly transgresses inland. Mass accumulation rates for the sediment traps are shown in table 2 and Figure 21. The total mass accumulation was divided by the appropriate number of days the trap was deployed yielding a rate of grams per day. The mass accumulation rates were generally higher over the 2 week period than the 2 month period. The only exceptions were traps not recovered and trap ST09-04A&B. Trap ST09-04A&B is in the proximal zone of the sand flat environment, near the vegetated dunes (Figures 1 & 30). ST09-04A (2 week period) had the lowest accumulation rate between the two with 0.55 g/day and 1.92 g/day during the 2 month period. This anomalous rate may be due to the proximity of the dunes for this particular trap which may have prevented direct flooding by overwash. One possible reason for the lower accumulation rates for the 2 month period (~ 63 days) is the increased frequency of storms. Only one minor rain shower occurred during the two week deployment, while multiple storm systems passed through during the 2 month period leaving the traps more vulnerable to a higher frequency of erosion. Initially these storm deposits are erosive, but as flow wanes, it has been observed that storm deposits remain, such as the obstacle scours (Figure 39 C & D).

The spatial arrangement of the sediment traps and their associated mass accumulation results suggests the erosional capacity generally increased distally within the sand flat environment probably due to overland flow and sheet wash during flooding stages. However, within the channel facies, relief along erosional surfaces decreased distally. Trap ST09-09

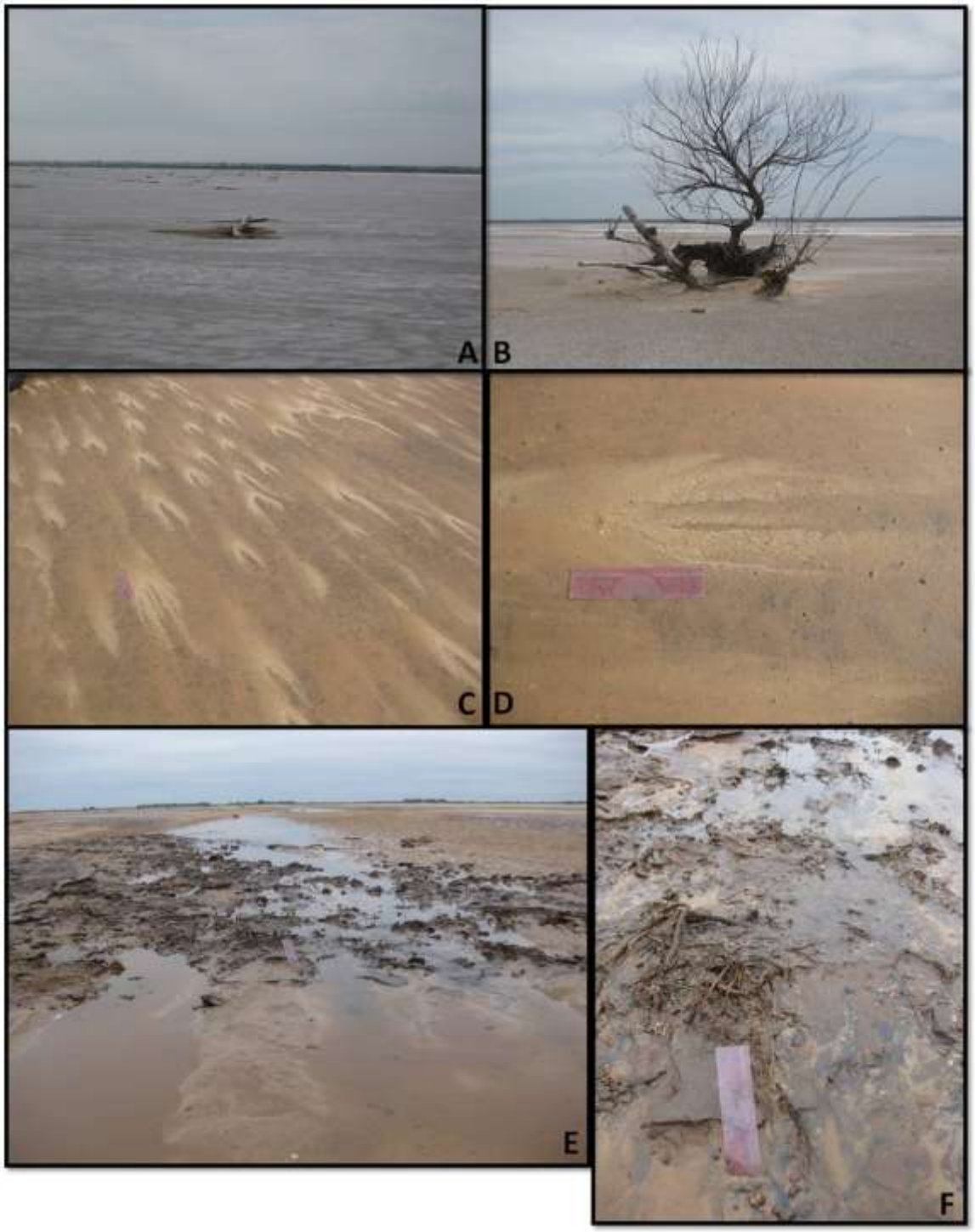

Figure 39: Features produced across the GSP during the flooding stage. A: Debris (logs) extent inland on the sand flats. B: Debris washed in from Clay Creek system, close to a riparian island. C: Obstacle scours from sheet wash on sand flats. D: Obstacle scour. E: New ephemeral channel washout debris deposits. F: Wash out debris deposits.

retained trace amounts of sediment for the first two weeks of deployment and was completely gone for the 2 month retrieval. Depositional surfaces were generally tied to the channel facies environment within the medial and distal zones.

Grain-size data was collected for sediment traps, however, their values are subject to the depression each trap was observed to have created, which was not desired and allowed for a potentially unnatural enhanced accumulation of sediments.

Stages: Sedimentary Processes

Observations of the GSP through the course of this study suggest the GSP undergoes three stages of development in which a unique set of processes control the character of its surfaces and the natures of sediments deposited. These stages start with a rain event marking the flooding stage and are followed by the evaporation-concentration and desiccation stages as the waters recede.

Flooding stage

During this stage, water leaves the channels and expands into the sand flat environment to compensate for discharge producing ephemeral channels (Figure 39-E & F). Bifurcation increases in the medial zone for the channel environment, as well as within newly formed ephemeral streams that appear across sand flat environment. Distally, during this stage the GSP reservoir levels rise (causing the shoreline to transgress resulting in suspended load deposition on top of the sand flat and channel environments. The landward extent of this transgression determines the spatial distribution of the mud/algal flat facies. During times of frequent rain storms such as in the spring, portions of the sand flat environment (particularly on the South side) can be submerged with up to 3 cm of water, as measured/observed (Figure 40). This standing water eventually evaporates or flows via overland flow into the GSP reservoir. Some ephemeral isolated pools remain scattered throughout the flats resulting in the deposition of mud and evaporites. Additionally, sand sized sediment is transported by sheet-wash within shallow

Figure 40: Lineations on sand flat surface within 30 hours of a rainstorm, ovals circle standing water.

gradient settings, as also observed by Fisher et al. (2007). This process in addition to eolian processes is responsible for much of the sand deposits of the sand flat environment. Debris is introduced across the environment from sheet-flood flows. This debris includes dead logs, plant debris, animal remains and anthropogenic debris (Figure 39). Relatively large logs found on the sand flat surface are likely introduced during heavier rain events (Figure 39-A).

Additional surface features formed during the flooding stage include scours. Scours are found in the proximal zone of the channel environment and are attributed to higher velocities breaching the thin algal mat left behind from the previous evaporation-concentration stage. Debris, i.e. branches, logs, etc, breaks the thin algal surface and the high-velocity channel flow experienced during the flooding stage infiltrates the sandier deposits below resulting in erosion. Obstacle scours are also interpreted to be the result of sheet wash. Obstacle scours, found in the proximal zone are dotted granule to pebble sized deposits (Figure 39-C&D). The noses of these features are generally a large or a collection of large pebble-granule grains pointing upstream.

Evaporation-Concentration Stage

During the evaporation-concentration stage, precipitation of halite and selenite (gypsum variety) occurs at the surface and in the shallow subsurface. Sparse isolated evaporation pools are found throughout the sand flat and channel environments and the site of deposition of halite hoppers (cubic habit of precipitating halite) and halite rafts (Figure 41-A, D, E, F)(Lowenstein et al., 1985). Halite precipitation is not restricted to these pools as it also precipitates across the GSP in every zone and environment (Figure 41-B, C & Figure 42). Figure 42 illustrates the desiccation stage; however, the original process that introduced the halite occurs during the evaporation-concentration stage. Figure 41-B and C, both show unique habits of halite within the medial zone on the sand flats. Figure 41-B shows a prominent accumulation of halite along a log which is interpreted to have created a scour, which later formed an isolated puddle for halite hoppers and

Figure 41: Evaporation-concentration stage. A: Isolated halite encrusted ephemeral pool. B: Accumulation of halite along log. C: Cross hatched pattern of dynamic features, asymmetrical straight swept ripples (halite covered) and lineations with adhered sand lenses. D: Halite hoppers. E: Selenite clusters precipitate in the subsurface and exposed due to erosion. F: Halite rafts.

Figure 42: Desiccation Stage. A: Desiccated ephemeral pool, tumble weed in the left background. B: Syneresis cracks and rolling log trail. C: Abandoned ephemeral channel with adhesion ripples and eolian sand lenses trapped in the troughs. D: Eolian halite ripples with noses pointed up wind, long continuous white lines are halite actively being transported.

rafts to form. Additional halite accumulates as the evaporation-concentration stage transitions into the desiccation stage and reworked halite grains were observed accumulating in the field by wind transport. Figure 41-C is show a unique cross hatched geometry in the medial zone of the sand flat environment. In this situation, asymmetrical straight-crested ripples are highlighted during the evaporation-concentration stage by the halite precipitation superimposed on lineations formed during the flooding stage. The lineations are composed of sand lenses transported by the wind and adhering to (at the time) the moist sand flat surface.

During this stage, isolated pools from abandoned ephemeral channels are observed in all three sub-environments. These pools are commonly halite filled and encrusted around their perimeters (Figure 41-A). These observed pools are most likely accountable for the discontinuous thin mud deposits found in trenches in both the channel facies and sand flat facies.

Desiccation Stage

The desiccation stage is dominated by eolian processes and impacts all zones. The medial zone was modified the most by eolian processes during the desiccation stage. Figures 42-B & C both have features that originate from the evaporation-concentration stage, but additional accumulation of halite and sand lenses occurred due to wind transport during the desiccation stage. Figure 42-A & B shows the surface of a dried ephemeral pool and faint syneresis cracks, respectively. Figure 42-B illustrates the trial of a log seen in the distance similar to deposits found in Racetrack playa of Death Valley (Stanley 1955). Whether the log traveled solely due to sheet-wash processes or was aided by wind is uncertain. Sand, halite or any available fragments or particles from the abandoned channel is redistributed by the wind and deposited on top of over-bank deposits. This process was also observed in active channels, although, the wind tended to redistribute over-bank deposits of sand and halite. Additional wind transport during this stage is

shown in Figure 42-D. Asymmetrical ripples of reworked halite and sediment occur discontinuously across the surface.

Depending on the length of the desiccation stage, perennial channels can also be reworked. Image J in Figure 46, shows a trench that illustrates this cyclicity between wet and dry stages along the channel and sad flat facies. Wetter periods (flooding stage) are represented by clay drapes and darker, finer sediment cutting in the laminates sands (drier – desiccation stage). The paramount characteristic of the desiccation stage is its ability to redistribute sediment from all zones and its subsequent environments. This reworking of grains makes it difficult to quantify the relative importance of eolian and fluvial contribution.

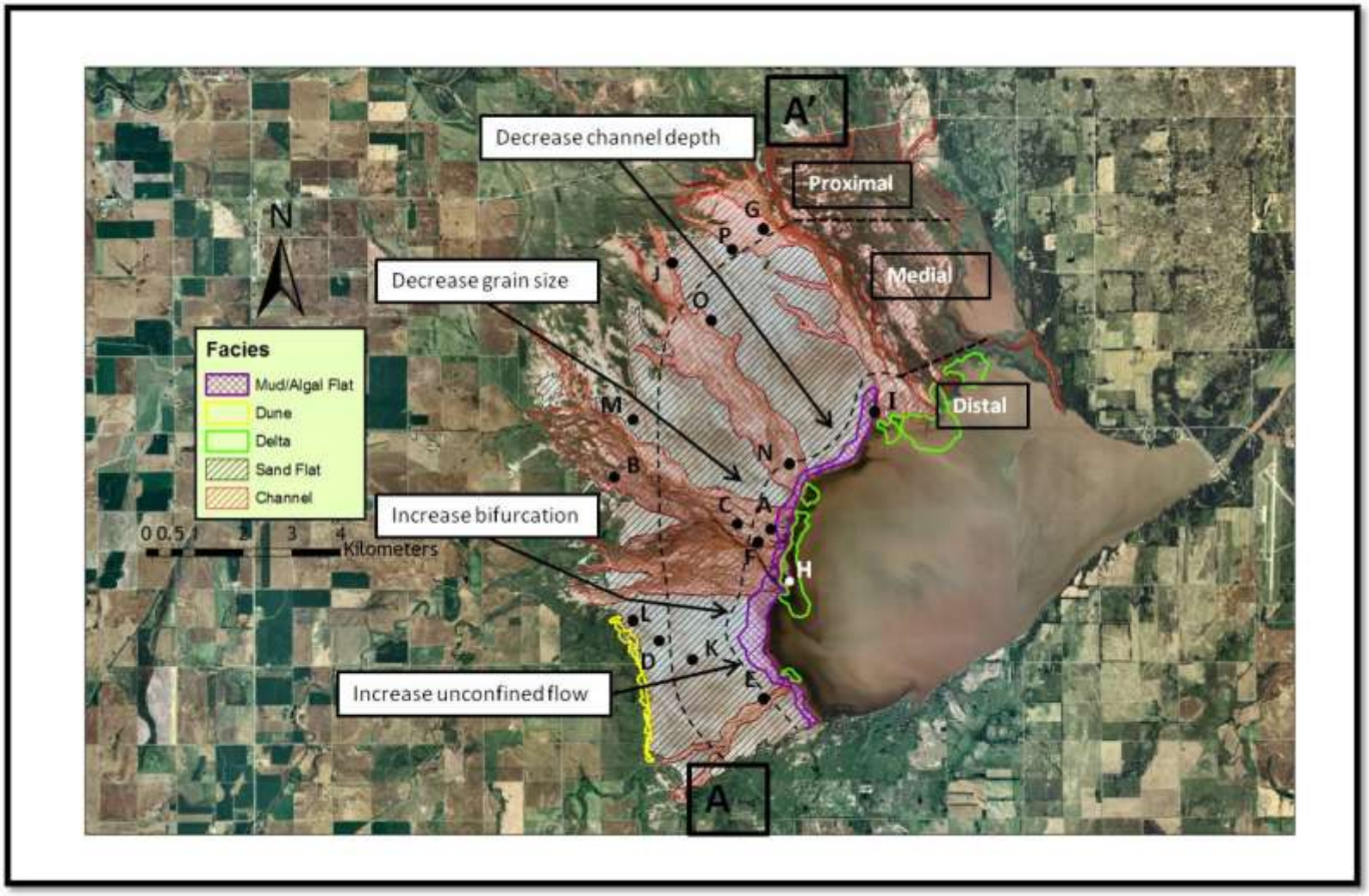

Figure 43: Zones of the GSP including some of the major trends found within some of the environments.

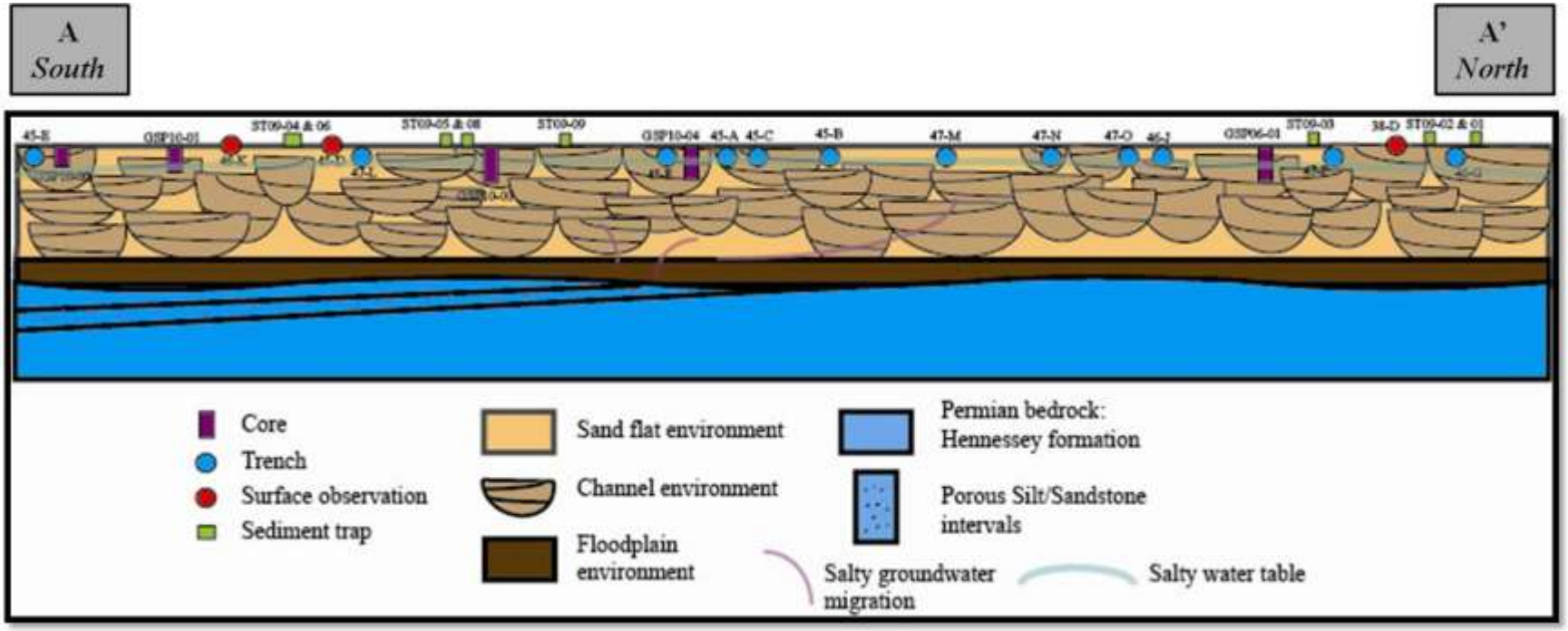

Figure 44: GSP Schematic cross section from South to North. Numbers and letters correspond to figures.

Figure 45: A-F photographs of the GSP summarizing the key characteristics of the depositional model. A: Rip up layer within the distal zone of the channel environment. B: Trough of cross bedding, with coarse grains and rip ups at base within the proximal zone within the channel environment. C: Clay layer overlying sand lenses and parallel lamina of the medial – distal transition zone of the sand flat environment. D: Side swept catenary ripples from sheet wash processes in the proximal zone of the sand flat environment. E: Ripple cross lamination, with a degrading black wood fragment from the medial zone within the channel environment. F: Lunate ripples found in the distal zone within the sandflat environment.

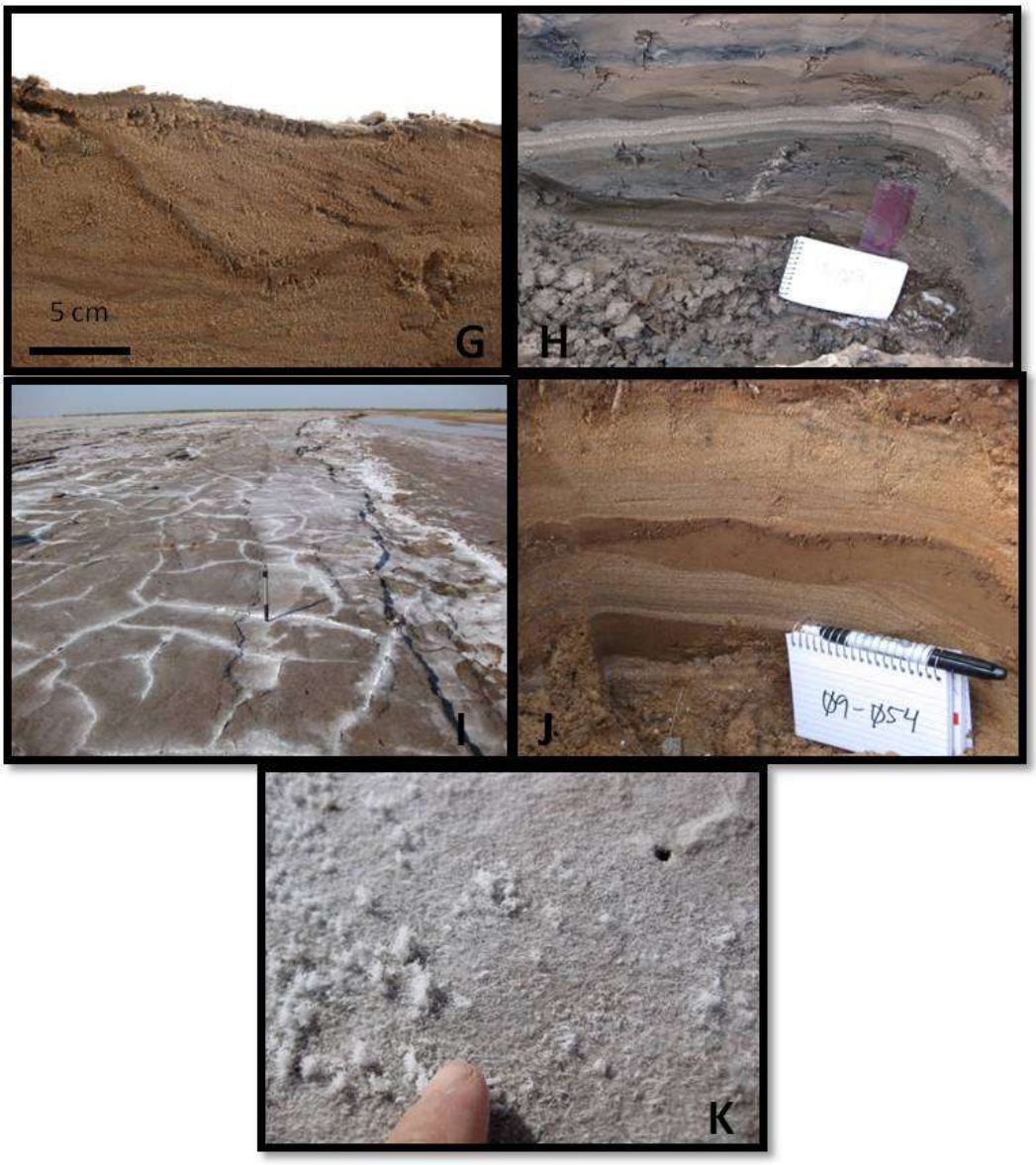

Figure 46: G-K photographs of the GSP depositional model. G: Cut and fill feature overlying ripple cross stratification in the proximal zone of the channel environment. H: Dark organic rich sand/mud lamination package overlain by coarser sand package and another package of dark organic rich sand/mud package in the distal zone of the channel environment. I: Syneresis cracks in over-bank deposits in the distal zone of the channel environment. J: Dark sand – very fine sand deposits overlain by lighter, coarse sand lamination and cross stratification cycles; dark: wetter times, light: drier times in the proximal zone straddling the channel and sand flat environments. K: Efflorescence surface, halite crust from the medial zone of the sand flat environment.

Figure 47: Images L – P of the GSP depositional model. L: Organic fragments, close to dunes in the proximal zone in the sand flat environment. M: Rip up clasts, parallel laminations and ripples capped by fine grained sandstone with sparse ripples in the proximal zone of the sand flat environment. N: Nearing distal zone, dark very fine sand and clay layer capped by organic rich silty to fine sand laminations in the channel environment. O: Dark organic rich sand and very fine grained sand layer capped by medium – coarse grained sand with thin organic rich layers with sparse ripples in the medial zone of the boundary of the channel and sand flat environment. P: Organic rich sand ripples with clay drapes capped by med grained sand with sparse ripples and organics in the proximal zone of the channel environment.

ERI – Paleoclimate Potential

Figure 44 illustrates our conceptual stratigraphic framework for the Holocene section of the GSP. The GSP stratigraphy is generally a thin layer of sand flat facies overlying a 5 – 10 m thick interval of coalesced fluvial channels represented by the three sub-facies of the channel facies. It is unclear whether the low-conductivity unit beneath the channel unit shown in Figure 32 represents an earlier period of sand flats or the finer-graines deposits of a more active Salt Fork of the Arkansas River. If it represents the former, a section of sandflat facies may provide a continuous record of Holocene sediments. However, nothing was identified with in the sand flat facies that could be used as a sedimentary proxy (e.g. laminations, preserved eolian lenses, etc) of climate.

CHAPTER VI

CONCLUSIONS

The GSP is a continental sabkha located within the central plains of Oklahoma. Its potential to hold a Holocene paleoclimate record was evaluated by documenting its sedimentary environments and general stratigraphy. Five (5) sedimentary environments were identified with in the GSP: sand flat, channel, mud/algal flat delta and dunes. The facies of each environment were described using field observations, shallow trenches, cores, grain-size measurements and aerial photography. All of the environments are subject to three different stages of evolution: flooding, evaporation-concentration and desiccation. The dominant processes that control sedimentation include: fluvial, sheet-flood, eolian and reservoir (anthropogenic) flooding processes.

From proximal to distal zones of the GSP, a decrease in channel depth, decrease in grain-size, an increase in channel bifurcation, and an increase in unconfined flow was observed. The channel depth trend is the most notable as it is contrary to the results of North et al. (2007), when stated that there is no systematic variation in channel dimension in the splay environment. However, a decrease in channel depth was found in this environment.

Both geophysical (ERI) and core analysis documented the presence of paleo-channels underlying most of the GSP. The presence of a continuous sheet of fluvial deposits beneath most of the GSP as well as the absence of a distinct sedimentary structures needed to produce a

Holocene climate proxy (e.g. laminations, eolian lenses, etc.) suggest that producing a climate record for the GSP may be unattainable.

REFERENCES

Amiel, A. J., Friedman, G. M., 1971. Continental Sabkhas in Arava Valley Between Dead Sea and Red Sea: Significance for Origin of Evaporites. The American Association of Petroleum Geologists Bulletin, v. 55, p. 581 – 592.

Ardnt, D. Assistant State Climatologist. Oklahoma State Climatology Survey. http://climate.mesonet.org/county_climate/Products/oklahoma_climate_overview.pdf

Benison, K.C., Beitler Bowen, B., Oboh-Ikuenobe, F.E., Jagniecki, E.A., LaClair, D.A., Story, S.L., Mormile, M.R., and Bo-Young, H., 2007. Sedimentology of Acid saline Lakes in Southern Western Australia: Newly described processes and products of an extreme environment. Journal of Sedimentary Research, v. 77, p. 366-388.

Brady, R.G., 1989. Geology of the Quaternary Dune Sands in Eastern Major and Southern Alfalfa Counties, Oklahoma. Unpublished Doctoral Thesis. Oklahoma State University. Stillwater, Oklahoma. 1-164.

Chairi, R., Derenne, S., Abdeljaoued, Largeau, C., 2010. Sediment cores representative of contrasting environments in salt flats of the Moknine continental sabkha (Eastern Tunisia): Sedimentology, bulk features of organic matter, alkane sources and alteration. Organic Geochemistry (2010) 41, p. 637-652.

Cheetham, M. D., Keene, A. F., Bush, R. T., Sullican, L. A., Erskine, W. D., 2008. A Comparison of grain-size analysis methods for sand-dominated fluvial sediments. Sedimentology (2008) 55: 1905-1913.

Cordova, C. E., Porter, J. C., Lepper, K., Kalchgruber, R. and Scott, G., 2005. Preliminary assessment of sand dune stability along a bioclimatic gradient, north-central and northwestern Oklahoma. Great Plains Research v. 15, p 227-249.

Fisher, J.A., Krapf C.B.E., Lang, S.C., Nichols, G.J., and Payenberg, T.H.D., 2008. Sedimentology and architecture of the Douglas Creek terminal splay, Lake Eyre, central Australia. Sedimentology (2008) 55: 1915-1930.

Fisher, J.A., Waltham, D., Nichols, G.J., Krapf, C.B.E., Lang, S.C., 2007. A Quantitative model for deposition of thin fluvial sand sheets. Journal of the Geological Society, London, v. 164, p. 67-71.

Fredlund, G.G., 1994. Late Quaternary Pollen Records from Cheyenne Bottoms, Kansas. Quaternary Research (1995) 43, p. 67-79.

Forman, S. L., Oglesby, R., Markgraf and V., Stafford, T., 1995. Paleoclimatic significance of Late Quaternary eolian deposition on the Piedmont and High Plains, Central United States. Global and Planetary Change v. 11, issue 1-2, p 35-55.

Gunatilaka, A., Mwango, S., 1987. Continental sabkha pans and associated nebkhas in southern Kuwait, Arabia Gulf. Geological Society, London, Special Publications, v. 35, p. 187-203.

Gustavson, T.C., and Holliday, V.T., 1999.Eolian sedimentation and soil development on a semiarid to subhumid grassland, Tertiary Ogallala and Quaternary Blackwater Draw Formations, Texas and New Mexico high plains. Journal of Sedimentary Research, v. 69, n. 3, p. 622-634.

Handford, C. R., 1982. Sedimentology and evaporate genesis in a Holocene continental-sabkha playa basin—Bristol Dry Lake, California. Sedimentology v. 29, p. 239-253.

Handford, C.R., 1981. Coastal sabkha and salt pan deposition of the lower Clear Form Formation (Permian), Texas. Journal of Sedimentary Petrology, v. 51, n. 3, p. 761-778.

Holliday, V.T., 1999. Folsom Drought and Episodic Dying on the Southern High Plains from 10,900 – 10,200 14C yr B.P. Quaternary Research v. 53, p. 1-12.

Hussain, M., Rohr, D.M., Warren, J.K., 1988. Depositional environments and facies in a quaternary continental sabkha, west Texas. West Texas Geological Society Publication: West Texas Geological Society 1988 Field Seminar: Guadalupe Mountains Revisited, Texas and New Mexico. October 13,14,15,16, 1988 Carlsbad, New Mexico.

Hyne, N. J. and Glass, C. R., 1977. A Process-Response Model for a Lacustrine Delta Orifice: Geological Society of America, v. 9, p. 28.

Johnson, K.S., 1972. Guidebook for Geologic Field Trips in Oklahoma Book II: Northwest Oklahoma. Oklahoma Geological Survey Educational Publication, 3. University of Oklahoma, Norman Oklahoma

Kinsman, D. J. J., 1969. Modes of formation, sedimentary associations and diagnostic features of shallow-water and supratidal evaporites. American Association of Petroleum Geologists Bulletin, v. 53, p. 830-840.

Kocurek, G. and Fielder, G., 1982. Adhesion structures. Journal of Sedimentary Petrology, v. 62, i. 4, p. 1229-1241.

Lepper, K., and Scott, G. F., 2005. Late Holocene Aeolian activity in the Cimarron River valled of west-central Oklahoma. Geomorphology v. 70, p. 42-52.

Lowenstein, T.K., and Hardie, L.A., 1985. Criteria for the recognition of salt-pan evaporites. Sedimentology (1985) 32: 627-644.

Miao, X., Mason, J.A., Johnson, W.C., and Wang, H., 2006. High-resolution proxy record of Holocene climate from a loess section in Southwestern Nebraska, USA. Palaeogeography, Palaeoclimatology, Palaeoecology.

Muhs, D.R., Bettis, E.A., III, Aleinikoff, J.N., McGeehin, J.P., Beann, J., Skipp, G., Marshall, B.D., Roberts, H.M., Johnson, W.C. and Benton, R., 2008. Origin and paleoclimatic significance of late Quaternary loess in Nebraska: Evidence from stratigraphy, chronology, Sedimentology, and geochemistry. Geological Society of America Bulletin, v. 120, p. 1378-1407.

Muhs, D.R., and Bettis, E.A., III, 2003. Quaternary loess-paleosol sequences as examples of climate-driven sedimentary extremes, *in* Chan, M.A., and Archer, A.W., eds., Extreme depositional environments: Mega end members in geologic time: Geological Society of America Special Paper 370, p. 53-74.

Nanson, G.C., Tooth, S. and Knighton, D., 2002. A global perspective on dryland rivers: perceptions, misconceptions and distinctions. Dryland Rivers: Hydrology and Geomorphology of Semi-arid Channels, pp. 17-54.

North, C.P. and Warwick, G.L., 2007. Fluvial fans: myths, misconceptions, and the end of the terminal-fan model. Journals of Sedimentary Research, 77: 693-701.

North, C.P., Nanson, G.C. and Fagan, S.D., 2007. Recognition of the sedimentary architecture of dryland anabranching (anastomosing) river. Journal of Sedimentary Research, 77: 925-938.

Olsen, H., Due, P.H., and Clemmensen, L.B., 1989. Morphology and genesis of symmetric adhesion warts – a new adhesion surface structure. Sedimentary Geology, v. 61, p. 277-285.

Porter, S.C., 2001. Chinese loess record of monsoon climate during the last glacial-interglacial cycle: Earth Science Reviews, v. 54, p. 115-128.

Purdue, J. R., 1976. Adaptations of the Snowy Plover on the Great Salt Plains, Oklahoma. The Southwestern Naturalist, v. 21, n. 3, p. 347-357.

Reilly, M., Lang, S., Fisher, J., Krapf, C., Payenberg, T. and Kassan, J., 2006. Variabilities of dryland terminal splay complexes; examples from western *Lake Eyre*, Australia. American Association of Petroleum Geologists, Annual Meeting 2006 15: p. 90

Slaughter, C. B. and Cody, R. D., 1989, Geochemistry of Near-Surface Ground Water, Great Salt Plains, Alfalfa County, Oklahoma: Oklahoma Geology Notes, v. 49, p. 200-219.

Stephens, J.J., Stratigraphy and Paleontology of late Pleistocene Basin, Harper County, Oklahoma. Bulletin of the Geological Society of America, 71: p. 1675-1702

Stanley, G.M., 1953. Origin of play stone tracks, Racetrack playa, Inyo County California. The Geological Society of America bulletin: 1955.

Soil Conservation Service (1968 & 1975). Soil Survey of Major and Alfalfa Counties, Oklahoma. United States Department of Agriculture.

Tooth, S., 2005. Splay formation along the lower reaches of ephemeral rivers on the northern plains of arid central Australia. Journal of Sedimentary Research, v. 75, p. 636-649.

Wakelin-King, G.A., Webb, J.A., 2007. Upper-flow-regime mud floodplains, Lower-flow-regime sand channels: sediment transport and deposition in a drylands mud-aggregate river. Journal of Sedimentary Research, 77: 702-712.

Warren, J.K., 2006. Evaporites: Sediments, Resources and Hydrocarbons. Springer – Verlag Berlin Heidelberg.

http://www.mesonet.org/

http://www.ogs.ou.edu/pubsscanned/EP9p12_14water.pdf

http://www.saltplains.fws.gov/

http://www.swt-wc.usace.army.mil/GSAL.lakepage.html

http://www.topozone.com/states/Oklahoma.asp?county=Alfalfa

APPPENDICES

GRAIN-SIZE DATA

Core	Mean Φ	Std Deviation	Skewness	Facies	Trench & Surface	Mean Φ	Std Deviation	Skewness	Facies
01A_0 cm	3.9814594	1.6206394	1.0294616	sand flat	09_022	0.8638812	2.0522815	0.7147217	delta
01B_50 cm	2.7502972	1.9677537	1.2592617	sand flat	09_030F	2.9365468	1.3921222	2.7139553	channel
01C_100 cm	2.801759	2.186906	1.4219312	sand flat	09_031B	2.7554119	1.6071553	1.4409417	channel
01D_150 cm	3.5258267	2.5371471	0.4814897	sand flat	09_030D	1.7655835	2.0893622	0.5518395	channel
01E_200 cm	1.9972041	2.0919077	1.4714975	channel	09_032B	3.2657441	1.0801064	3.4746454	channel
01F_250 cm	0.5655404	1.4684138	3.0769617	channel	09_033B	3.831832	1.6048542	0.938065	channel
02_15cm	4.3804367	1.8048575	0.3777556	channel	09_034	2.6450885	0.8418368	3.8716356	channel
03A_0 cm	3.3041104	1.3576147	1.992888	channel	09_036	2.9786337	0.8855289	3.4926096	channel
03B_50 cm	2.1564625	1.9449407	1.6971896	channel	09_037	3.2153392	1.0326605	2.8518361	Mud/algal flat
03C_100 cm	4.7809809	2.2603823	0.5393604	channel	09_043	2.1453052	1.0747535	2.1418039	channel
03D_150 cm	4.1752629	2.4228927	0.499392	channel	09_045	3.2187244	1.2654936	1.8756317	channel
03E_200 cm	2.8902096	1.3915868	2.4292172	channel	09_046	2.2847572	0.7994803	4.4918528	channel
03F_250 cm	2.2071707	1.9605797	1.4871468	channel	09_048	2.4412941	1.0386202	3.3316991	channel

03G_300 cm	1.9115298	1.3486604	2.4031328	channel	09_OB01	3.1267738	1.4134759	2.7710165	sand flat
03H_350 cm	2.1686011	1.4881832	2.4942131	channel	10_061A	2.0792271	0.9850025	2.5065339	sand flat
04_0 cm	3.936504	1.7246673	1.6438671	channel	10_061B	3.8445863	1.4605579	2.1298219	sand flat
04_56 cm	1.992308	1.0083013	2.501313	channel	10_061C	2.8244358	1.3762984	2.4654916	sand flat
04_75 cm	3.1789206	1.7394746	1.0962409	channel	10_062	2.4062994	0.8632424	3.9043071	sand flat
04_210 cm	3.730136	1.4528132	2.0438416	channel	10_063	2.6583642	1.5015632	2.9897446	sand flat
					10_064	4.0558	1.2347323	2.4933504	sand flat
					beach_sand	2.8149431	1.4849161	1.7614475	sand flat
					ss_001	1.3616948	2.2824185	0.4697215	mud/algal flat - surface

ERI DATA

Line Name	GPS - Electrode	Latitude	Longitude	Electrodes	Spacing (m)
GSP01N	E 1	N 36° 42.371'	W 98° 15.875'	56	2
GSP01N	E 14	N 36° 42.381'	W 98° 15.876'	56	2
GSP01N	E 28	N 36° 42.396'	W 98° 15.876'	56	2
GSP01N	E 42	N 36° 42.411'	W 98° 15.878'	56	2
GSP01N	E 56	N 36° 42.429'	W 98° 15.880'	56	2
GSP02NA	E 1	N 36° 42.367'	W 98° 15.996'	56	2
GSP02NA	E 14	N 36° 42.382'	W 98° 15.996'	56	2
GSP02NA	E 28	N 36° 42.393'	W 98° 15.996'	56	2
GSP02NA	E 42	N 36° 42.411'	W 98° 15.996'	56	2
GSP02NA	E 56	N 36° 42.425'	W 98° 15.996'	56	2
GSP04NA	E 1	N 36° 42.368'	W 98° 15.989'	56	2
GSP04NA	E 14	N 36° 42.381'	W 98° 15.989'	56	2
GSP04NA	E 28	N 36° 42.398'	W 98° 15.990'	56	2
GSP04NA	E 42	N 36° 42.413'	W 98° 15.990'	56	2
GSP04NA	E 56	N 36° 42.429'	W 98° 15.990'	56	2
GSP05N	E 1	N 36° 42.429'	W 98° 15.984'	56	2
GSP05N	E 14	N 36° 42.382'	W 98° 15.984'	56	2
GSP05N	E 28	N 36° 42.398'	W 98° 15.984'	56	2
GSP05N	E 42	N 36° 42.413'	W 98° 15.984'	56	2
GSP05N	E 56	N 36° 42.369'	W 98° 15.984'	56	2
GSP06N	E 1	N 36° 42.368'	W 98° 15.978'	56	2
GSP06N	E 14	N 36° 42.382'	W 98° 15.978'	56	2
GSP06N	E 28	N 36° 42.398'	W 98° 15.978'	56	2
GSP06N	E 42	N 36° 42.413'	W 98° 15.978'	56	2
GSP06N	E 56	N 36° 42.428'	W 98° 15.978'	56	2

GSP07N	E 1	N 36° 42.369'	W 98° 15.970'	56	2
GSP07N	E 14	N 36° 42.383'	W 98° 15.970'	56	2
GSP07N	E 28	N 36° 42.398'	W 98° 15.970'	56	2
GSP07N	E 42	N 36° 42.413'	W 98° 15.970'	56	2
GSP07N	E 56	N 36° 42.429'	W 98° 15.970'	56	2
GSP08N	E 1	N 36° 43.727'	W 98° 15.240'	56	2
GSP08N	E 14	N 36° 43.743'	W 98° 15.241'	56	2
GSP08N	E 28	N 36° 43.758'	W 98° 15.243'	56	2
GSP08N	E 42	N 36° 43.774'	W 98° 15.245'	56	2
GSP08N	E 56	N 36° 43.789'	W 98° 15.248'	56	2

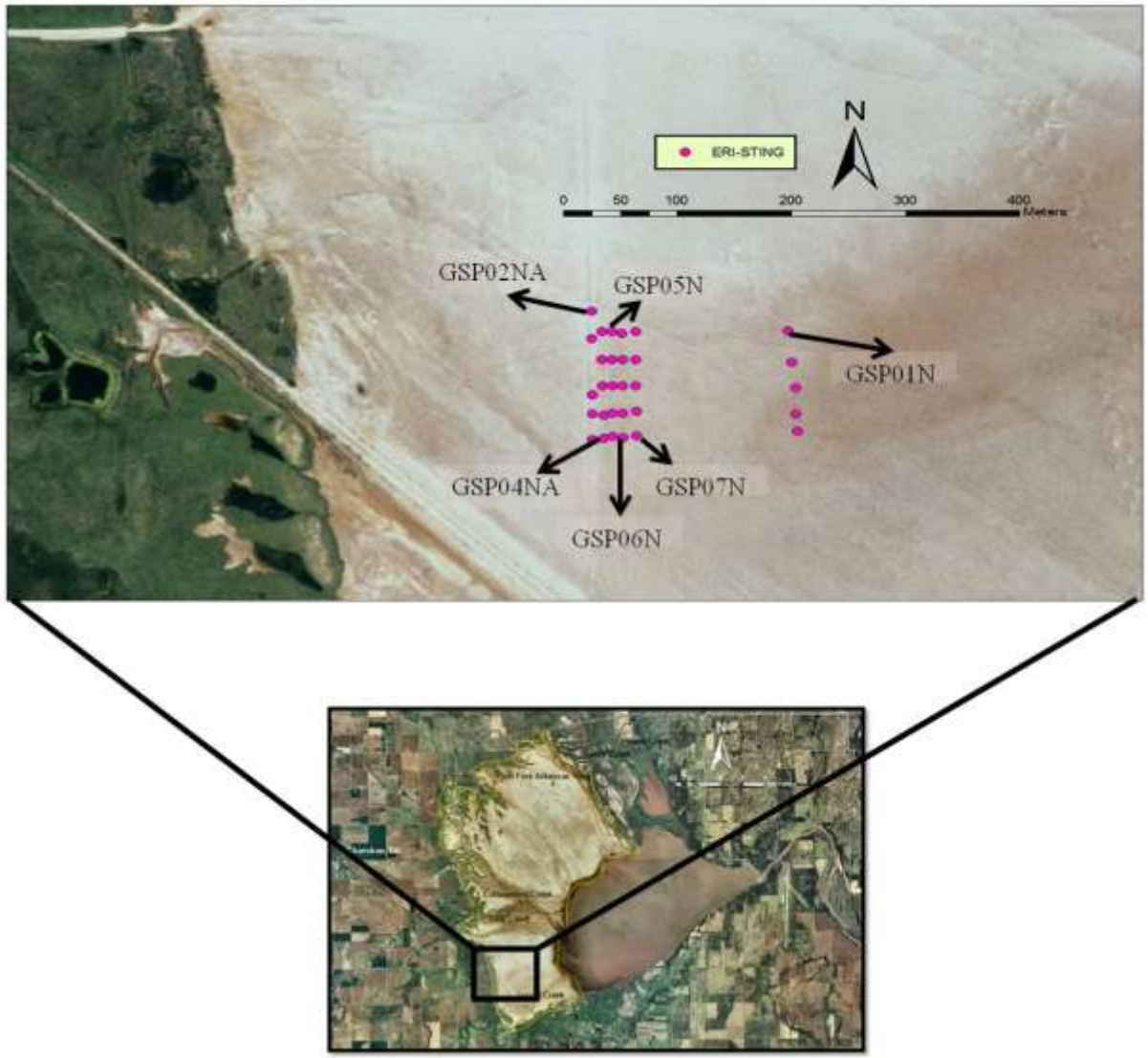
ERI-STING
N
0
50
100
200
300
400
Meters
GSP02NA
GSP05N
GSP01N
GSP04NA
GSP07N
GSP06N

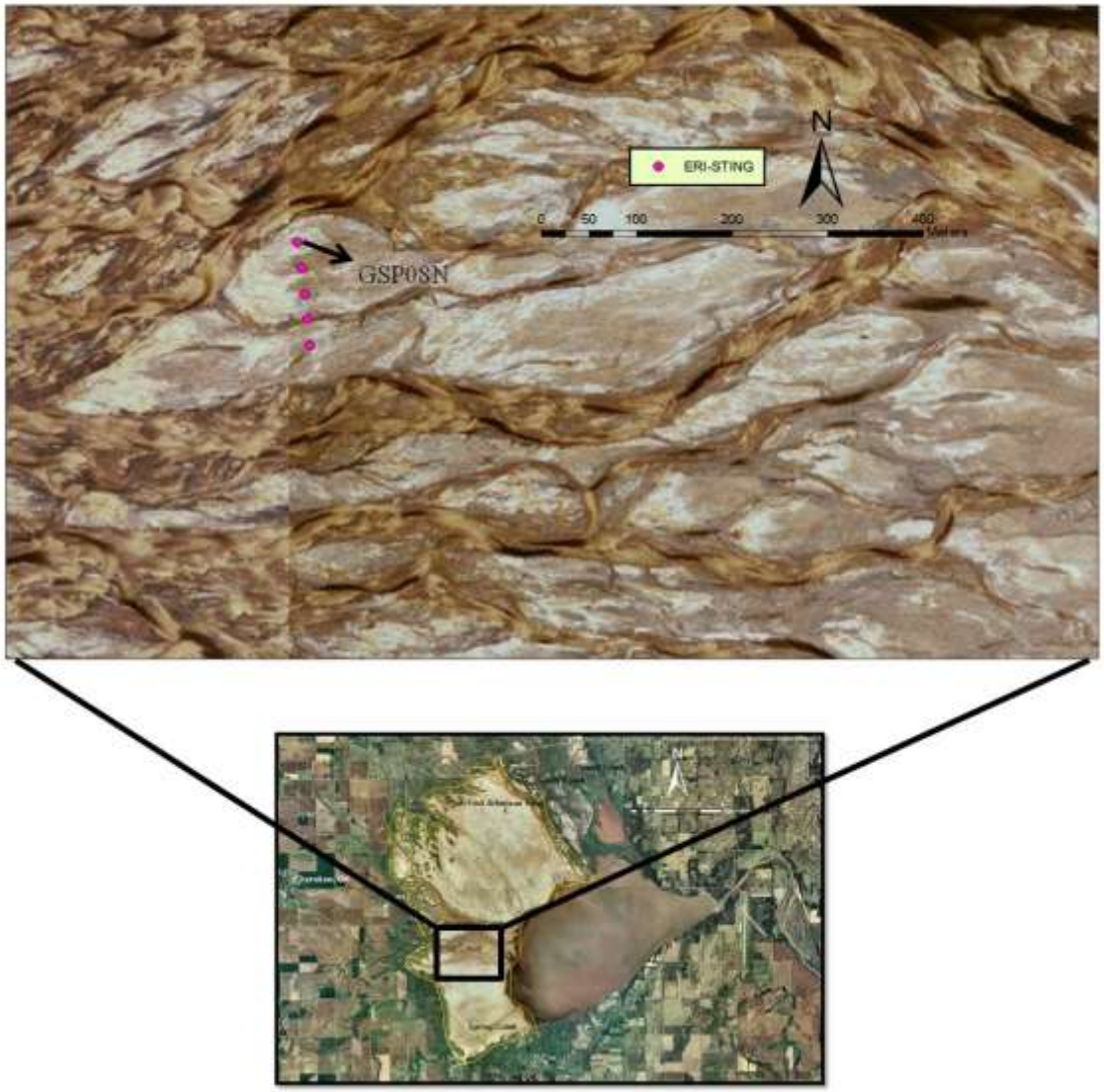
ERI-STING
N
0 50 100 200 300 400
Meters
GSP08N

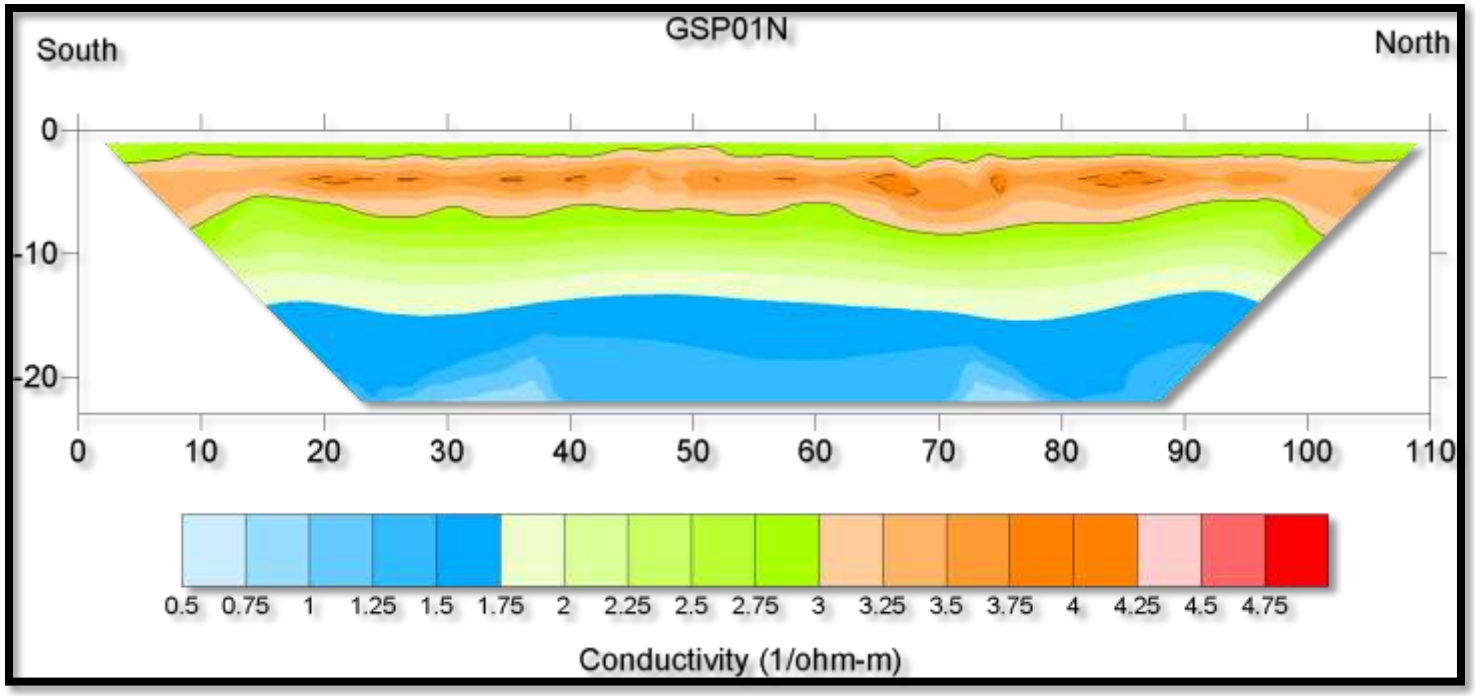
GSP01N
South
North
0
-10
-20
0
10
20
30
40
50
60
70
80
90
100
110
0.5
0.75
1
1.25
1.5
1.75
2
2.25
2.5
2.75
3
3.25
3.5
3.75
4
4.25
4.5
4.75
Conductivity (1/ohm-m)

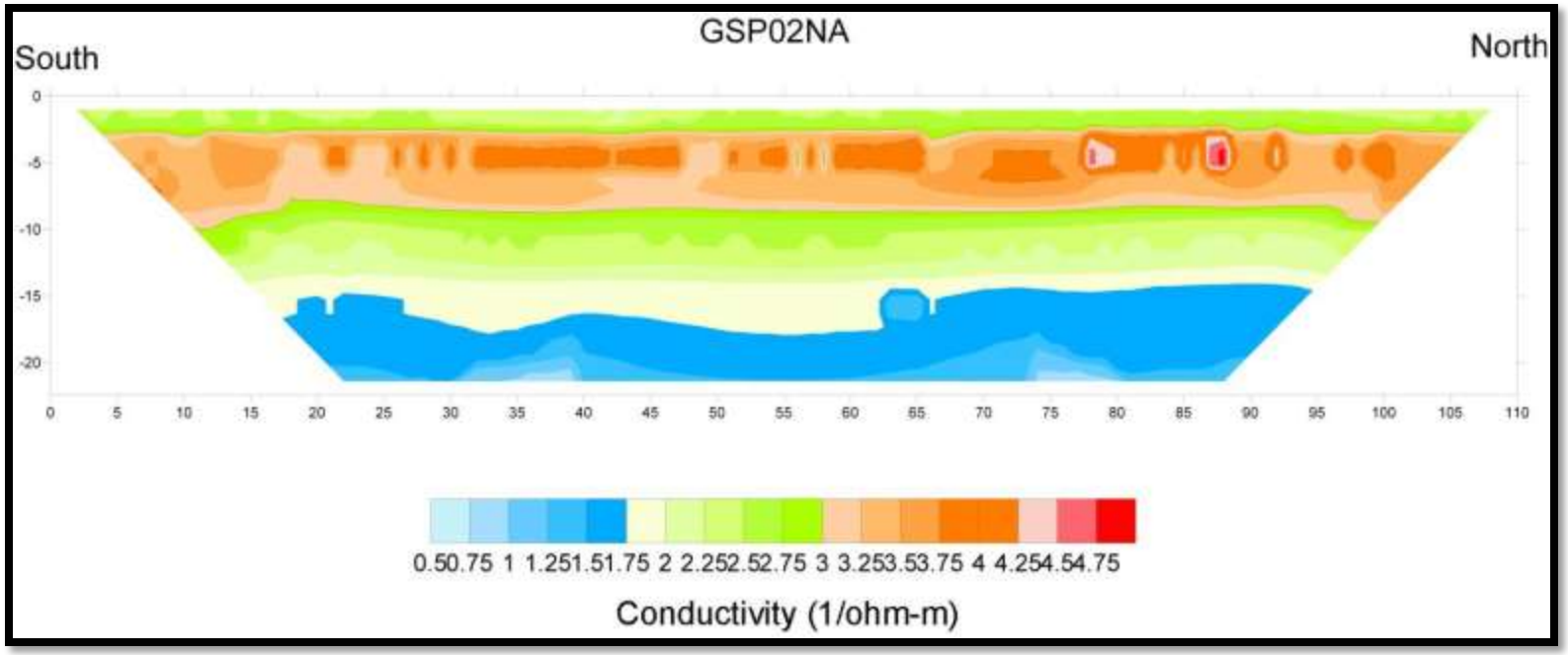
GSP02NA
South
North
0
-5
-10
-15
-20
0 5 10 15 20 25 30 35 40 45 50 55 60 65 70 75 80 85 90 95 100 105 110
0.50.75 1 1.251.51.75 2 2.252.52.75 3 3.253.53.75 4 4.254.54.75
Conductivity (1/ohm-m)

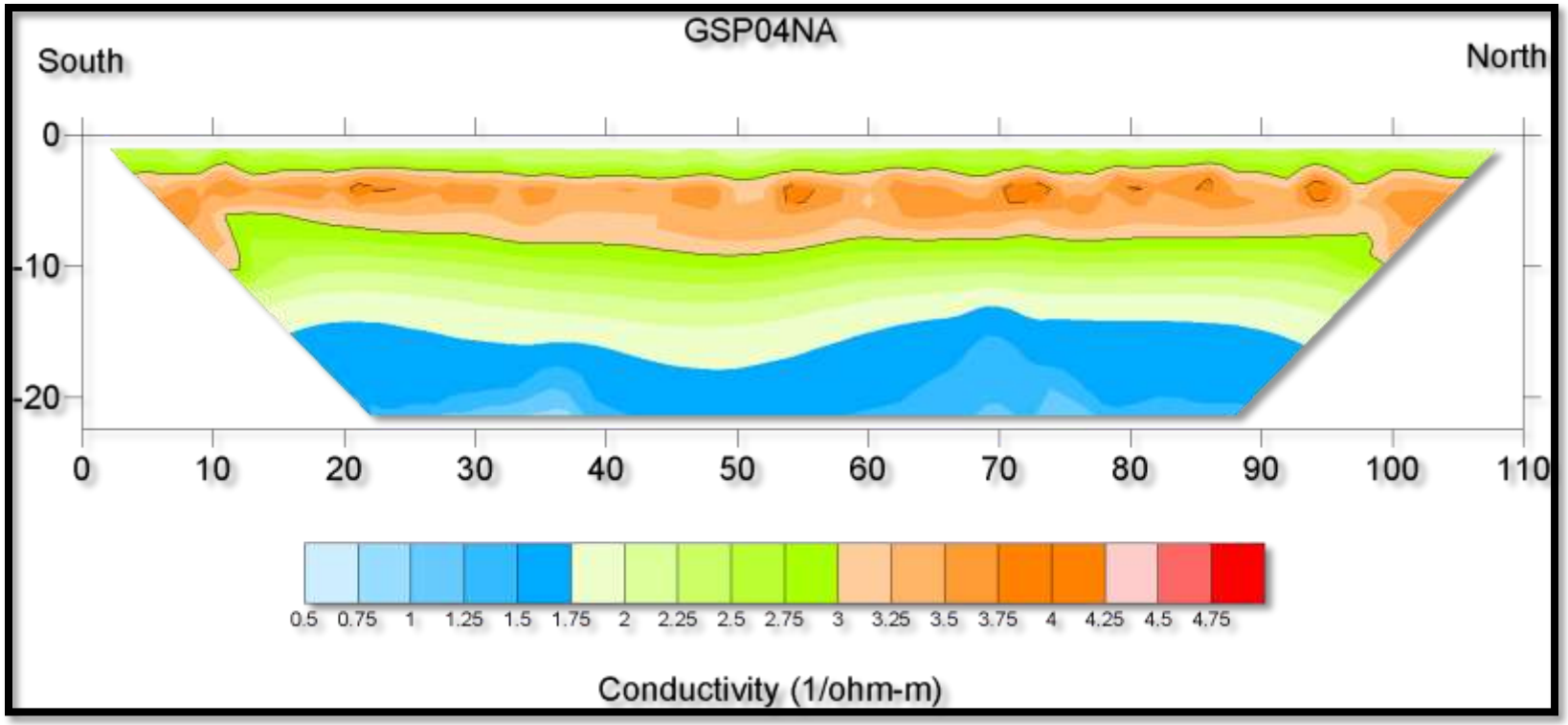
GSP04NA
South
North
0
-10
-20
0
10
20
30
40
50
60
70
80
90
100
110
0.5
0.75
1
1.25
1.5
1.75
2
2.25
2.5
2.75
3
3.25
3.5
3.75
4
4.25
4.5
4.75
Conductivity (1/ohm-m)

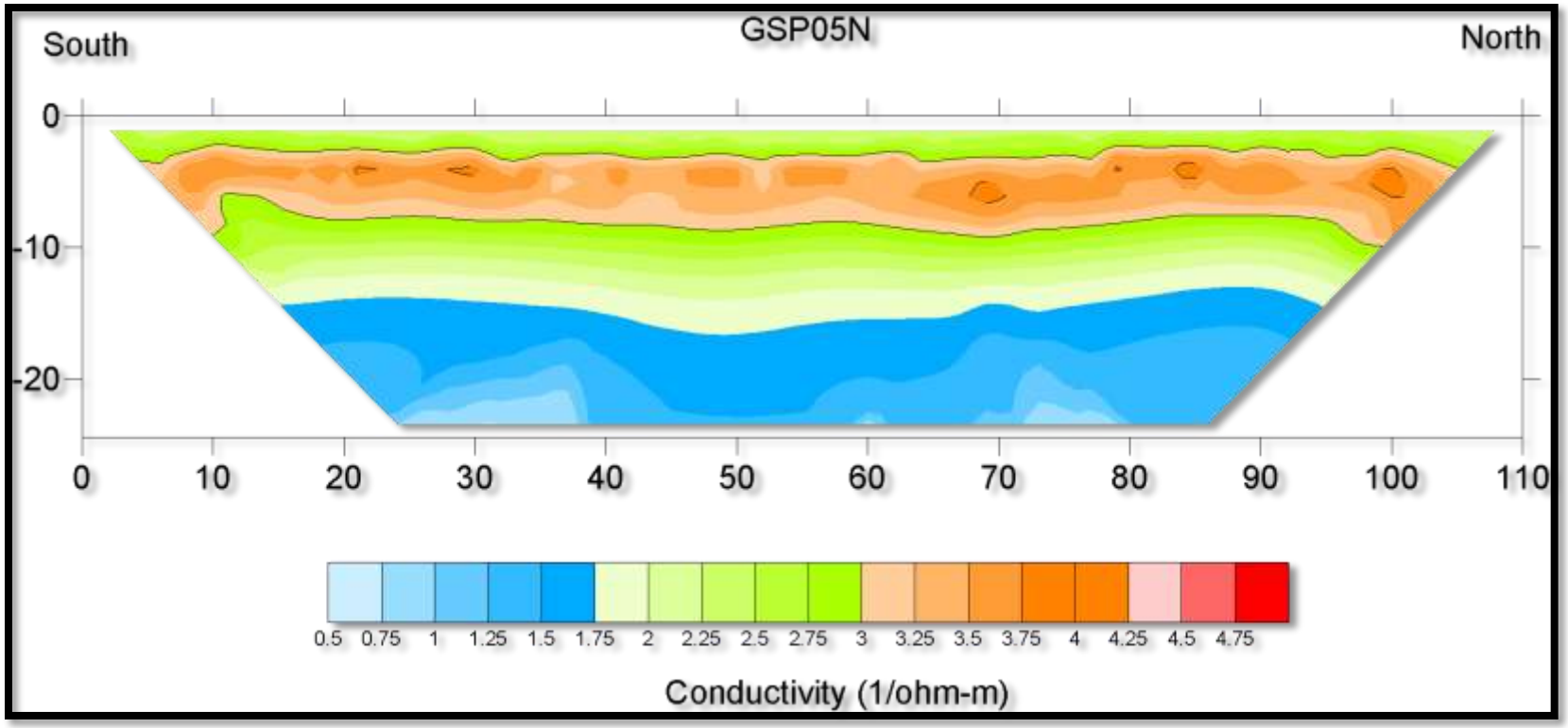
South
GSP05N
North
0
-10
-20
0
10
20
30
40
50
60
70
80
90
100
110
0.5
0.75
1
1.25
1.5
1.75
2
2.25
2.5
2.75
3
3.25
3.5
3.75
4
4.25
4.5
4.75
Conductivity (1/ohm-m)

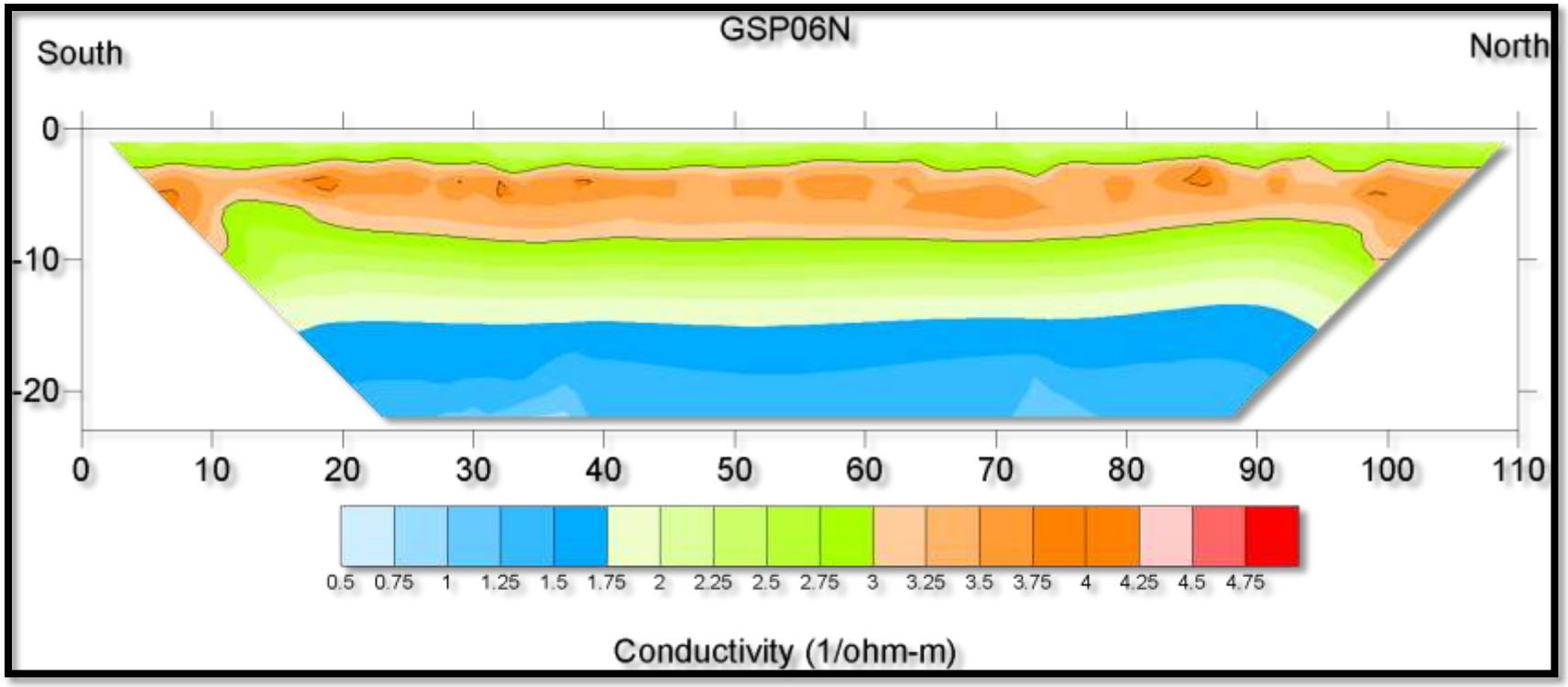
GSP06N
South
North
0
-10
-20
0
10
20
30
40
50
60
70
80
90
100
110
0.5
0.75
1
1.25
1.5
1.75
2
2.25
2.5
2.75
3
3.25
3.5
3.75
4
4.25
4.5
4.75
Conductivity (1/ohm-m)

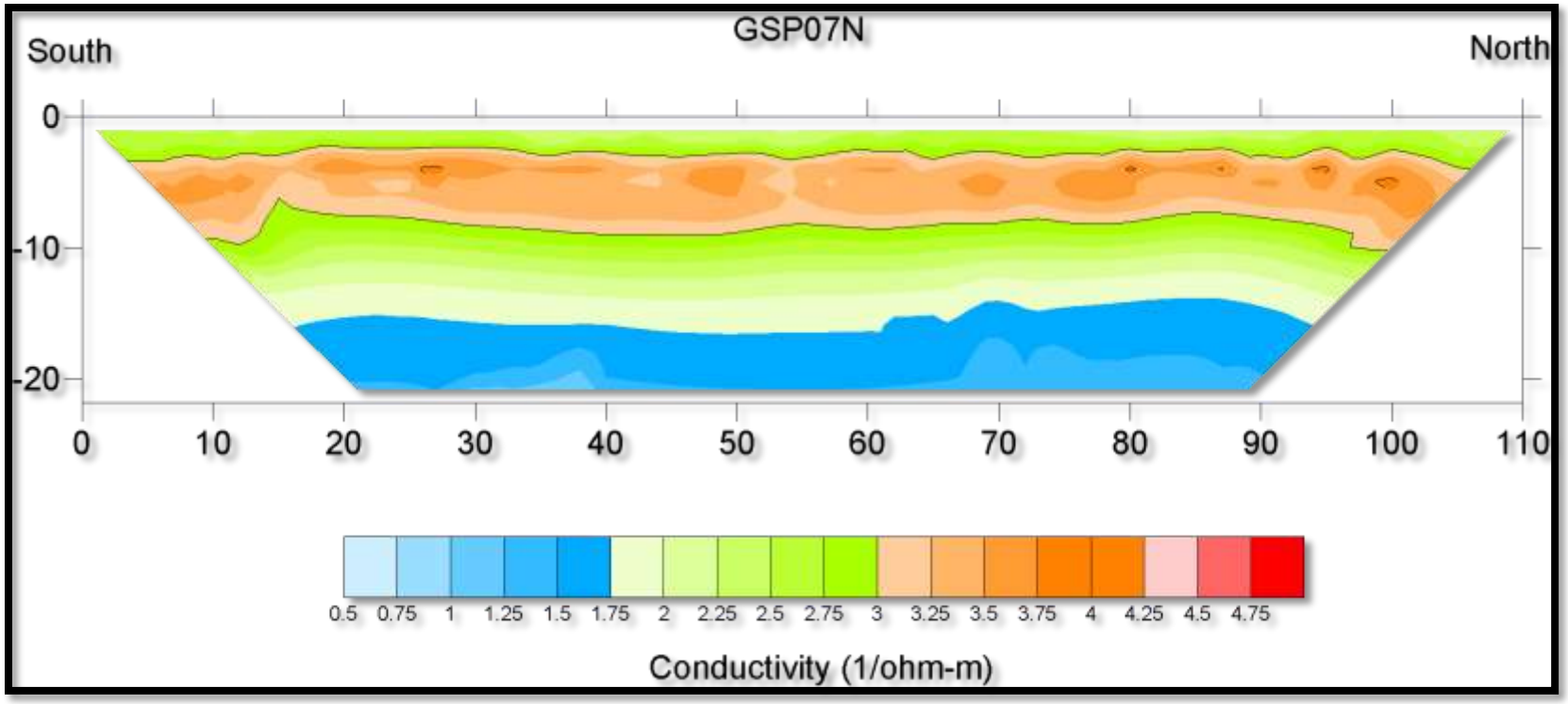
GSP07N
South
North
0
-10
-20
0
10
20
30
40
50
60
70
80
90
100
110
0.5
0.75
1
1.25
1.5
1.75
2
2.25
2.5
2.75
3
3.25
3.5
3.75
4
4.25
4.5
4.75
Conductivity (1/ohm-m)

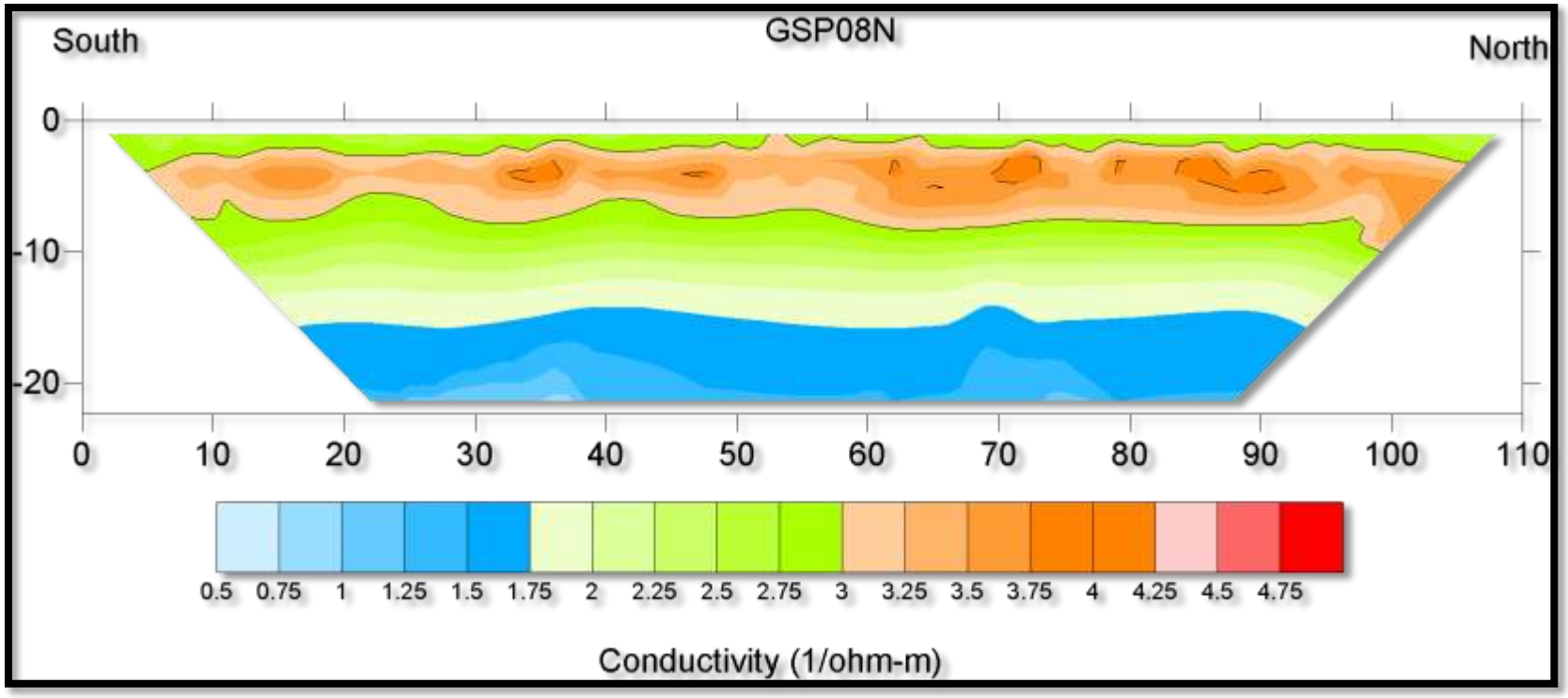
South
GSP08N
North
0
-10
-20
0
10
20
30
40
50
60
70
80
90
100
110
0.5
0.75
1
1.25
1.5
1.75
2
2.25
2.5
2.75
3
3.25
3.5
3.75
4
4.25
4.5
4.75
Conductivity (1/ohm-m)

ABSTRACT

We investigate the potential of the Great Salt Plains (GSP) of northwestern Oklahoma for containing a climate archive by documenting the modern environments and creating a depositional model using trenches, cores, surface observations, aerial photographs, and GPS surveys. The GSP can be subdivided into five environments. These environments include sand flat, channel, mud/algal flat, delta and dunes. Each environment is marked by at least one distinct facies documented in trenches and surface observations. The most geographically widespread environment is the sand flat. Large expanses of sand flat are broken by many branching ephemeral channels of Spring, Clay, Powell Creeks and The Salt Fork of the Arkansas River. Cores and resistivity profiles were used to determine the vertical distribution of facies within the GSP. This subsurface data shows that although the sand flat environment is the most widespread environment today, the majority of the sedimentary deposits represent the channel environment with three (3) distinct sub-facies: sub-facies 1: tan-light brown to orange, coarse – granule sands with minor amounts of clay drapes, rip up clasts and cross bedding; sub-facies 2: brown-dark brown to black, fine – mud sized grains with plant fragments, trough cross bedding and inter-laminated sands and muds; and sub-facies 3: tan, to grey and rusty yellow, medium – coarse sands with flaser bedding, minor starved ripples and woody fragments. The avulsive nature of the Spring, Clay, Powell Creeks and The Salt Fork of the Arkansas River probably continuously reworks the sand flat facies making the preservation of a long continuous record of fine-grained sediments necessary for paleo-climate archive unlikely. Thus it is doubtful that the GSP contains a continuous long-term record of Holocene climate.

VITA

Kathryn Gail Jackson

Candidate for the Degree of

Master of Science

Thesis: A MODERN DEPOSITIONAL MODEL OF THE GREAT SALT PLAINS AND ITS POTENTIAL AS A CLIMATE ARCHIVE

Major Field: Master of Science in Geology

Biographical:

Personal Data:
Born: May 23rd, 1986 Austin, Texas
Parents: Johnny and Lisa Jackson

Education:
B.S. Texas Tech University, Lubbock, Texas May, 2008.
M.S. Oklahoma State University, Stillwater, Oklahoma December 2011

Experience:
Geology intern with SM Energy (formerly St. Mary Land & Exploration), Billings, Montana May – August 2010
Geologist with SM Energy, Midland, Texas March 2011 – present

Professional Memberships:
Geological Society of America (GSA)
American Association of Petroleum Geologists (AAPG)
Society for Sedimentary Geology (SEPM)
West Texas Geological Society (WTGS)

Name: Kathryn Gail Jackson Date of Degree: December, 2011

Institution: Oklahoma State University Location: Stillwater, Oklahoma

Title of Study: A MODERN DEPOSTIONAL MODEL OF THE GREAT SALT PLAINS AND ITS POTENTIAL AS A CLIMATE ARCHIVE

Pages in Study: 98 Candidate for the Degree of Master of Science

Major Field: Geology

Scope and Method of Study:

The purpose of this study was to create a comprehensive depositional model of a modern continental sabkha: The Great Salt Plains in Alfalfa County Oklahoma. This was achieved through shallow trenches, surface observations, sediment traps, aerial photography, grain size analysis, ERI – resistivity lines and vibra-cores. This was done in order to determine if a meaningful climate proxy could be extracted from the GSP.

Findings and Conclusions:

Five separate environments were identified: sand flat, channel, algal/mud flat, dune and delta. These environments are affected by three stages of evolution: flooding, evaporation-concentration and desiccation. The main processes controlling sedimentation are fluvial and eolian. The avulsive nature of the ephemeral streams entering the GSP constantly reworks sediments, especially during the flooding stage. Eolian processes also constantly rework sediments and make it very difficult to distinguish between fluvial and eolian contribution. Paleo-channel deposits were identified with ERI lines and verified with vibra-cores, however, being that the nature of the GSP is constantly being reworked, the likelihood of extracting an continuous climate archive is doubtful.